April 2014

Stochastic Dynamic Optimization Models for Societal Resource Allocation

Armagan Bayram
University of Massachusetts - Amherst

STOCHASTIC DYNAMIC OPTIMIZATION MODELS FOR SOCIETAL RESOURCE ALLOCATION

A Dissertation Presented

by

ARMAGAN BAYRAM

Submitted to the Graduate School of the
University of Massachusetts Amherst in partial fulfillment
of the requirements for the degree of

DOCTOR OF PHILOSOPHY

February 2014

Isenberg School of Management

STOCHASTIC DYNAMIC OPTIMIZATION MODELS FOR SOCIETAL RESOURCE ALLOCATION

A Dissertation Presented

by

ARMAGAN BAYRAM

Approved as to style and content by:

Senay Solak, Chair

Anna Nagurney, Member

Robert Nakosteen, Member

James M. Smith, Member

Michael Johnson, Member

George Milne, Ph.D. Program Director
Isenberg School of Management

ABSTRACT

STOCHASTIC DYNAMIC OPTIMIZATION MODELS FOR SOCIETAL RESOURCE ALLOCATION

FEBRUARY 2014

ARMAGAN BAYRAM

B.Sc., ISTANBUL TECHNICAL UNIVERSITY

M.Sc., ISTANBUL TECHNICAL UNIVERSITY

Ph.D., UNIVERSITY OF MASSACHUSETTS AMHERST

Directed by: Professor Senay Solak

We study a class of stochastic resource allocation problems that specifically deals with effective utilization of resources in the interest of social value creation. These problems are treated as a separate class of problems mainly due to the nonprofit nature of the application areas, as well as the abstract structure of social value definition. As part of our analysis of these unique characteristics in societal resource allocation, we consider two major application areas involving such decisions.

The first application area deals with resource allocations for foreclosed housing acquisitions as part of the response to the foreclosure crisis in the U.S. Two stochastic dynamic models are developed and analyzed for these types of problems. In the first model, we consider strategic resource allocation decisions by community development corporations (CDCs), which aim to minimize the negative effects of foreclosures by acquiring, redeveloping and selling foreclosed properties in their service areas. We model

this strategic decision process through different types of stochastic mixed-integer programming formulations, and present alternative solution approaches. We also apply the models to real-world data obtained through interactions with a CDC, and perform both policy related and computational analyses. Based on these analyses, we present some general policy insights involving tradeoffs between different societal objectives, and also discuss the efficiency of exact and heuristic solution approaches for the models. In the second model, we consider a tactical resource allocation problem, and identify socially optimal policies for CDCs in dynamically selecting foreclosed properties for acquisition as they become available over time. The analytical results based on a dynamic programming model are then implemented in a case study involving a CDC, and social return based measures defining selectivity rates at different budget levels are specified.

The second application area involves dynamic portfolio management approaches for optimization of surgical team compositions in robotic surgeries. For this problem, we develop a stochastic dynamic model to identify policies for optimal team configurations, where optimality is defined based on the minimum experience level required to achieve the maximum attainable performance over all ranges of feasible experience measures. We derive individual and dependent performance values of each surgical team member by using data on operating room time and team member experience, and then use them as inputs to a stochastic programming based framework that we develop. Several insights and guidelines for dynamic staff allocation to surgical teams are then proposed based on the analytical and numerical results derived from the model.

TABLE OF CONTENTS

LIST OF TABLES

LIST OF FIGURES

Figure **Page**

CHAPTER 1

INTRODUCTION

We study resource allocation problems where mainly social benefits and non-quantitative objectives are considered in determining the allocation of the resources. Resource allocation can be defined as the systematic use of scarce resources, especially in the near term, to achieve goals for the future.

Because of its social characteristics, our problem falls into the research area of community-based operations research (CBOR) which is a new sub-discipline within operations research and the management sciences. CBOR was created to provide operations research expertise to public sector that addresses societal problems such as poverty, homelessness and equity. Like other areas of public sector operations research, the objective function is not directly profit maximization or cost minimization, rather it is mostly related to the maximization of social utility and welfare (Johnson, 2011).

In general, CBOR is a well-studied field of problem structuring methods and soft systems methodologies, but quantitative focus involving many of operations research methodologies has been limited. On the other hand, given that most of the real-world resource allocation problems include uncertainty in the problem parameters, stochastic optimization is one of the quantitative tools that can be used to model societal resource allocation problems.

In this thesis, we propose stochastic dynamic modeling methodologies to solve certain societal problems based on two motivating applications. The non-financial structure of the objectives, which require an additional phase of objective definition in model development, as well as the similarity of the implemented methodologies in these problems form the common elements among a seemingly diverse set of application areas.

In the remainder of this chapter we describe the methodologies that we utilize in our analyses and present the specifics of the two motivating applications that form the focus of our research.

1.1 Methodology

1.1.1 Stochastic Programming

Stochastic programming (SP) with recourse is a method for solving optimization problems where there is uncertainty. Dantzig (1955) was the first to introduce a recourse model where the solution could be adapted based on the outcome of a random event. Since then, the field of SP has grown and become an important tool for optimization under uncertainty.

A stochastic program results when some of the parameters in a mathematical program are described as random variables. A key assumption in SP is that probability distributions of these random parameters are known. The objective of SP is to identify a feasible policy that minimizes or maximizes the expected value of a function of decision variables and parameters over all possible realizations of the random variables. The most widely studied SP models are two-stage models. In these problems, a decision is made at the beginning of the first stage without any certainty as to the values of the random parameters. At the beginning of the second stage, after observations regarding the uncertain parameters are made during the first stage, a recourse decision can be made to compensate for or fine-tune the first-stage action. The optimal policy for a two stage model includes the best decision in the first stage considering the possible realizations of the random parameters, as well as the best recourse decision in the second stage for each possible realization. A generalization of the two-stage problems is multistage SP models. In these models, a sequential structure exists, in which certain decisions are made at the beginning of each stage, followed by observations of the random parameters during that stage.

1.1.2 Dynamic Programming

Dynamic programming is a methodology for sequential decision making over periods which was originally used in the 1940s by Richard Bellman to describe the process of solving problems where one needs to find the best decisions one after another Puterman (1994). At each decision epoch, a decision maker observes the state of a system and chooses an action, and then gets an immediate reward and moves to a new state according to the probability distribution determined by the action choice. Because of the dynamical structure of the problem, this process continues, but now the system may be in a different state and there may be a different set of actions. Different from stochastic programming, dynamic programming involves many decision epochs and few constraints, so solution approaches proposed for these methods are different from each other. The value of each state at a given time can be found by working backwards, using a recursive relationship called the Bellman equation. Bellman's equation is useful because it reduces the choice of a sequence of decision rules to a sequence of choices for the control variable. There are different algorithms to solve dynamic programming problems suitability of which depend on the planning horizon. For instance, backward induction is a methodology used for finite horizon problems, while it is not appropriate for infinite horizon problems as there is no last period in which to start. A dynamic programming model is symbolically represented in Figure 1.1.

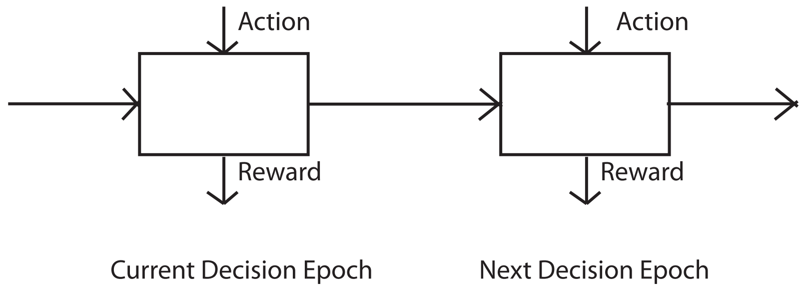

Figure 1.1. Symbolic representation of a dynamic programming problem.

1.2 Motivating Application: Nonprofit Foreclosed Housing Acquisition

The recent U.S. economic recession has had adverse effects in all sectors of the economy, particularly residential housing. A root cause of the recession was a dramatic increase in mortgage foreclosures, originating in decreases in home price appreciation that amplified the effects of increases in mortgage rates and the number of risky mortgage origination (Bernanke, 2008). The impacts of this crisis on the U.S. housing market have been broad and profound: there have been substantial decreases in housing values, home equity, home sales, and total housing starts (Joint Center for Housing Studies, 2009). As a result, home foreclosures have resulted in massive losses of consumer wealth: on average U.S. households lost $2.2 trillion in home value over the last four years, with losses totaling around $3 trillion in 2011 (CNN, 2009; Business Insider, 2012).

Policies to mitigate these losses include efforts to reduce the number of foreclosed homes in neighborhoods, which in turn will result in the appreciation of home prices and stabilization of the housing market. For example, U.S. Department of Housing and Urban Development has established a neighborhood stabilization program, which provides billions of dollars as assistance to state and local governments in the acquisition and rehabilitation of foreclosed property (HUD, 2008). Similar initiatives also exist at local or regional levels in many states. Key actors in these efforts with access to several federal and state funds are nonprofit community development corporations (CDCs), which acquire and rehabilitate foreclosed properties in their service areas using resources available to them. CDCs are local organizations that provide services and engage in other activities to build and revive neighborhoods. When a foreclosed property is put on sale, an important advantage for CDCs and other similar entities is their priority in making offers on the property. This is due to requirements put in place by most financial institutions through the National First Look Program, which provide owner occupants and public entities that are committed to the community an early opportunity to bid for a foreclosed property. As part of this policy, only offers from owner occupants and buyers using public funds are considered during the first 15 days a property is on the market, and offers from investors are considered only after the first 15 days have passed. This allows for a higher likelihood of a successful offer for CDCs due to the relatively fewer competitors in the process (Axel-Lute and Hersh, 2011).

CDCs exist in nearly every major urban area of the United States with approximately 5,000 CDCs spread throughout all 50 states (Community Wealth, 2012). Given the large number of CDCs operating in different parts of the U.S., the decision problems they face in their efforts to respond to the foreclosure problem have implications for the overall economy and public good. This is especially of importance, as the foreclosure crisis is not yet over, and the limited resources need to be used as effectively as possible to meet the challenges of the current or any other future crisis.

1.2.1 Strategic Societal Resource Allocation

In this motivating application area, we focus on the strategic resource allocation problem faced by CDCs. Strategic resource allocations need to consider potential availability and acquisitions of individual foreclosed units in the future, as well as the social impacts associated with these acquisitions which are all redeveloped and placed on market for sale. Given that all acquired properties are redeveloped, by acquisition we imply both the acquisition and redevelopment activities on a property unless noted otherwise in the study. Another key issue is that all these decisions are made under uncertainty, as several relevant inputs for the decision making process are determined by the state of the local and national economy, which is inherently uncertain. For example, the number of foreclosures to occur in a given region over the planning horizon, the purchase price of a foreclosed property, as well as the value generated by an acquired property are directly related to the economic conditions, and thus are not known in advance. Our decision framework is intended to capture these complexities in determining optimal resource allocations to different geographical regions by considering the specific acquisition decisions to be made in response to different realizations of future uncertainty. Our objective in this application is to develop tractable decision models whose solutions can provide general guidance to CDCs as they attempt to define priorities and budget allocations for residential real estate investments, which are intended to minimize the negative local impacts associated with housing foreclosures. To this end, we develop strategic resource allocation models under uncertainty, apply these multi-period stochastic models to a case study of a community-based organization, and discuss the solutions with respect to their policy implications and computational efficiency.

1.2.2 Tactical Societal Resource Allocation

In the second part of this motivating application we focus on tactical decisions that are led by CDCs in urban neighborhoods to support neighborhood stabilization and revitalization. Since the scale of the foreclosure crisis in most neighborhoods exceeds the response capacity of any particular CDC, our fundamental research question is the following: Given resource limitations and the uncertainty on the impacts of the foreclosure crisis, what are socially optimal acquisition policies that a CDC should implement while selecting foreclosed properties for potential acquisition?

A CDC seeking to purchase a foreclosed property faces a decision problem under uncertainty: should they make an offer on a given property - with a certain probability of success -, or should they wait for another property which may have a higher value for neighborhood stabilization? And if an offer is to be made on a property, what should be the offer amount? These decision alternatives are complicated by the fact that a property with a greater probability of high social returns may have higher costs than one with a lower probability of high social returns. Our approach to this problem involves a dynamic and stochastic resource allocation model where a limited budget is allocated dynamically to maintain an optimal portfolio of acquired properties. Each property has some associated cost defined by the dollar value required for purchase, and return defined by a social utility value, also defined in dollars. The problem involves stochasticity due to the uncertainty in the costs and returns of the properties, as well as their availability based on the conditions of the housing market and foreclosures. The costs and returns of properties are characterized by probability distributions, and are known for a property that has become available for potential bidding or acquisition. Upon observing the cost and return value of a property that arrives randomly over time, a CDC decides on whether to make an offer on the property, and if so how much to offer. Through our analysis, we obtain analytical and numerical results that characterize the optimal policies for a CDC under the cases with and without a deadline at which time the budget expires.

1.3 Motivating Application: Team Allocation in Robotic Surgery

Robotic surgery is a method to perform surgery using very small tools attached to a robotic arm where the surgeon controls the robotic arm through a computer. The use of robotic surgery has many advantages over open or conventional surgeries, as it results in reduced surgical error rates, shorter recovery times, and reduced levels of patient scarring and other lasting effects of surgery. In 1985 a robot, the Unimation Puma 200, was first used in a surgery to place a needle and then in 1988 a robot was developed to perform prostatic surgery. Four years later in 1992, another robotic system was introduced to mill out precise fittings in the femur for hip replacement (Ebme Articles, 2013). Nowadays, the Da Vinci surgical system, which is the most sophisticated robotic platform designed to expand a surgeon's capabilities, is widely used in a variety of operations such as gynecologic, cardiovascular, or urological surgeries.

Applications of robotic surgery and its importance have increased dramatically over time, and more than 300 hospitals across the United States currently use surgical robots in their procedures (GLG, 2013). Besides its benefits, the robotic systems are costly investments and have complex, time-consuming setups, requiring additional training or experience for the entire surgery team (Lanfranco et al., 2004; Wall et al., 2008). More specifically, each robotic system ranges in price from \$1 million to \$2.5 million, and the use of robotic surgery increases the cost of procedures anywhere from \$3,000 to \$8,000 (Creators.com, 2010).

Given the high costs and the increasingly common usage of robots in surgeries, it has become essential to evaluate operating room efficiency and cost effectiveness in these types of surgeries. It is clear that the composition of the surgical team, and the experience and competence of each team member play an important role in all surgeries, but it is especially of significance in robotic surgery. This is because the surgeon is not immediately at the bedside during the major components of the procedure, and several steps are performed by other team members during the surgery. Such steps, which require skill development by all team members, include docking of the robot, some surgical manipulation, and troubleshooting for minor technical and operational aspects of this highly sophisticated procedure.

The surgical team always includes a *primary surgeon*, who operates the surgery and uses the robot as necessary. A first assistant who is usually a designated *physician assistant* (PA) but sometimes another physician, assists the surgeon during the surgery, and is mainly responsible for robot docking and positioning. *A nurse anesthetist* provides anesthesia care during the surgery. The surgical team also includes a *scrub technician*, referred to as a scrub tech (ST), who works under the supervision of the surgeon, and handles the instruments, scrubs, medications, and other supplies during the surgical procedure. In addition, a *circulating nurse* (CN) "circulates" the operating room, ensuring proper procedures are being followed. Some of his/her responsibilities include preparing the operating room and all the required equipment, staying in the room during the surgery, and aiding in counting the equipment after the surgery. These tasks that each team member perform in robotic surgery differ with respect to those in a classical surgery, mainly due to the surgeon not being directly performing the operation, as well as due to the different procedures and equipments used.

Overall, the role that each surgical team member plays during the surgery is crucial and essential. Moreover, given the higher level of dependence of tasks in robotic surgery, any mishaps by any member can affect the performance of the entire team. Hence, the composition of the surgical team, specifically the joint experience, competence and cohesion among surgical team members are key determinants of efficiency and effectiveness in a robotic surgery. In many cases, failure to work together effectively has been cited as a common cause of adverse events and errors in surgery (Jeffcott, 2009). On the other hand, it is important to note that the ability to work as a team is a dynamic behavior that is acquired over time.

Our analysis in this application is based on the observation that although the individual experiences of team members make a difference in a robotic surgery, there may be an optimal combination of experiences and an optimal team composition, defined by the individual and joint number of surgeries performed. Considering this observation, in this study we aim to answer the following questions: (1) Given a range of potential experience measures for each team member, how would operating room performance vary as a function of these experience measures, and what is the marginal value of an increase in the experience of a specific team member? (2) What is an optimal team configuration, where optimality is defined based on the minimum experience level required to achieve the maximum attainable performance over all ranges of feasible experience measures?

Our methodology to answer these questions involve several statistical analyses, as well as a stochastic programming approach that is used to identify optimal team configurations by taking into account the dynamics of learning and experience building over time. The analyses are based on actual robotic surgery data involving records of around 400 robotic sacrocolpopexy operations, i.e. urologic and pelvic surgeries.

1.4 A Cohesive Framework for the Two Motivating Applications

In this thesis, we combine the problems described as part of the two motivating applications above under the general framework of stochastic dynamic societal resource allocation models. More specifically, we note that the objectives in these applications involve social dimensions which are different from classical applications with cost or profit based objectives. The social perspective in these problems requires additional phases in model building which involve definitions of social value. This is typically not necessary in cost based optimization. Another common element in the presented analyses in this thesis is the set of methodological approaches used, as all three problems are modeled and solved using stochastic dynamic optimization procedures.

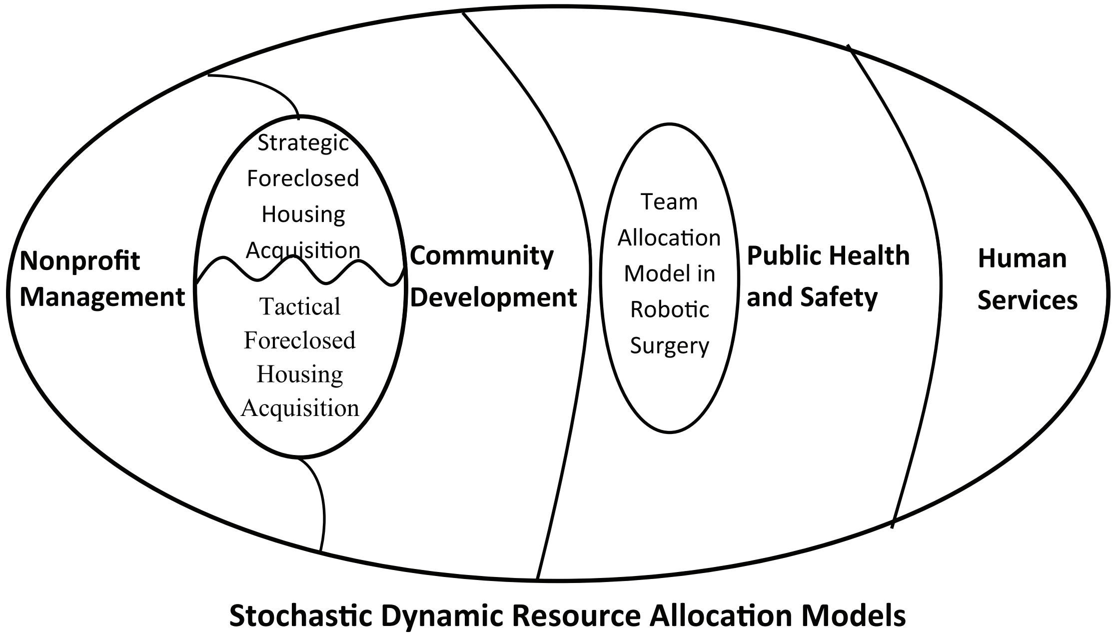

Figure 1.2. Conceptual map showing the relationship between the applications studied in this thesis.

In the foreclosed housing acquisition problem, a number of social objectives are considered. For the strategic planning model, these include measures such as collective efficacy, equity based on budget allocation rate, social utility and equity based on owner occupation of properties, while the tactical planning model uses only a social utility measure. Note that the strategic and tactical models for the foreclosed housing acquisition problem are connected and sequential. A CDC would first perform strategic planning involving budget allocations to different neighborhoods, and then given the budget allocations, tactical acquisition decisions for individual properties are made. These two decision problems are both addressed through stochastic dynamic optimization models, which is the general methodological structure combining all the applications in the thesis.

In our second application, the objective involves the maximization of performance in robotic surgical operations. Performance in this setting is defined by operating room time which is a proxy for health and safety based social value. More specifically, reduced operating room time through better utilization of team members implies fewer complications and faster recovery periods, which directly relate to benefits realized for patients or the society in general. The resulting problem is modeled and solved through a stochastic programming approach, which again represents the stochastic dynamic structure in the applications studied in this thesis.

To better display the cohesive framework for the two motivating applications in this thesis, in Figure 1.2 we show a conceptual map that we envision for stochastic dynamic societal resource allocation problems in general, which also displays where our three analyses fall within this framework. We assume that stochastic dynamic resource allocation problems with social objectives can be categorized based on the types of application area defined for community based operations research. To this end, Johnson and Smilowitz (2007) provide a taxonomy consisting of four major areas: nonprofit management, community development, public health and safety, and human services. Each of these application areas involves of a variety of resource allocation problems. Nonprofit management points out common problems in management of community-based or community-oriented service providers (Berenguer, 2013), while community development applications address economic growth and welfare improvement of segregated communities. Some subareas of community development can be listed as housing, community/urban planning, and transportation (Johnson and Smilowitz, 2007). One sample resource allocation study in this area includes Johnson et al. (2010), where the authors propose a deterministic and static multi-objective integer program for foreclosed housing acquisition and redevelopment by allocating available resources to different acquisitions. In public health and safety, general issues related to the public wellness and security are covered, such as healthcare, criminal justice, food insecurity, emergency studies, and dangerous/undesirable facility location. Aaby et al. (2006) and Bodily (1978) are two resource allocation related studies in the literature related to public health. In the first paper, Aaby et al. (2006) propose models for clinics to improve resource planning activities in their contagious disease management decisions, where the authors use discrete event simulations and queuing models as their methodologies. Bodily (1978) investigate a police sector planning problem where the workloads of the police officers are equalized by satisfying service equity and system efficiency. As another major area, humanitarian services typically include studies in public education, family supportive services, humanitarian logistics, and public libraries. Related to this field of study, Campbell et al. (2008) propose models to ensure both equity and efficiency during the allocation of the resources after a disaster. Another example involves the library vehicle fleet management problem studied by Francis et al. (2006), where the authors build models to improve vehicle routing operations and management by considering budget limitations of the library.

Our first application in the thesis can be placed in the intersection of nonprofit management and community development, because the foreclosed housing acquisition activities of a CDC can be classified as being related to both nonprofit management and housing/urban planning. On the other hand, we classify our second application under the public health and safety application area, as it involves a social value based implementation based on practice at a private hospital. Overall, as depicted through Figure 1.2, the three studies presented in this paper fall under the umbrella of the larger class of stochastic dynamic societal resource allocation problems, which constitute relatively small but relevant components - especially as the first such models in the corresponding application areas.

CHAPTER 2
LITERATURE REVIEW

In this section, we discuss the relevant literature separately for the two main motivating applications in our analysis. To this end, we first present a summary of the relevant literature on the foreclosed housing acquisition problem, and then discuss related studies in surgical team allocation. The discussions also include references to dynamic stochastic resource allocation problems in general. In addition, we also discuss in this chapter how this thesis contributes to the corresponding areas of research.

2.1 Related Research on Foreclosed Housing Acquisition

The foreclosed housing acquisition problem faced by CDCs is a stochastic resource allocation problem where a limited budget is allocated to maximize expected social returns. One stream of research on these problems involves dynamic resource allocation decisions on a set of *given* investment options, attributes of which evolve stochastically over time. Some examples to these studies include Mild and Salo (2009), where the authors develop a multi-criteria decision model for the allocation of resources to road maintenance activities, and Loch and Kavadias (2002), who develop a dynamic model for allocating resources to different new product development projects and identify analytical solutions by considering different types of return functions. Bertsimas and Popescu (2003) and Calafiore (2008) are other examples where dynamic policies are investigated for allocating scarce resources to stochastic demand through approximation based procedures.

In addition to these studies, Chalabi et al. (2008) propose a two-stage stochastic mathematical programming formulation to optimally allocate resources within and between healthcare programs when there is an exogenous budget and the parameters of the healthcare models are uncertain. Chalabi et al. (2008) limit their analysis to a small-scale two stage formulation without any algorithmic discussion or numerical analysis. In contrast to Solak et al. (2010), our first application addresses multiple objectives, including a measure of social utility, and uses novel return functions.

As a stochastic resource allocation model with a multi-objective structure, Medaglia et al. (2007) describe allocating limited resources to R&D projects by considering multi-criteria under uncertainty. Cheng et al. (2003) propose an investment strategy model for firms based on two-stage multi-objective optimization framework. The problem formulation leads to a multi-objective Markov decision problem representation, which is used to define Pareto optimal design strategies. Our first application extends the limited scope of Medaglia et al. (2007), which is static and uses a Monte Carlo simulation analysis, and extends that of Cheng et al. (2003) through the use of multi-stage stochastic programming.

Given the knapsack-type offer/no-offer decisions on properties that become available over time in the foreclosed housing acquisition decision process, a more relevant stream of research is the literature on dynamic stochastic knapsack problems. These problems have been formally defined by Kleywegt and Papastavrou (1998), where the authors study optimal acceptance policies for equal-sized items that arrive randomly over time with stochastic return structures. This framework is then extended by Kleywegt and Papastavrou (2001) to include items with random sizes. These two papers form the basis for some other studies in the literature, which involve models and solution approaches proposed for various applications with a dynamic stochastic knapsack structure. One such application is Kilic et al. (2010), where the authors study a model for raw material allocation in food production and propose a heuristic algorithm to derive an optimal policy. Similarly, Dizdar et al. (2011) derive simple policies under some limiting assumptions for revenue-maximization based general resource allocation problems. In another general analysis, Lu (2005) proposes a computational procedure to calculate the optimal policy for infinite horizon dynamic stochastic knapsack problems. In addition, Lin et al. (2008) apply stochastic knapsack type models in revenue management and dynamic pricing, while Nikolaev and Jacobson (2010) study resource allocation to a random number of jobs and present optimal policies for the sequential stochastic assignment problem. All these studies involve variations of the dynamic stochastic knapsack problem with different characteristics or algorithmic implementations in various applications. Our second application adds to this stream of research by considering a distinct application in the nonprofit sector, and extends this general framework by considering additional decisions, such as the selection of an overbid rate when making offers to selected foreclosed properties.

For housing policy based literature, we note that while foreclosures have many negative impacts on neighborhoods Kingsley et al. (2009), data limitations generally result in analyses of property value impacts of foreclosures. Campbell et al. (2009) use regression analyses of house prices and extend their analysis to estimate the total lost value from properties proximate to a foreclosed unit. Harding et al. (2009) estimate different effects on sales of non-distressed properties also by using regression analysis and present findings related to specific features of neighborhoods, foreclosed units, or the surrounding market conditions. Harding et al. (2009), along with Schuetz et al. (2008), also assess the impact of multiple foreclosures in an area, where the authors conclude that the number of proximate foreclosures generally multiplies the effects on neighboring house prices. In contrast to these descriptive and exploratory studies, our prescriptive decision models are intended to mitigate these negative impacts.

There also exist some related works on CDCs and their involvement in housing markets through property acquisitions. Swanstrom et al. (2009) describe acquisition strategies that CDCs employ to acquire and redevelop foreclosed housing, and NeighborWorks (2009) describes the difference of these strategies from those used for traditional community development. Key challenges encountered by CDCs during implementation of foreclosure acquisition and redevelopment strategies are investigated by Bratt (2009). Based on the observations from those studies, Simon (2009) describes some suggestions for CDCs and policy makers to implement. We add to this qualitative literature through a quantitative rigorous approach aimed to help CDCs in their long term strategic decision processes.

A relevant stream of research for the traditional housing market that focuses on purchasing strategies also exists. Such an analysis is performed by Drew et al. (2001), where the authors use regression analysis to measure competitiveness and offer a purchasing strategy model in selecting which properties to bid for. In another related paper, Yao and Zhang (2005) develop optimal dynamic portfolio decisions on housing investments for individual investors over a lifetime. Different from us, they build a long term economic model using a dynamic programming structure, and present some numerical analysis. Unlike these papers, we explicitly consider stochasticity in a portfolio model involving both near and long term decisions, as well as multiple objectives, in our first application. Moreover, we specifically address both the budget allocation and foreclosed property acquisition decisions for CDCs with social objectives, which differs significantly from the decisions of an individual investor.

There are a few recent papers that directly address problems similar to those we study in this thesis. These involve Johnson et al. (2010), where the authors describe the formulation and solution of a deterministic and static multi-objective integer program for foreclosed housing acquisition and redevelopment, applied to multifamily foreclosed housing in a small city. Bayram et al. (2011a) and Bayram et al. (2011b) investigate optimal policies for resource allocation and foreclosed property acquisition under some restrictive assumptions such as dominancy, in which the social utility values of different property categories are assumed to follow a dominancy based relationship throughout the planning period. By building on the framework discussed in these papers, we model and analyze the dynamic stochastic decision process for nonprofit housing investments over multiple periods.

2.2 Related Research on Surgical Team Allocation

The surgical team allocation problem we study falls into the general category of performance based team allocation problems. We summarize some relevant descriptive and prescriptive models for team performance and discuss their applicability to the problem we study. There are many papers involving data based analyses of medical team performance, where the factors affecting team performance are determined through statistical analysis. Cassera et al. (2009) and Burtscher et al. (2011) show the importance of information sharing during a surgery, and suggests enhancing communication to improve the overall surgical team performance. In addition to these studies, Ortega et al. (2013) note that team learning through experience has a significant effect on nurse performances. Fransen et al. (2012) also highlight the importance of experience and team training, specifically focusing on obstetric surgeries. Different from these descriptive studies, in our study we provide a team performance function based on statistical analysis, and utilize this function to prescribe an optimal team composition structure.

Although there exist some studies that focus on optimal team composition to maximize expected utility, Zakarian and Kusiak (1999) note that multi-functional team selection/formation process is a complex problem for which comprehensive analytical approaches are difficult to obtain. Hence, studies in this area are mostly limited approaches. Some studies consider team formation by using the analytical hierarchy process (AHP), where they solve a linear programming model to find optimal team compositions. As an example, Chen and Lin (2004) develop an analytical hierarchy model to aid in establishing an efficient multifunctional team by selecting team members for each project according to their skills. Zakarian and Kusiak (1999) also develop a methodology which is based on the AHP approach and the quality function deployment method for determining optimal team formations. In another paper, Zhang and Zhang (2013) propose a multi-objective team formation optimization model for new product development projects by considering capabilities and interpersonal relationships of all members, and again address the problem through AHP. Distinct from such studies, in our application we develop a stochastic dynamic team optimization model and address the problem through stochastic programming methods.

For additional relevant research, Slomp and Suresh (2005) build a multi-objective goal programming model for the problem of assigning operators to teams that work in three daily-shift systems. They propose a two phase solution approach in which the shift systems, machines and the sizes of each shift team are identified first, and in the second phase the team members are assigned to the corresponding teams. Team formation models are also applicable to the sport teams. For example, Ahmed et al. (2012) define a constrained multi-objective optimization model in selection of players for a cricket team using a finite budget. The authors propose a multi-objective evolutionary metaheuristic to optimize the overall batting and bowling strength of a team with eleven players. Unlike these papers, we identify the optimal assignment of available surgery team members to each operation dynamically over time, in order to improve expected performance over all operations by considering the uncertainty in observed performances.

To the best of our knowledge, there is no literature that specifically addresses optimal team formation in healthcare applications, where the team assignments are made according to experiences and performances of team members. Team allocation is typically integrated into scheduling models, where the performance of all physicians and nurses are assumed to be the same. On the other hand, there are several studies on nurse and physician scheduling, where cost minimization is mainly considered. We summarize below some of these team scheduling and planning studies, and how our study complements these analyses.

As an example to assignment and staffing problems in healthcare, Stolletz and Brunner (2011) addresses a shift scheduling problem in which physicians are assigned to demand periods to minimize the paid out hours by integrating physician preferences and fairness aspects into the scheduling model. In another paper, Choi and Wilhelm (2013) develop a block scheduling policy by proposing a newsvendor-based model in order to minimize the sum of expected lateness and earliness costs in surgeries. In addition to these studies, Wright and Mahar (2012) and Dowsland (1998) develop scheduling models where the objective is to ensure that enough nurses are on duty at all times while taking account individual preferences and requests for days off to treat all employees fairly. Another relevant paper is a literature review on operating room planning and scheduling, where the authors evaluate and list the literature on multiple fields that are related to either the problem setting or the technical features (Cardoen et al., 2010). As an optimal team configuration study, Harper et al. (2009) propose a method to find optimal size and skill-mixes for nursing teams to match with patient needs through combining simulation and optimization tools. They consider the demand uncertainty and dynamically identify the size and mix of the teams based on changing patient needs over time. In addition, Bordoloi and Weatherby (1999) present a linear program to determine the optimum mix of different staff categories for a hospital medical unit, where cost is minimized subject to constraints of patient demand and minimum staffing policies. Different from these papers, in our application we assign team members based on their experiences in order to maximize the minimum performance over all teams, where surgery time is taken as the main performance measure.

CHAPTER 3

STRATEGIC SOCIETAL RESOURCE ALLOCATION IN FORECLOSED HOUSING ACQUISITION

Consider a CDC making strategic decisions in advance of a planning horizon for their property acquisition investments. These decisions may involve prioritization and resource allocation to individual geographically distinct service areas, which we refer to as 'neighborhoods'. It is assumed that the strategic resource allocation decisions will be made at the beginning of the planning horizon and certain information will become available over subsequent planning periods. Tactical acquisition decisions, i.e. those involving specific purchasing decisions for available properties, will be made based on this information as well as the probabilistic information on social and economic impacts of each acquisition. The resource in our problem refers to an available budget, while the planning periods are typically defined in years. Hence, such terms are used interchangeably throughout the study.

A more specific representation of this general decision process is depicted visually in Figure 3.1, which can be described as follows. The decision maker, i.e. the CDC, initially decides on a tentative budget allocation to each neighborhood. Subsequently, properties become available for acquisition, i.e. foreclosures occur over time, and their acquisition costs become known to the CDC. Once this information is available, individual acquisition decisions are made under uncertain return characteristics. The process can continue for multiple periods where resource reallocations can take place based on any new information that becomes available. Hence, depending on the planning horizon considered, this process can be represented through a two-stage or

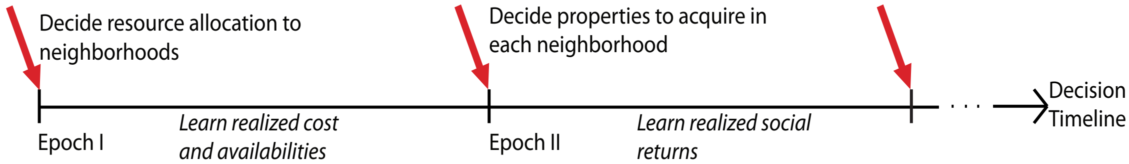

Figure 3.1. The general decision process for the strategic foreclosed housing acquisition problem.

multi-stage decision structure. The models we develop capture these different levels of complexity in the problem.

A key assumption in this strategic planning framework is that information on all foreclosed properties, particularly acquisition costs, in a particular planning period is available immediately after the resource allocation decision is made, and tactical acquisition decisions are made based on such information. In reality, however, real estate development is a dynamic process, and tactical acquisitions are performed over time as properties become available. Given the strategic planning nature of the problem and the relatively small gap in dynamic and static tactical decision making in this setting, we believe that this assumption does not detract significantly from the validity of the model.

The goal in the foreclosed housing acquisition problem (FHAP) is to decide on an initial strategic resource allocation plan such that an expected value function based on multiple potentially conflicting criteria is optimized. In other words, the problem is:

$$\max_{x\in\mathcal{X}} \mathbb{E}_{\Psi}\left[\max_{h\in\mathcal{H}(x)} [G(x,h,\Psi)]\right] \tag{3.1}$$

where $G(x,h,\Psi)$ is a function based on multiple objectives, with $x \in \mathcal{X}$ representing the resource allocation decisions that take on values in the feasible set $\mathcal{X}$, $h \in \mathcal{H}(x)$ modeling the tactical acquisitions to be made based on the allocations as defined by the set $\mathcal{H}(x)$, and Ψ being a vector of random parameters with known joint probability distributions. This vector of random parameters corresponds to costs, availabilities and returns of properties in the service area of a CDC. To allow for a tractable stochastic programming approach, we assume discrete distributions of these random parameters, and refer to each possible realization $\psi \in \Psi$ as a scenario with a corresponding probability p_{ψ}. Using this framework, we develop two stochastic programming approaches to the problem with different levels of complexity, which we describe in detail below. We note here that our models are based on interactions with CDCs and are thus informed by an inclusive, and cross-disciplinary view of community-based or community-oriented decision modeling.

3.1 Model I: FHAP with Simple Resource Allocation (FHAP-S)

First, we consider a basic strategic resource allocation framework that is typically applicable for annual planning. While an annual timeline may be short for most strategic planning problems, the CDC operations and specifically fund availabilities are strictly dependent on the condition of the economy and government policies. Hence, a very long strategic planning framework is not typical for these organizations. On the other hand, our general modeling framework is flexible enough to handle longer planning periods, and indeed the more advanced models in Section 3.2 are typically applicable to a multi-year planning structure. In FHAP with simple resource allocation, which we refer to as FHAP-S, we consider a planning horizon consisting of two decision periods where initially a budget allocation decision is made, followed by acquisition decisions determined according to realizations of foreclosed property availability, costs and expected returns.

We assume that a CDC can acquire units from a set of foreclosed properties $\mathcal{N}$. Each property is associated with a neighborhood $i \in \mathcal{I}$, based on its geographic location, and a category $l \in \mathcal{L}$, based on a pre-defined categorization scheme such that properties in each category have similar characteristics some of which are stochastic and dependent on external market environments. The CDC wants to determine the optimal amount of budget x_i to be allocated to neighborhood i given a limited available budget B, and potential future acquisition decisions h_{il}^{ψ}. The acquisition decisions h_{il}^{ψ} denote the number of properties of category $l \in \mathcal{L}$ acquired from neighborhood $i \in \mathcal{I}$ under scenario $\psi \in \Psi$.

3.1.1 Model Inputs

Model formulations for our decision framework involve several probabilistic and deterministic parameters. While we describe them in detail in this section, a summary list of these parameters is also provided in Appendix A. In the following paragraphs, we discuss these model inputs, and based on analysis of numerical data, we note for each parameter as to why that parameter is treated in a deterministic or stochastic manner.

3.1.1.1 Stochastic Parameters

The uncertainty in the modeling framework is represented through the attributes of the property categories $l \in \mathcal{L}$, which are defined by three stochastic parameters, corresponding to costs, returns and availabilities of foreclosed properties. More specifically, we let c_{ψ}^{il} denote the *acquisition and redevelopment cost* for a category l property in neighborhood i under scenario ψ. Note that for clarity in notation, the scenario index ψ in the stochastic parameters is denoted as a subscript, while a superscript is used for decision variables. When a foreclosed property is put on sale by the lender, it has an associated asking price, usually based on the price opinion of a broker with experience in the area. In addition to this purchasing cost, for each such property, CDCs perform an analysis to estimate the redevelopment costs for the property. The cost parameter c_{ψ}^{il} refers to the sum of these two cost components, and is defined by a probability distribution based on historical data. We demonstrate the observed variation in acquisition and redevelopment costs through a histogram of these costs for a specific category of properties in a given neighborhood within the service area of the CDC that we obtained operational data from. The histogram is included in Appendix A, where the distribution of these costs suggests a need for their consideration as a stochastic parameter. While the numerical analyses performed in Section 3.4 are based on data from 2011 where the economy was consistently in a poor state, dynamics based on the state of the economy and the markets are important in estimating the probability distribution of future acquisition and redevelopment costs. Clearly, an improving trend in the economy would imply a higher likelihood of higher costs, while a slowing economy would result in the opposite. The dynamic nature of residential property prices, which can be used as a proxy for the acquisition and redevelopment costs of foreclosed properties, is demonstrated in Appendix A through a plot of U.S. house prices over time. These dynamics can be captured in our modeling framework by defining scenario probabilities such that they reflect potential trending effects due to market factors.

The second stochastic parameter μ_{ψ}^{il} denotes the *social return* from the acquisition of a category l property in neighborhood i under scenario ψ. Foreclosures have significant effects on social and community life of the surrounding neighborhoods since they result in depreciation of a neighborhood's image and residents' quality of life (Immergluck and Smith, 2006). Therefore the acquisition and redevelopment of foreclosed properties yield in social value for the society, where estimating this social return is clearly difficult. Johnson et al. (2013) highlight this challenge, and develop a measure validated by some CDCs, which is based on the impact of the acquisition of a foreclosed property on the appreciation of the value of nearby properties. More formally, the property value impact (PVI) measure is defined as the expected impact on proximate property values from a given foreclosure. This measure is directly related to the geographical location of a property, and can be calculated for each foreclosed property through a procedure described by Johnson et al. (2013), where the authors calculate an approximation to the expected total property value losses associated with a property by using Markov chains and cost-benefit analysis. PVIs are the results of several determinants which are associated with foreclosures, i.e. increased blight, crime and social disorder (Harding et al., 2009). While any social return measure can be used when implementing the decision models, we utilize the PVI values to represent the social returns from the acquisition of a foreclosed property in our empirical analysis. PVI values are calculated as a dollar amount by Johnson et al. (2013), however in the strategic foreclosed acquisition problem analyzed in Chapter 3 we consider normalized values that vary between 0 and 1. This normalization is achieved dividing all PVI values by the maximum observed PVI in the data set directly obtained from Johnson et al. (2013). Note that the PVI measure is assumed to be a random variable, where a histogram based on a sample set of calculated PVI values is depicted in Figure A.2 in Appendix A. The PVI values in the figures are distributed uniformly between 0.85 and 1.0. Similar to the acquisition and redevelopment costs, the probability distribution of PVI values is defined based on historical data. A statistical analysis of costs and PVI values has shown almost no correlation between the two within the same category of properties, hence the stochastic process for social returns is assumed to be independent of the costs in the numerical study discussed later in the study. In Appendix A we show how PVI values vary for a set of properties considered for potential acquisition by the partner CDC, as well as how the PVI values and the acquisition and redevelopment costs lack correlation based on the same data set. We note that, although there does not exist any data for a quantitative analysis, the PVI measure is likely to be negatively correlated with the state of the economy and the housing market. If the economy is good, depreciation of property values due to presence of a foreclosed property in a neighborhood will typically be limited. Thus, the impact of the acquisition and redevelopment of a foreclosed property in a neighborhood in a good economic state is not likely to be as high either. While such dynamic effects due to market factors may not be as significant, they can again be captured through scenario probabilities used within our stochastic programming framework.

As the final stochastic parameter, we let θ_{ψ}^{il} refer to the *total required budget to acquire all properties of category l available for acquisition in neighborhood i under scenario ψ*. The stochasticity in this parameter is due to the inherent uncertainty in the housing market and the overall economy. Note that the definition of θ_{ψ}^{il} implicitly represents the number of foreclosed properties of category l available for acquisition in neighborhood i, as the cost of each property in a given category is assumed to have the same probability distribution. Hence, a high realization of this parameter would correspond to a high rate of foreclosures occurring for the corresponding category of properties in a given neighborhood. The stochastic structure in this parameter definition is also based on data analysis involving the transitions of properties in different pre-foreclosure stages to foreclosed status over a given period. These transition probabilities, derived from historical property data, are described in detail in Johnson et al. (2013). Given the current pre-foreclosure stage information for the properties and using the transition probability structures, a probability distribution defining the number of properties in a neighborhood that will be in foreclosed status in the next period can be derived. Such a probability distribution for a sample category and neighborhood is included in Appendix A.

We note here that there exists a correlation between the stochastic parameters c_{ψ}^{il} and θ_{ψ}^{il}, which correspond to the acquisition and redevelopment costs and the total required budget to acquire all properties of category l in neighborhood i. When the housing market or the economy worsens, property values are expected to decrease, which should normally imply that the total required budget to acquire all foreclosed properties would also decrease. At the same time, however, there is a negative correlation between number of foreclosures and property prices as shown through an empirical analysis by McDonald and Stokes (2013). Thus, the reduced property prices due to a worsening economy would also imply an increase in the number of foreclosed properties. This could result in an increase in the total required budget to acquire all properties. Given this interplay between the costs and the number of foreclosures, the correlation between c_{ψ}^{il} and θ_{ψ}^{il} can be either negative or positive. We capture such correlation in our modeling framework by considering scenarios that reflect both types of correlation, and assigning appropriate probabilities to each scenario based on the likelihood of each type of correlation. The positive correlation case corresponds to the situations where the property prices are high and at the same time there is a high number of foreclosures, or vice versa, i.e. low costs and low number of foreclosures. Based on an analysis by Chen (2009), we assume that the total likelihood of these cases is 0.2. Hence, the negative correlation cases of low cost-high required budget and high cost-low required budget outcomes have a total probability of 0.8. The numerical analyses described in Section 3.4 have been implemented under these assumptions on the correlation between the two parameters.

3.1.1.2 Deterministic Parameters

In addition to the stochastic parameters described above, several deterministic inputs representing neighborhood and category properties are used as part of the modeling framework. One such parameter is ϕ_{il}, which corresponds to the expected *financial return* from the sale of an acquired category l property in neighborhood i. In other words, this is the expected revenue in excess of costs associated with the eventual sale of a foreclosed property that has been acquired and redeveloped to a defined community standard. We assume for modeling and tractability purposes that the financial returns ϕ_{il} from an acquired property are deterministic. This is mostly a reasonable assumption as financial returns from acquired properties are typically better estimated than social returns, especially considering the 1-2 year timeline used in the problem definition. In addition, these profit amounts are typically constant for each category of properties. More specifically, the profit amount is determined by adding a specific dollar amount on the total acquisition and redevelopment cost of a property before its sale, as opposed to a percentage. The specific planned profit amounts are determined by CDC management. Hence, financial returns in general are independent of the costs incurred for a property, and they only vary over different neighborhoods or categories of properties. To demonstrate the mostly constant structure of the financial returns, in Appendix A we provide a plot of the financial returns realized through a set of historical acquisitions by the CDC from which we obtained historical acquisition data. In addition, given that a CDC typically uses a fixed financial return objective, and does not use different markup rates under different economic and market conditions, it can be assumed that such dynamics do not play a significant role in this model parameter.

Another important measure assumed to be deterministic in the model is the *collective efficacy* measure for a given neighborhood i, which is denoted as e_i. The collective efficacy e_i is defined by Sampson et al. (1997) as the social cohesion among neighbors combined with their willingness to intervene on behalf of the common good. This measure is a hard-to-quantify social value and is typically based on expert opinions. Thus, we include it in the model as a strategic value measure through which we attempt to capture the benefits from a property's location that relate to the CDC's mission and objectives for property redevelopment. Morenoff and Smapson (2001) state that violent activities involving crime is directly related to the collective efficacy of a neighborhood. More specifically, the authors note that criminal activities can be ecologically concentrated because of the absence of guardianship defined by the collective efficacy level of a neighborhood. The authors show a negative correlation between crime rate and collective efficacy where collective efficacy is expected to be higher for the neighborhoods having lower crime rates. Based on this analysis, we quantify the collective efficacy of a neighborhood using neighborhood-level crime data. Given that crime statistics for a neighborhood are fixed and known, we naturally assume this measure to be a deterministic parameter. We further standardized crime rate information in each neighborhood to vary between 0 and 1 by dividing each crime rate value by the maximum over all neighborhoods. Note that it is implicitly assumed that $e_i > 0$, as no neighborhood is likely to have a crime rate equal to zero. While there exists some correlation between the state of the economy and this model parameter, it is possible to assume that the impacts are likely going to be similar in proximate neighborhoods, resulting in minor fluctuations in the relative values for different neighborhoods. This is especially the case because the decision epochs do not cover an extensive length of time, and any impacts on crime rates due to economic dynamics or investment decisions are likely to take a longer time.

In order to model the fact that not all acquired properties might be redeveloped and sold within the planning horizon, we introduce the parameter r_{il} denoting the *probability that a category l property in neighborhood i will be sold within a given time frame.* While it is assumed that all acquired properties will be redeveloped and sold over time, it may be that the CDC will consider a shorter planning horizon for some return related parameters, during which not all properties might be sold. Such dynamics play a more significant role in the more complex models we study later in the study. This probability is estimated based on historical sales data, and for FHAP-S it will be used to reflect the projected impact of acquisitions on home ownership in a neighborhood, as redeveloped properties are typically sold to owner occupants only. Given that the period length used to determine this probability, and thus the probability r_{il}, can vary based on the return type, we append the notation for r_{il} with a superscript corresponding to the return type. To this end, we let r^o_{il} denote the probability used for owner occupancy modeling purposes, and also define

o_i and n_i as the *current number of owner occupied and total number of properties in a given neighborhood* i, respectively. Similarly, we define r_{il}^{ϕ} as the probability of sales used for financial return calculations. The values for r_{il}^{o} and r_{il}^{ϕ} are obtained through past property sales ratios, and are fixed and known by definition. These values can vary based on the state of the economy and the housing market, but this is likely to take a longer amount of time than the planning horizons considered in the models.

Finally, d_{ij} is used to denote the *distance between two neighborhoods* i and j, which will be utilized as part of an objective involving the allocation of the budget in a way that would take advantage of synergistic effects of investing in proximate neighborhoods. We note here that the distance between neighborhoods is an ambiguous notion, which in this study is approximated as the straight-line distance between centroids of two neighborhoods. Thus, by definition it is a deterministic parameter. In addition, by synergistic effects we mean a social value arising between certain number of properties that produce a value greater than the sum of their individual PVI values, which we discuss further as part of objective descriptions in Section 3.1.2.

3.1.2 Model Definition

In addition to the budget allocation decisions x_i and the tactical acquisition decisions h_{il}^{ψ} which were defined above, a set of additional decision variables are also utilized in the model formulation. To this end, we first define z_i^{ψ} as the unused budget allocated to neighborhood i in scenario ψ. This variable will be used as part of an objective to maximize expected budget utilization, noting that having any unused funds would imply that the resources are not being utilized.

All other variables used in the formulation are auxiliary variables that help define different objectives and constraints. Of these, y_{ij} relates the investments in neighborhoods i and j with respect to the distance between the neighborhoods. R^{ψ} and S^{ψ}, on the other hand, define the minimum expected home ownership rate and minimum

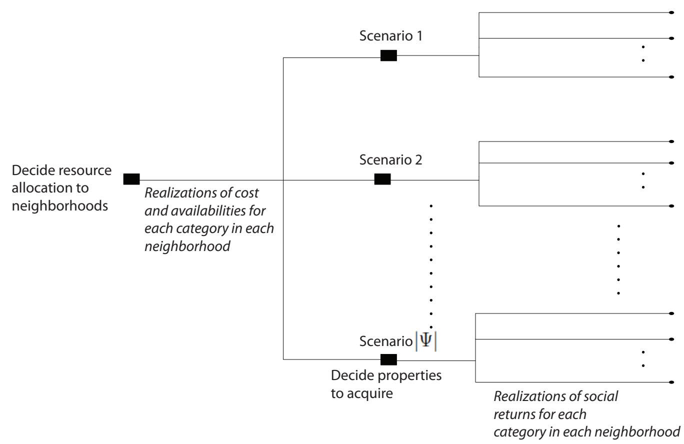

Figure 3.2. Scenario tree illustrating the decisions and stochastic parameter realizations in FHAP-S.

allocation rate over all neighborhoods for scenario ψ. The allocation rate in the definition of S^{ψ} refers to the ratio of the budget allocated to a given neighborhood over the observed value of available housing units for acquisition in that neighborhood.

Using the notation described above, we model FHAP-S as a two stage stochastic mixed-integer programming problem. In this recourse model, the first-stage decisions involve x_i, i.e. the allocation of budgets to each neighborhood, and the auxiliary variables y_{ij}. Once the components of the random vector Ψ corresponding to costs and availability of properties are realized, the tactical acquisition decisions are made as defined by the second stage variables h_{il}^{ψ} and z_i^{ψ}. While it is assumed that the returns μ_{ψ}^{il} from the acquired properties will be realized further into the future, no decisions are assumed to be made after the return realizations. Hence, we incorporate the stochasticity in the returns by considering the expected returns for each scenario. The corresponding scenario tree for FHAP-S is illustrated in Figure 3.2, where the dark rectangles represent the decision nodes. This assumption is relaxed in the more comprehensive models described in the later sections. We first summarize the notation used in FHAP-S below, and then describe the objectives and constraints in detail.

3.1.2.1 Notation Used in FHAP-S

Variables Used in FHAP-S

h_{il}^{ψ} : Integer variable denoting the umber of properties of category l acquired from neighborhood i under scenario ψ

R^{ψ}: Auxiliary variable defining the minimum home ownership rate among all neighborhoods for scenario ψ

S^{ψ}: Auxiliary variable defining the minimum allocation rate among all neighborhoods for scenario ψ

x_i : Amount of budget allocated to each neighborhood i

y_{ij} : Auxiliary variable relating the investments in neighborhoods i and j with respect to the distance between the neighborhoods

z_i^{ψ} : Unused allocated budget for neighborhood i in scenario ψ

Parameters Used in FHAP-S

B : Available budget over the planning horizon

c_{ψ}^{il} : Acquisition cost for a category i property in neighborhood l under scenario ψ

d_{ij} : Distance between neighborhoods i and j

e_i : Collective efficacy measure for a given neighborhood i

n_i : Current number of properties for a given neighborhood i

o_i : Current number of owner occupied properties for a given neighborhood i

p_{ψ} : Probability of scenario ψ

r_{il}^{o} : Probability that a category l property in neighborhood i will be sold within the time frame used for measuring owner occupancy

μ_{ψ}^{il} : Social return from the acquisition of a category l property in neighborhood i under scenario ψ

λ_k: Weight importance for objective k

θ_ψ^{il} : Total required budget to acquire all properties of category l available for acquisition in neighborhood i under scenario ψ

ϕ_{il} : The financial return from the acquisition of a category l property in neighborhood i

$\overline{u}_k$: An upper bound value for objective k.

u_k : An auxiliary value for objective k.

3.1.2.2 Model Formulation

Based on this framework, the multi-objective two-stage stochastic mixed-integer programming formulation for FHAP-S is as follows:

$$\mathbf{F}(\mathbf{x},\mathbf{y},\mathbf{\Psi}) = \max \quad \lambda_1 \sum_{i=1}^{|\mathcal{I}|} \frac{x_i}{e_i} + \lambda_2 \sum_{i=1}^{|\mathcal{I}|} \sum_{j=1}^{|\mathcal{I}|} y_{ij} + \mathbb{E}_{\mathbf{\Psi}}[Q(\boldsymbol{x},\boldsymbol{y},\Psi)] \tag{3.2}$$

$$\text{s.t.} \quad \sum_{i=1}^{|\mathcal{I}|} x_i \leq B \tag{3.3}$$

$$y_{ij} = \frac{x_i}{d_{ij}} \qquad \forall i,j \tag{3.4}$$

$$x_i, y_{ij} \geq 0 \qquad \forall i,j,l,\psi \tag{3.5}$$

where $\mathbf{F}(\mathbf{x},\mathbf{y},\mathbf{\Psi})$ is a weighted sum of all objectives and $Q(\boldsymbol{x},\boldsymbol{y},\Psi)$ is the optimal objective value of the second stage decision problem for any given realization ψ of the random vector Ψ. $Q(\boldsymbol{x},\boldsymbol{y},\psi)$ is defined as:

$$Q(\boldsymbol{x},\boldsymbol{y},\Psi) = \max \lambda_3 S^\psi + \lambda_4 \sum_{i=1}^{|\mathcal{I}|} \sum_{l=1}^{|\mathcal{L}|} \phi_{il} h_{il}^\psi + \lambda_5 \sum_{i=1}^{|\mathcal{I}|} \sum_{l=1}^{|\mathcal{L}|} \qquad \mu_\psi^{il} h_{il}^\psi + \lambda_6 R^\psi + \lambda_7 \left(1 - \frac{\sum_{i=1}^{|\mathcal{I}|} z_i^\psi}{\sum_{i=1}^{|\mathcal{I}|} \sum_{l=1}^{|\mathcal{L}|} \theta_\psi^{il}}\right) \tag{3.6}$$

$$\frac{x_i}{\sum_{l=1}^{|\mathcal{L}|} \theta_\psi^{il}} \geq S^\psi \qquad \forall i,\psi \tag{3.7}$$

$$\frac{o_i + \sum_{l=1}^{|\mathcal{L}|} r_{il}^o h_{il}^{\psi}}{n_i} \geq R^{\psi} \qquad \forall i, \psi \quad (3.8)$$

$$x_i - \sum_{l=1}^{|\mathcal{L}|} c_{\psi}^{il} h_{il}^{\psi} = z_i^{\psi} \qquad \forall i, \psi \quad (3.9)$$

$$c_{\psi}^{il} h_{il}^{\psi} \leq \theta_{\psi}^{il} \qquad \forall i, l, \psi \quad (3.10)$$

$$x_i, y_{ij}, z_i^{\psi}, S^{\psi}, R^{\psi} \geq 0 \qquad \forall i, j, l, \psi \quad (3.11)$$

$$h_{il}^{\psi} \in \mathbf{Z}^+ \qquad \forall i, l, \psi \quad (3.12)$$

where λ_k is the weighting factor coefficient for objective $k = 1, \ldots, 7$, where $\sum_{k=1}^{7} \lambda_k = 1$ and $\lambda_k \geq 0$. Although there are many algorithms in the literature to determine weight values, no fundamental guidelines have been presented for selecting weights. Eckenrode (1965), Hobbs (1980), Voogd (1983) can be given as examples to the proposed approaches in weight determination. In our application, we determine weights accordingly based on discussions with CDC staff. Since they are indifferent between objectives and do not have any priorities, we use equal λ_k values for the objectives in our implementations.

Note that our objective function is a weighted combination of several objectives. To derive this function, we first normalize each objective value function separately by performing the following steps:

1. Set the corresponding weighting factor for the given objective k to 1 while setting other weighting factors to 0.

2. Solve the model and let the value of the overall objective function be $\overline{u}_k$, where $\overline{u}_k$ represents an upper bound for objective k.

3. Use the current values of all weighting factors (e.g. in our implementations all λ_k's are assumed to be equal), and solve the model. Let the corresponding value for objective k be u_k.

4. Normalize each objective value as $\frac{u_k}{\overline{u}_k}$.

Through these steps we ensure that each objective value is between 0 and 1. In order to combine separate objectives, we multiply each objective by its weight and sum them up. Since $\sum_{k=1}^{7} \lambda_k = 1$ and $\lambda_k \geq 0$, the overall objective function will be between 0 and 1 as well. Note that our solution methods for FHAP-S, as well as its variants and extensions, are applied to a single-objective version of this model using a weighted representation of the objectives with weights where the weights are determined by the CDC. On the other hand, other multi-objective frameworks can be considered for the optimization as well. We further note that, we obtained the value of our weighted objective function by using mathematical programming tools instead of generating a seven dimensional noninferior set of alternatives. However, in Section 3.4.4, we perform Pareto analysis for grouped sets of objectives where we grouped our objectives into two groups and investigate the noninferior set of alternatives between new two objectives.

3.1.2.3 Objectives and Constraints

As noted above, our optimization model includes seven types of objectives, which reflect different goals involving maximization of overall socio-economic utility and equity through the decisions made. These objectives were developed based on consultations with CDCs which involved formal value focused thinking sessions with CDC staff. Modeling of the objectives requires introduction of various constraints, which we also describe below.

The first and second objectives shown in (3.2) constitute the first stage objective function, which implies that they are only a function of the first stage variables, i.e. the resource allocation decisions. Objective 1 is an equity related objective defined according to neighborhood-level collective efficacy measures introduced in Section 3.1.1. This objective, similar to those of Leclerc and McLay (2012), maximizes total collective efficacy of a budget allocation strategy over all neighborhoods by allocating higher budgets to neighborhoods with relatively lower efficacy values. This is ensured by the ratio $\frac{x_i}{e_i}$ in the objective definition. Given the efficacy measures e_i for each neighborhood, the ratio will be maximized if larger x_i values are assigned to neighborhoods with lower e_i levels.

Objective 2 is related to the economies of scale and aims to maximize efficiencies associated with proximity of acquired units. The objective is modeled through the variable y_{ij} and the constraint (3.4) and standardized by following steps described in Section 3.1.2.2. The structure of the objective involves the minimization of a function of the total distance between neighborhoods to which resources are allocated. Notice that we use the distance between neighborhoods, as opposed to actual properties, because property availability is an uncertain parameter and thus specific location information is not known within the modeling framework. So the intended objective is assumed to be achieved by considering that higher allocations to a neighborhood would result in a higher number of properties to be acquired with closer proximity. This is done by the maximization of the y_{ij} values, for which larger x_i and x_j values need to be assigned for neighborhoods i and j that are geographically closer, i.e. where d_{ij} is small. The utility of having more acquisitions in proximate neighborhoods is mainly due to ease of managing redevelopment activities in nearby regions. If the acquired properties are closer to each other, then it also becomes more convenient to locate municipal services. In the absence of an explicit function representing such economies of scale, the model tries to allocate the budget proportionally to the distances between neighborhoods through this function, where the distances between neighborhoods are based on the centroids of the neighborhoods. Related to this structure, Galster et al. (2006) show that concentrated long-term investments in small areas produce beneficial results when compared with areas without such focused investments.

The remaining five objectives correspond to the second stage objective function as shown in (3.6), as their values depend on the realization of the uncertain parameters. Objective 3 another equity related objective and involves the maximization of the minimum allocation rate, i.e. the ratio of the budget allocated to a given neighborhood and realized value of available housing units for acquisition to provide equitable service to different neighborhoods. Hence, this objective aids to allocate resources equally to neighborhoods. This is modeled through constraint (3.7), the structure of which implies that S^{ψ} will be maximized if the ratio on the left hand side is as high and close as possible for all neighborhoods. This objective is a ratio and varies between 0 and 1 but similar to the other objectives it is also standardized by using steps in Section 3.1.2.2.

Objective 4 considers the financial returns from the resource allocation strategy by maximizing the total expected profit based on the financial return structures for each category of housing. This is a relevant objective for CDC operations, despite the fact that CDCs are nonprofit organizations. This is because any financial profits made in the current planning period will enable more acquisitions in the future. The profit amounts are defined based on the product of expected per unit profit and the number of properties acquired as shown in the formulation. Although the unit of this objective is in dollars, after standardization, it varies between 0 and 1.

Objective 5 ensures the social utility maximization of a foreclosed housing acquisition strategy, where social utility is based on the social return measure μ_{ψ}^{il} defined for each category of housing in each neighborhood. As noted previously, we adapt a social return measure based on the impact of the acquisitions on the values of nearby properties (PVI). Similar to the financial returns, PVI based social returns in FHAP-S are defined by the product of realized per unit PVI and the number of properties acquired in each category in a neighborhood. The objective value is standardized and changes between 0 and 1.

Objective 6 represents an equity related goal based on owner occupation rates in neighborhoods. Maximization of owner occupied housing units in each neighborhood is one of the missions of CDCs (Galster et al., 2005), and this objective tries to achieve it in an equitable way by maximizing the minimum owner occupation rate among neighborhoods. The objective structure is modeled through constraint (3.8), where expected increase in the number of owner occupied properties in a neighborhood is defined in the numerator on the left hand side of the constraint. The increase is based on the probability r_{il}^{o} that a property in a specific category will be sold to an owner occupant within a predefined period, where the length of this period is dependent on a CDC's overall goals with regard to owner occupancy. Maximizing R^{ψ} would imply a more evenly distributed owner occupancy rates among neighborhoods after the acquisitions. This objective also varies between 0 and 1 after standardization by following steps in Section 3.1.2.2.

Finally, Objective 7 ensures that the available budget is utilized in the most efficient manner across different scenarios. To this end, constraint (3.9) defines the variable z_i^{ψ}, which corresponds to any unused portion of the allocated budget to a neighborhood. Hence, the expression $\frac{\sum_{i=1}^{|\mathcal{I}|} z_i^{\psi}}{\sum_{i=1}^{|\mathcal{I}|}\sum_{l=1}^{|\mathcal{L}|} \theta_{\psi}^{il}}$ in (3.6) is the ratio of unused budget to the total value of available properties for a given scenario. This ratio is used to ensure that the consideration of the unused budget amounts for different scenarios is consistent, as the availabilities differ for each scenario.

In addition to the constraints described above, the optimization model involves constraints (3.3), (3.10), (3.11) and (3.12). In constraint (3.3), we ensure that amount of allocated resources are less than the total budget available, while constraint (3.10) ensures that total amount of acquired properties does not exceed the total amount of available properties. We further define nonnegativity and integrality through constraints (3.11) and (3.12), respectively.

This model reflects fundamental policy-analytic concerns with tradeoffs between efficiency, effectiveness and equity (Bardach, 2005), as well as an understanding of policy and practice in foreclosure mitigation activity derived from observations of specific CDCs. In addition, observing that the expectation in (3.2) can be represented through the scenario probabilities p_ψ, the overall model can be expressed in the following compact form:

$$\max \Big\{ \lambda_1 \sum_{i=1}^{|\mathcal{I}|} \frac{x_i}{e_i} + \lambda_2 \sum_{i=1}^{|\mathcal{I}|} \sum_{j=1}^{|\mathcal{I}|} y_{ij} + \sum_{\psi \in \Psi} p_\psi \big[\lambda_3 S^\psi + \lambda_4 \sum_{i=1}^{|\mathcal{I}|} \sum_{l=1}^{|\mathcal{L}|} \phi_{il} h_{il}^\psi + \lambda_5 \sum_{i=1}^{|\mathcal{I}|} \sum_{l=1}^{|\mathcal{L}|} \mu_\psi^{il} h_{il}^\psi + \lambda_6 R^\psi + \lambda_7 (1 - \frac{\sum_{i=1}^{|\mathcal{I}|} z_i^\psi}{\sum_{i=1}^{|\mathcal{I}|} \sum_{l=1}^{|\mathcal{L}|} \theta_\psi^{il}}) \big] \quad \text{s.t.} \quad (3.3), (3.4), (3.7) - (3.12) \Big\} \tag{3.13}$$

Note that by setting $\lambda_{k'} = 1$ and $\lambda_k = 0$ for all $k \neq k'$, we may analyze the corner points of the Pareto frontier associated with a solution to FHAP-S. In addition to such an implementation, we also generate estimates of the Pareto frontier associated with aggregations of various FHAP-S objectives through an application of the constraint method (Collette and Siarry, 2003) later in the study.

3.2 Model II: FHAP with Gradual Uncertainty Resolution (FHAP-G)

The second model we consider for FHAP has a more complex representation of the resource allocation decision process. While this representation is more realistic as it considers potential reallocation of budget depending on gradual realization of information on the economy and its impacts on neighborhoods, the resulting model is a more complex multi-stage stochastic mixed-integer programming problem.

The multi-stage decision process that involves gradual resolution of uncertainty is depicted in Figure 3.4. We assume a longer strategic planning timeline consisting of two budgeting periods, e.g. two years, with a pooled budget to be allocated over the two periods. Such a strategic decision timeline has been observed to be used by CDCs (Frisch and Servon, 2006). Given the longer planning horizon of two years, a CDC can perform better planning by taking into account the learning effects that will take place over time. More specifically, the state of the economy and market conditions two years into the future will be better estimated in the next year based on realized conditions in the first year. Hence, a model that captures such dynamics is likely to be more valuable when deciding on optimal budget allocations. At the beginning of the planning horizon, i.e. in the first decision epoch, initial resource allocation decisions for each neighborhood are made separately for each of the next two years. Foreclosed properties then become available for potential acquisition along with the associated costs, and acquisition decisions are made in the second decision epoch based on the social return distribution information available at that time. It is assumed that additional new information on returns will be revealed after the second decision epoch based on the state of the economy, which will be followed by a potential reallocation of second year resource allocations, as well as new allocations of any unused budgets and realized returns from any sales in the first year. These represent the decisions in the third decision epoch, while in the fourth epoch acquisitions for the second budgeting period will be performed after new availability and cost information becomes known. We note here that the realizations of the cost parameters in the second period are dependent on the social return, i.e. PVI realizations in the first period. More specifically, a high PVI value in the first period would imply a higher appreciation of house prices which is then reflected in the acquisition costs of foreclosed properties in the same area in the second period. Hence, scenarios for the stochastic programming formulation are defined based on this dependent structure.

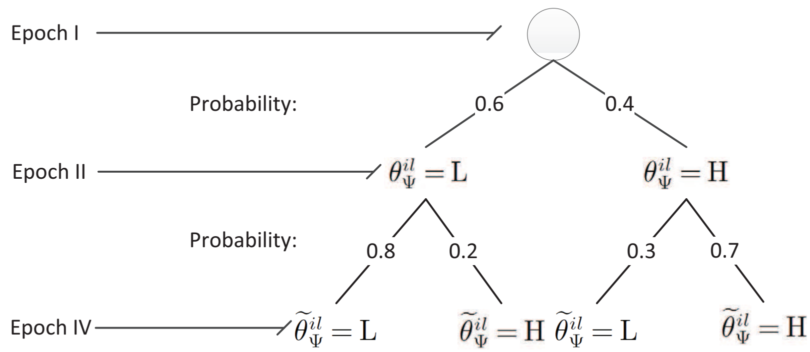

Figure 3.3. Demonstration of gradual resolution of uncertainty for the random availability parameter θ_{Ψ}^{il}.

We further describe gradual uncertainty realization through Figure 3.3, which shows an example where the availability information θ_{Ψ}^{il} is learned over time. In this example the availability is assumed to be either at low or high levels, indicated by L and H, respectively. At Epoch I, the probability of a low realization is 0.6, while the probability is 0.4 for a high availability level. Information becomes available over time, and preliminary availability information is known at Epoch II. If this information is $\theta_{\Psi}^{il} = \mathrm{L}$, then the probability distribution for low and high availabilities in the second period, which is to be realized at Epoch IV, is updated to be 0.8 and 0.2, respectively. On the other hand, if $\theta_{\Psi}^{il} = \mathrm{H}$ at Epoch II, then the corresponding probabilities are 0.3 and 0.7 for low and high availabilities as shown in the figure. This representation suggests four combinations of realizations for the random availability parameter θ_{Ψ}^{il}, namely LL, LH, HL, HH, which form part of the scenario definitions involving all uncertain parameters.

Based on the description above, we expand the notation used in Section 3.1 by referring to the first stage allocation variables as $x_{i\rho}$ where $\rho \in \{1, 2\}$ refers to the planning period. Note that x_{i2} represents the tentative allocations for period two made at the first decision epoch. This tentative allocation can be changed in the third decision epoch, as represented through variables $x_i^{+\psi}$ and $x_i^{-\psi}$ which correspond to

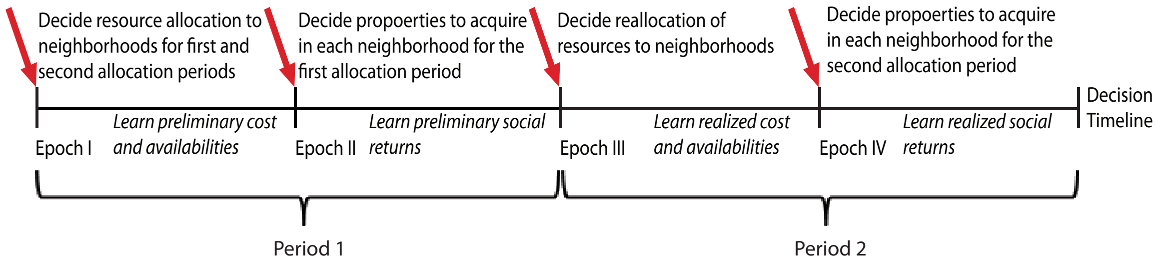

Figure 3.4. The decision process for the strategic foreclosed housing acquisition problem with gradual resolution of uncertainty in social returns.

the positive and negative reallocation decisions for scenario $\psi \in \Psi$. The definitions of all other decision variables are also extended through the subscript $\rho \in \{1, 2\}$. The realized values of the stochastic parameters after the reallocation period are denoted as follows: $\widetilde{\mu}^{il}_{\psi}$, $\widetilde{\theta}^{il}_{\psi}$, $\widetilde{c}^{il}_{\psi}$. Finally, a penalty parameter ν_i is introduced for the costs associated with budget reallocation to/from a given neighborhood i. This reallocation cost corresponds to variable overhead and other expenses due to changes in the initial allocated budgets to neighborhoods. We include the minimization of the expected value of this cost as a new objective and associate it with the weighting parameter λ_8. The notation used in FHAP-G and the formulation of the model are as follows:

Variables Used in FHAP-G

$h^{\rho\psi}_{il}$: Number of properties of category l acquired from neighborhood i at period ρ under scenario ψ

$R^{2\psi}$: Auxiliary variable defining the minimum home ownership rate among all neighborhoods at second period for scenario ψ

$S^{2\psi}$: Auxiliary variable defining the minimum allocation rate among all neighborhoods at second period for scenario ψ

$x^{\rho\psi}_{i}$: Amount of allocated budget to each neighborhood i at period ρ

in scenario ψ

$x_i^{+\psi}$: Amount of positive reallocation budget of neighborhood i in scenario ψ

$x_i^{-\psi}$: Amount of negative reallocation budget of neighborhood i in scenario ψ

$y_{ij}^{\rho\psi}$: Auxiliary variable relating the investments in neighborhoods i and j at period ρ in scenario ψ with respect to the distance between the neighborhoods

$z_i^{\rho\psi}$: Unused allocated budget for neighborhood i at period ρ in scenario ψ

Parameters Used in FHAP-G

$\widetilde{c}_{\psi}^{il}$: Acquisition cost for a category l property in neighborhood i at second period under scenario ψ

r_{il}^{ϕ} : Probability that a category l property in neighborhood i will be sold within the second period under time frame used for measuring financial returns

$\widetilde{\mu}_{\psi}^{il}$: Social return from the acquisition of a category l property in neighborhood i at second period under scenario ψ

$\widetilde{\theta}_{\psi}^{il}$: Total required budget to acquire all properties of category l available for acquisition in neighborhood i at second period under scenario ψ

α_η : Parameter defining the vertex point η in the piecewise linear approximations

Θ : Upper bound on the amount of allocation to any neighborhood

τ_1, τ_2 : Threshold values used in the definition of the investment dependent return function

$$\Upsilon_{\rho}^{\psi\psi'} : \begin{cases} 1, \text{ if } \psi \text{ and } \psi' \text{ have the same history at a given decision epoch} \\ \quad \text{in period } \rho \\ 0, \text{ otherwise} \end{cases}$$

This objective function for the resulting multi-stage stochastic mixed-integer programming formulation for FHAP-G can be expressed in nested expectation form as follows, where the notation Ψ_t denotes the vector of random parameters that realize after each epoch t as described in Figure 3.4. $\mathbf{G}(\mathbf{x}, \mathbf{y}, \mathbf{S}, \mathbf{h}, \mathbf{R}, \mathbf{z}, \mathbf{\Psi})$ is defined as a scalar value which is the weighted sum of all objectives:

$$\mathbf{G}(\mathbf{x}, \mathbf{y}, \mathbf{S}, \mathbf{h}, \mathbf{R}, \mathbf{z}, \mathbf{\Psi}) = \max \lambda_1 \sum_{i=1}^{|\mathcal{I}|} \frac{x_{i1}}{e_i} + \lambda_2 \sum_{i=1}^{|\mathcal{I}|} \sum_{j=1}^{|\mathcal{I}|} y_{ij1} \tag{3.14}$$

$$+ \mathbb{E}_{\mathbf{\Psi_2}} \Big[\lambda_3 S_1^{\Psi_2} + \lambda_4 \sum_{i=1}^{|\mathcal{I}|} \sum_{l=1}^{|\mathcal{L}|} \phi_{il} h_{il1}^{\Psi_2} + \lambda_5 \sum_{i=1}^{|\mathcal{I}|} \sum_{l=1}^{|\mathcal{L}|} \mu_{\Psi_2}^{il} h_{il1}^{\Psi_2} + \lambda_6 R_1^{\Psi_2}$$

$$+ \lambda_7 (1 - \frac{\sum_{i=1}^{|\mathcal{I}|} z_{i1}^{\Psi_2}}{\sum_{i=1}^{|\mathcal{I}|} \sum_{l=1}^{|\mathcal{L}|} \theta_{\Psi_2}^{il}}) \tag{3.15}$$

$$+ \mathbb{E}_{\mathbf{\Psi_3} | \mathbf{\Psi_2}} \Big[\lambda_1 \sum_{i=1}^{|\mathcal{I}|} \frac{x_{i2} + x_i^{+\Psi_3} - x_i^{-\Psi_3}}{e_i} + \lambda_2 \sum_{i=1}^{|\mathcal{I}|} \sum_{j=1}^{|\mathcal{I}|} y_{ij2}^{\Psi_3} - \lambda_8 \sum_{i=1}^{|\mathcal{I}|} \nu_i (x_i^{+\Psi_3} + x_i^{-\Psi_3}) \tag{3.16}$$

$$+ \mathbb{E}_{\mathbf{\Psi_4} | \mathbf{\Psi_3}, \mathbf{\Psi_2}} \Big[\lambda_3 S_2^{\Psi_4} + \lambda_4 \sum_{i=1}^{|\mathcal{I}|} \sum_{l=1}^{|\mathcal{L}|} \phi_{il} h_{il2}^{\Psi_4} + \lambda_5 \sum_{i=1}^{|\mathcal{I}|} \sum_{l=1}^{|\mathcal{L}|} \widetilde{\mu}_{\Psi_4}^{il} h_{il2}^{\Psi_4} + \lambda_6 R_2^{\Psi_4}$$

$$+ \lambda_7 [(1 - \frac{\sum_{i=1}^{|\mathcal{I}|} z_{i2}^{\Psi_4}}{\sum_{i=1}^{|\mathcal{I}|} \sum_{l=1}^{|\mathcal{L}|} \widetilde{\theta}_{\Psi_4}^{il}})] \Big] \Big] \Big] \tag{3.17}$$

The components of the objective shown in (3.14) and (3.15) are respectively the objective functions for the first and second stages, and are defined similar to the FHAP-S formulation described in Section 3.1.2. The nested expectation in (3.16) corresponds to the third stage objective function, which consists of a similar setup as (3.14) plus Objective 8. The third stage objective function is calculated assuming the realization of preliminary costs, availabilities, and social returns in the first and second stages. The structure of Objective 1 in (3.16) involves the reallocation decisions as part of the numerator defining the final resource allocation amount to each neighborhood for the second period. The fourth stage objective is shown through the expectation in

(3.17) which is defined over the uncertainty in social returns given the information on realized costs and availabilities in the third stage.

Defining a scenario ψ with probability p_ψ for each possible combination of realizations of the random parameters over the entire planning horizon, where conditional realizations are also taken into account, the overall formulation for FHAP-G can be stated by combining the components of the objective function that are multiplied by the same weighting factor λ_k, $k = 1, \ldots, 8$:

$$\begin{aligned}
\mathbf{G}(\mathbf{x}, \mathbf{y}, \mathbf{S}, \mathbf{h}, \mathbf{R}, \mathbf{z}, \mathbf{\Psi}) = \max \lambda_1 \sum_{i=1}^{|\mathcal{I}|} \frac{x_{i1}}{e_i} + \lambda_2 \sum_{i=1}^{|\mathcal{I}|} \sum_{j=1}^{|\mathcal{I}|} y_{ij1} \\
+ \sum_{\psi \in \Psi} p_\psi \Big[\lambda_1 \sum_{i=1}^{|\mathcal{I}|} \frac{x_{i2} + x_i^{+\psi} - x_i^{-\psi}}{e_i} + \lambda_2 \sum_{i=1}^{|\mathcal{I}|} \sum_{j=1}^{|\mathcal{I}|} y_{ij2}^{\psi} + \lambda_3 (S_1^\psi + S_2^\psi) \\
+ \lambda_4 \sum_{i=1}^{|\mathcal{I}|} \sum_{l=1}^{|\mathcal{L}|} \phi_{il} (h_{il1}^\psi + h_{il2}^\psi) + \lambda_5 \sum_{i=1}^{|\mathcal{I}|} \sum_{l=1}^{|\mathcal{L}|} (\mu_\psi^{il} h_{il1}^\psi + \widetilde{\mu}_\psi^{il} h_{il2}^\psi) + \lambda_6 (R_1^\psi + R_2^\psi) \\
+ \lambda_7 \big[(1 - \frac{\sum_{i=1}^{|\mathcal{I}|} z_{i1}^\psi}{\sum_{i=1}^{|\mathcal{I}|} \sum_{l=1}^{|\mathcal{L}|} \theta_\psi^{il}}) + (1 - \frac{\sum_{i=1}^{|\mathcal{I}|} z_{i2}^\psi}{\sum_{i=1}^{|\mathcal{I}|} \sum_{l=1}^{|\mathcal{L}|} \widetilde{\theta}_\psi^{il}}) \big] - \lambda_8 \sum_{i=1}^{|\mathcal{I}|} \nu_i (x_i^{+\psi} + x_i^{-\psi}) \Big] \quad (3.18)
\end{aligned}$$

$$\text{s.t} \quad (3.4), (3.7) - (3.12)$$

$$\sum_{i=1}^{|\mathcal{I}|} \sum_{\rho=1}^{2} x_{i\rho} \leq B \quad (3.19)$$

$$y_{ij2}^\psi = \frac{x_{i2} + x_i^{+\psi} - x_i^{-\psi}}{d_{ij}} \qquad \forall i, j, \psi \quad (3.20)$$

$$\frac{x_{i2} + x_i^{+\psi} - x_i^{-\psi}}{\sum_{l=1}^{|\mathcal{L}|} \widetilde{\theta}_\psi^{il}} \geq S_2^\psi \qquad \forall i, \psi \quad (3.21)$$

$$\frac{o_i + \sum_{l=1}^{|\mathcal{L}|} r_{il}^o h_{il1}^\psi - \sum_{l=1}^{|\mathcal{L}|} \widetilde{\theta}_\psi^{il} + \sum_{l=1}^{|\mathcal{L}|} r_{il}^o h_{il2}^\psi}{n_i} \geq R_2^\psi \qquad \forall i, \psi \quad (3.22)$$

$$x_{i2} + x_i^{+\psi} - x_i^{-\psi} - \sum_{l=1}^{|\mathcal{L}|} \widetilde{c}_\psi^{il} h_{il2}^\psi = z_{i2}^\psi \qquad \forall i, \psi \quad (3.23)$$

$$\widetilde{c}_\psi^{il} h_{il2}^\psi \leq \widetilde{\theta}_\psi^{il} \qquad \forall i, l, \psi \quad (3.24)$$

$$\sum_{i=1}^{|\mathcal{I}|} x_i^{+\psi} - \sum_{i=1}^{|\mathcal{I}|} x_i^{-\psi} = \sum_{i=1}^{|\mathcal{I}|} \sum_{l=1}^{|\mathcal{L}|} r_{il}^{\phi} \phi_{il} h_{il1}^{\psi} + \sum_{i=1}^{|\mathcal{I}|} z_{i1}^{\psi} \qquad \forall \psi \quad (3.25)$$

$$\chi_{\rho}^{\psi} = \chi_{\rho}^{\psi'} \;\; \forall \rho, \psi, \psi' : \Upsilon_{\psi\psi'}^{\rho} = 1 \qquad (3.26)$$

$$x_{i\rho}, x_i^{+\psi}, x_i^{-\psi}, y_{ij\rho}^{\psi}, z_{i\rho}^{\psi}, S_{\rho}^{\psi}, R_{\rho}^{\psi} \geq 0 \qquad \forall i, j, l, \psi, \rho \quad (3.27)$$

$$h_{il\rho}^{\psi} \in \mathbf{Z}^{+} \qquad \forall i, l, \psi, \rho \quad (3.28)$$

We note that, similar to the FHAP-S model, $\sum_{k=1}^{8} \lambda_k = 1$ and $\lambda_k \geq 0$. In our calculations, we use equal weighting factors to evaluate the objective function and the same steps described in Section 3.1.2.2 are used to normalize the objective function. The constraints in the above formulation have a similar structure as FHAP-S except that they are defined both for the first and second planning periods, where the first period involves decision epochs I and II, and the second period involves decision epochs III and IV. The constraints also reflect the relationships between the two planning periods. More specifically, constraint (3.19) is the revised budget constraint which ensures that the sum of resource allocations to neighborhoods do not exceed the initially available budget B. Constraint (3.20) defines the variables y in relation to Objective 2 in the second period, where the numerator $x_{i2} + x_i^{+\psi} - x_i^{-\psi}$ represents the final second period allocation to neighborhood i at decision epoch III. Through the same allocation representation, constraint (3.21) is used to define Objective 3 for the second period, which involves maximization of the minimum allocation rate over neighborhoods. Note that constraint (3.21) involves an approximation where previous allocation decisions are only implicitly considered and not endogenously modeled in the denominator of the left hand side of the constraint. This is because second stage property availability should also take into account any remaining properties from the first period, i.e. the denominator in (3.21) should be $\sum_{l=1}^{|\mathcal{L}|} (\theta_{\psi}^{il} + \widetilde{\theta}_{\psi}^{il}) - x_{i1}$. However, this gives rise to a nonlinear and nonconvex structure, which we approximate by assuming that the second period availability will be exogenously determined, taking into account any potential remaining properties. In Section 3.3 we remove this assumption and reformulate the original model through a piecewise linear approximation approach.

The objective related to home ownership for the second period is modeled by constraint (3.22), which involves an endogenous structure as it captures the impact of previous period sales and new foreclosures in defining the owner occupancy rate. This is done by updating the number of owner occupied units in the numerator through the addition of number of sold properties as defined by the probability r^o_{il}, and the subtraction of the number of new foreclosures. Similar to its first period counterpart, constraint (3.23) represents the amount of unused budget in period two. More specifically, the amount of unused budget in neighborhood i is the difference between the final second period allocation of $x_{i2} + x_i^{+\psi} - x_i^{-\psi}$ and the total number of acquisitions $\sum_{l=1}^{|\mathcal{L}|} \widetilde{c}^{il}_{\psi} h^{\psi}_{il2}$. The inequality (3.24) is the availability constraint for the second period, modeling the fact that the number of acquisitions is limited by the available number of foreclosed properties. As a new constraint, (3.25) ensures that reallocations in the second period are feasible given the tentative allocations. The right hand side of this constraint represents the newly available funds for the second period, which corresponds to the sum of any unused budget in the first period and the financial returns from any property sales that might have occurred before the budget reallocation time, while the variables on the left hand side correspond to the reallocation decisions.

Constraints (3.26) are the nonanticipativity constraints for this multi-stage problem, which impose the condition that scenarios that share the same history at a decision epoch also make the same decisions during that history. Note that nonanticipativity is implied for the first decision epoch as the same variable definitions are used for all scenarios. Moreover, the fourth stage decisions are independent for each scenario, so no nonanticipativity requirements exist at that stage. Hence, explicit nonanticipativity representation is required for the second and third decision epochs only. Since these two epochs correspond to the first and second periods respectively, we utilize the period index in defining these constraints. More specifically, we introduce the indicator parameter $\Upsilon_\rho^{\psi\psi'}$, where $\Upsilon_\rho^{\psi\psi'} = 1$ if ψ and ψ' have the same history at the second and third decision epochs, which respectively correspond to $\rho \in \{1, 2\}$. Defining the sets χ_ρ as $\chi_1 = \{h_{il1}^{\psi}, z_{i1}^{\psi}, S_1^{\psi}, R_1^{\psi}\}$ and $\chi_2 = \{x_i^{+\psi}, x_i^{-\psi}, y_{ij2}^{\psi}\}$, we are able to represent the nonanticipativity in the formulation through constraints (3.26). We also define nonnegativity and integrality conditions thorough constraints (3.27) and (3.28).

3.3 Model Variations and Extensions

In this section we present two extensions to the core FHAP models presented. These variations of the model are used to capture some additional complexities that may exist in different practical settings.

3.3.1 Investment Dependent Social Return Functions

In this section we consider a different and more complex return structure for the two FHAP models by including synergistic effects that can be realized based on the number of acquisitions or the amount of investment in a given neighborhood. Such synergistic effects, specifically in social returns, have been discussed in the literature and also have been typically observed in practice (Bhide, 1993; Damodaran, 2005). Moreover, Harding et al. (2009) show that the contagion effect is a nonincreasing convex function of the number of foreclosures. This result implies that social returns can be considered as nondecreasing concave functions of the acquired foreclosed units. Hence, we expand our models to include this aspect by modeling the effect of acquisition decisions on social return characterizations. However, due to the introduction of new constraints and binary variables, the complexity of the resulting problem is increased.

To model this investment dependent return structure, we assume that the social returns μ_{ψ}^{il} in the first period and $\widetilde{\mu}_{\psi}^{il}$ in the second period are defined as piecewise step functions of the ratio of investment for each category and neighborhood over available acquisitions, which we refer to as the 'acquisition ratio', similar to the function type shown in Figure 3.5. The corresponding return structure has the following pattern: as the acquisition ratio in a property category and neighborhood increases, the return also increases up to a threshold level τ_1 and then remains constant in the range (τ_1, τ_2). If the acquisition ratio exceeds τ_2, then a synergistic joint return value $\overline{\mu}_{\psi}^{il}$ is realized for each scenario. We note here that while the structure of these return functions has been justified through practical discussions in the literature, there is no empirical evidence as to what the typical values for τ_1 and τ_2 should be for PVI based return functions. These parameters need to be subjectively defined by CDC practitioners, similar to what was done for our numerical implementations. On the other hand, we have also performed a sensitivity analysis around these parameter values as described in Section 3.4.3.

We also note that our modeling framework is quite general and can be adapted to different input characterizations. While in Figure 3.5 we show a piecewise linear structure, it is possible to define the returns using nonlinear functions as long as convexity of the optimization model is maintained and the model is solved as a stochastic nonlinear integer programming problem. Hence, in our representation of the investment dependent return functions we use generic notation and refer to the piecewise components of the return functions as $f_{\psi}^{\rho}(h_{il\rho}^{\psi})$ and $g_{\psi}^{\rho}(h_{il\rho}^{\psi})$, as indicated in Figure 3.5 for $\rho = 1$. The uncertainty in the social returns is modeled through the parameters of these functions. Based on the linearity assumption and for the empirical analysis in the study, we consider a probabilistic structure for the slope of

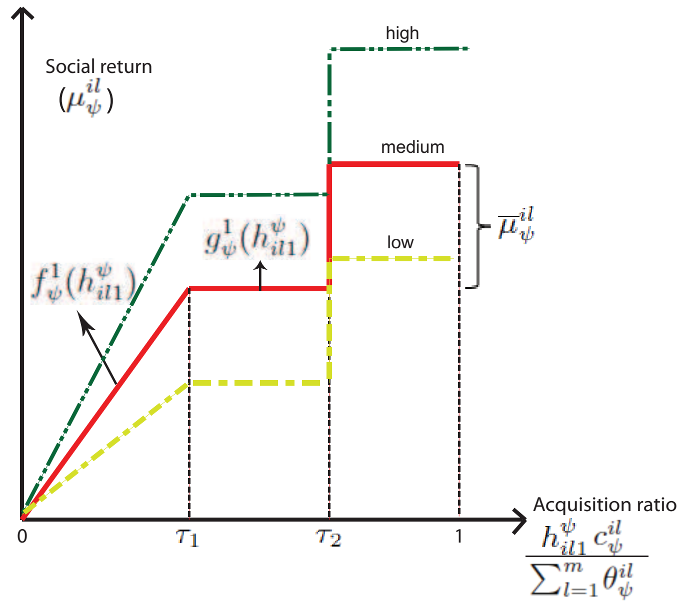

Figure 3.5. Investment dependent social return function modeling the synergistic effects of property acquisitions in a given neighborhood.

the function $f_{\psi}^{\rho}(h_{il\rho}^{\psi})$. Hence, different return realizations would imply different slopes for this function. This is demonstrated in Figure 3.5 for low, medium and high social return realizations for first period social returns μ_{ψ}^{il}. This uncertainty representation can be generalized by considering more uncertain parameters in the function definitions, such as the parameters of $g_{\psi}^{\rho}(h_{il}^{\psi})$ and the joint return value $\overline{\mu}_{\psi}^{il}$. Hence, these functions are also denoted using the scenario subscript ψ. In addition, we define the binary variables $\beta_{il\rho}^{\psi}$, which equal 1 if the joint return is realized, i.e. if the acquisition ratio exceeds τ_2, and 0 otherwise. Also while μ_{ψ}^{il} and $\widetilde{\mu}_{\psi}^{il}$ are defined as parameters in FHAP-S and FHAP-G, they become decision variables when investment dependent return is modeled. Note that second period returns are modeled through their expectations, so the parameters of the functions $f_{\psi}^{2}(h_{il2}^{\psi})$ and $g_{\psi}^{2}(h_{il2}^{\psi})$ in the second period are constant as they are based on these expectations.

Using this notation, it is possible to incorporate the investment dependent return structure into the two models as follows. For a more general representation, we show the modifications required for FHAP-G and describe how they would differ for

FHAP-S. The first modification involves the changes in the social return objective corresponding to the weighting parameter λ_5. We first summarize the added notation as follows:

Variables Added for FHAP-S and FHAP-G Extensions

ω_1^{ψ} : Approximated value of the square of S_2^{ψ}

ω_{2i} : Approximated value of the square of x_{i1}

ω_{3i}^{ψ} : Approximated value of the square of the summation of S_2^{ψ} and x_{i1}

$\gamma_{\eta}^{S\psi}$: SOS2 variable for approximation of the square of S_2^{ψ} defined at point η under scenario ψ

$\gamma_{i\eta}^{X}$: SOS2 variable for approximation of the square of X_i^1 defined at point η under scenario ψ

$\gamma_{i\eta}^{SX\psi}$: SOS2 variable for approximation of the square of the summation of S_2^{ψ} and x_{i1} for neighborhood i defined at point η under scenario ψ

$$\beta_{il\rho}^{\psi} : \begin{cases} 1, & \text{if the total category } l \text{ property acquisitions in neighborhood } i \\ & \text{exceed the threshold for joint return realization under scenario } \psi \\ & \text{in period } \rho \\ 0, & \text{otherwise} \end{cases}$$

To capture the investment dependent return structure, this function needs to be expressed in FHAP-G as:

$$\mathbf{G}(\mathbf{x},\mathbf{y},\mathbf{S},\mathbf{h},\mathbf{R},\mathbf{z},\widetilde{\boldsymbol{\mu}},\overline{\boldsymbol{\mu}},\boldsymbol{\beta},\boldsymbol{\Psi}) = \max \cdots + \lambda_5 \sum_{i=1}^{|\mathcal{I}|}\sum_{l=1}^{|\mathcal{L}|}(\mu_{\psi}^{il} + \overline{\mu}_{\psi}^{il}\beta_{il1}^{\psi} + \widetilde{\mu}_{\psi}^{il} + \overline{\mu}_{\psi}^{il}\beta_{il2}^{\psi}) + \dots \tag{3.29}$$

where the dots indicate that the remainder of the objective is exactly as shown in (3.18). Moreover, the following additional constraints need to be defined for the model, where the variables β_{il1}^{ψ} and μ_{ψ}^{il} are included into the group χ_1, while β_{il2}^{ψ} and $\widetilde{\mu}_{\psi}^{il}$ are included into the group χ_2:

$$\beta^{\psi}_{il1} - \frac{h^{\psi}_{il1} c^{il}_{\psi}}{\sum_{l=1}^{|\mathcal{L}|} \theta^{il}_{\psi}} \leq 1 - \tau_2 \qquad \beta^{\psi}_{il2} - \frac{h^{\psi}_{il2} \widetilde{c}^{il}_{\psi}}{\sum_{l=1}^{|\mathcal{L}|} \widetilde{\theta}^{il}_{\psi}} \leq 1 - \tau_2 \qquad \forall i, l, \psi \tag{3.30}$$

$$\beta^{\psi}_{il1} - \frac{h^{\psi}_{il1} c^{il}_{\psi}}{\sum_{l=1}^{|\mathcal{L}|} \theta^{il}_{\psi}} \geq -\tau_2 \qquad \beta^{\psi}_{il2} - \frac{h^{\psi}_{il2} \widetilde{c}^{il}_{\psi}}{\sum_{l=1}^{|\mathcal{L}|} \widetilde{\theta}^{il}_{\psi}} \geq -\tau_2 \qquad \forall i, l, \psi \tag{3.31}$$

$$\mu^{il}_{\psi} \leq f^1_{\psi}(h^{\psi}_{il1}) \qquad \widetilde{\mu}^{il}_{\psi} \leq f^2_{\psi}(h^{\psi}_{il2}) \qquad \forall i, l, \psi \tag{3.32}$$

$$\mu^{il}_{\psi} \leq g^1_{\psi}(h^{\psi}_{il1}) \qquad \widetilde{\mu}^{il}_{\psi} \leq g^2_{\psi}(h^{\psi}_{il2}) \qquad \forall i, l, \psi \tag{3.33}$$

$$\chi^{\psi}_{\rho} = \chi^{\psi'}_{\rho} \qquad \forall \rho, \psi, \psi' : \Upsilon^{\rho}_{\psi\psi'} = 1 \tag{3.34}$$

$$\mu^{il}_{\psi}, \widetilde{\mu^{il}_{\psi}} \geq 0 \qquad \forall i, l, \psi \tag{3.35}$$

$$\beta^{\psi}_{il\rho} \in \{0, 1\} \qquad \forall i, l, \psi, \rho \tag{3.36}$$

Constraints (3.30)-(3.31) ensure the realization of the joint return for the two periods if the acquisition ratio is greater than the threshold level τ_2. The piecewise structure of the return is modeled through constraints (3.32)-(3.33) due to the maximization objective involving the social returns. Constraint (3.34) represents the nonanticipativity constraints for the newly introduced variables as discussed above. Through constraints (3.35) and (3.36) we define nonnegativity and integrality conditions for the new decision variables.

For adaptation of the above modifications into FHAP-S, the term $\widetilde{\mu}^{il}_{\psi} + \overline{\mu}^{il}_{\psi}\beta^{\psi}_{il2}$ is removed from the objective function (3.29). In addition, constraints (3.30), (3.31), (3.32), and (3.33) are added to the formulation as shown, except the subscript of the acquisition variable is removed, to be denoted as h^{ψ}_{il}.

3.3.2 Reformulation of Allocation Rate Constraint

The second extension we introduce applies to FHAP-G only, and deals with the reformulation of constraint (3.21) which corresponds to one of the equity objectives in the model. Although this new extension adds to the complexity of the formulation, it is a more accurate representation of the equity objective as described in Section 3.2.

As noted previously, when remaining property information from the first planning period is included in the denominator on the left hand side of constraint (3.21), i.e. if the denominator is $\sum_{l=1}^{|\mathcal{L}|}(\theta_{\psi}^{il} + \widetilde{\theta}_{\psi}^{il}) - x_{i1}$, the resulting constraint is nonlinear and nonconvex. We deal with this issue by convexifying the model through a piecewise linear approximation of the nonlinear terms as follows. The nonlinear constraint can be rewritten as $x_{i2} + x_i^{+\psi} - x_i^{-\psi} \geq \sum_{l=1}^{|\mathcal{L}|} S_2^{\psi}(\theta_{\psi}^{il} + \widetilde{\theta}_{\psi}^{il}) - S_2^{\psi} x_{i1}$, where the second component on the right hand side involves the product of two decision variables. Through some algebraic manipulation, this bilinear term can be expressed as $S_2^{\psi} x_{i1} = -\frac{(S_2^{\psi})^2}{2} - \frac{(x_{i1})^2}{2} + \frac{(S_2^{\psi}+x_{i1})^2}{2}$ to involve three terms with squared values of decision variables. We utilize piecewise linear approximation methods on these three terms using a set of parameters corresponding to the vertices of the piecewise linear curves.

More specifically, we define new nonnegative variables $\gamma_{i\eta}^{X}$, $\gamma_{\eta}^{S\psi}$ and $\gamma_{i\eta}^{SX\psi}$ for each i, ψ, and $\eta = 0, 1, ...N$, where N is the number of vertices used to represent the nonlinear functions. Note that N can vary for each of the functions approximated. Moreover, the lower and upper bounds for x_{i1} are 0 and $\Theta = \min\{B, \max_{\psi} \sum_{l=1}^{|\mathcal{L}|} \theta_{\psi}^{il}\}$, while they are 0 and 1 for S_2^{ψ}. Hence, it is possible to define the vertices of the piecewise linear curves for the three functions using these bounds and ratio parameters $\alpha_{\eta} = \{0, \frac{1}{N}, \frac{2}{N}, \ldots, 1\}$ for $\eta = 0, 1, ...N$. A complexity in the piecewise linear representation involves the requirement that at most two adjacent values of $\gamma_{\cdot\eta}^{\cdot}$ are nonzero in each representation to ensure global optimality. We do this by defining the variables $\gamma_{i\eta}^{X}$, $\gamma_{\eta}^{S\psi}$ and $\gamma_{i\eta}^{SX\psi}$ as being members of specially ordered sets of type two (SOS2).

Given this structure, constraint (3.21) in FHAP-G can be replaced by the following set of constraints to more accurately model the allocation rate based equity structure:

$$x_{i2} + x_i^{+\psi} - x_i^{-\psi} \geq \sum_{l=1}^{|\mathcal{L}|} S_2^{\psi}(\theta_{\psi}^{il} + \widetilde{\theta}_{\psi}^{il}) + \frac{\omega_1^{\psi}}{2} + \frac{\omega_{2i}}{2} - \frac{\omega_{3i}^{\psi}}{2} \qquad \forall i, \psi \qquad (3.37)$$

$$S_2^{\psi} = \sum_{\eta=0}^{N} \gamma_{\eta}^{S\psi} \alpha_{\eta} \qquad \forall \psi \quad (3.38)$$

$$x_{i1} = \Theta \sum_{\eta=0}^{N} \gamma_{i\eta}^{X} \alpha_{\eta} \qquad \forall i \quad (3.39)$$

$$\omega_1^{\psi} = \sum_{\eta=0}^{N} (\alpha_{\eta})^2 \gamma_{\eta}^{S\psi} \qquad \forall \psi \quad (3.40)$$

$$\omega_{2i} = \Theta^2 \sum_{\eta=0}^{N} (\alpha_{\eta})^2 \gamma_{i\eta}^{X} \qquad \forall i \quad (3.41)$$

$$\omega_{3i}^{\psi} = \sum_{l=1}^{|\mathcal{L}|} (\Theta + 1)^2 \sum_{\eta=0}^{N} (\alpha_{\eta})^2 \gamma_{i\eta}^{SX\psi} \qquad \forall i, \psi \quad (3.42)$$

$$\sum_{\eta=0}^{N} \gamma_{\eta}^{S\psi} = 1 \qquad \forall \psi \quad (3.43)$$

$$\sum_{\eta=0}^{N} \gamma_{i\eta}^{X} = 1 \qquad \forall i \quad (3.44)$$

$$\sum_{\eta=0}^{N} \gamma_{i\eta}^{SX\psi} = 1 \qquad \forall i, \psi \quad (3.45)$$

$$\gamma_{\eta}^{S\psi}, \gamma_{i\eta}^{X}, \gamma_{i\eta}^{SX\psi} \in \text{SOS2} \qquad \forall i, \psi, \eta \quad (3.46)$$

Constraint (3.37) is the modified version of constraint (3.21) after linear approximation. Constraints (3.38) and (3.39) define the variables S_2^{ψ} and x_{i1}, and approximate the squares of S_2^{ψ} and x_{i1} as represented by ω_1^{ψ} and ω_{2i}. The square of the summation of S_2^{ψ} and x_{i1}, which is defined by ω_{3i}^{ψ}, is represented by constraint (3.42). Constraints (3.43), (3.44) and (3.45) imply that the summation of these piecewise approximation variables should be equal to 1. As the last constraint, (3.46) ensures the SOS2 requirement for the newly introduced approximation variables.

3.3.3 Heuristic Simplifications

While different versions of FHAP can potentially be solved using direct solutions of the deterministic equivalents for small number of scenarios, this becomes intractable for slight increases in the number of scenarios, especially for the enhanced formulations described in Sections 3.3.1 and 3.3.2. To this end, we introduce two heuristic approaches that simplify the solution process for the FHAP models, with the aim of establishing practical and efficient solution structures for CDCs that they can use more easily during potential implementations. We discuss the computational implications of these simplifications in the numerical analyses performed in Section 3.4.

In the first heuristic approach (Heuristic-1), we assume that given a budget allocation to a neighborhood, the property acquisitions from each category will be proportionally based on the availability in that category. In other words, acquisition levels are likely to be high for categories with high availability levels. This is reasonable from a practical perspective since CDCs would typically desire to acquire more housing units from categories and neighborhoods with high foreclosure rates.

The heuristic involves the solution of the corresponding FHAP models with these fixed relationships among the variable values. On the other hand, due to the integrality of the acquisition variables h_{il}^{ψ}, it is not possible to fix the acquisition variable values directly as a function of resource allocations x_i. Hence, we represent these conditions through inequality constraints, rather than using equalities, which is further described below. For presentation purposes, we describe the steps of the heuristic approaches by referring to FHAP-S and then state how they would differ for FHAP-G:

Step 1. Add the following constraints to fix the number of acquired units as a function of resource allocations:

$$h_{il}^{\psi} \leq \frac{\frac{\theta_{\psi}^{il}}{\sum_{l=1}^{|\mathcal{L}|} \theta_{\psi}^{il}} x_i}{c_{\psi}^{il}} \qquad h_{il}^{\psi} \geq \frac{\frac{\theta_{\psi}^{il}}{\sum_{l=1}^{|\mathcal{L}|} \theta_{\psi}^{il}} x_i}{c_{\psi}^{il}} - 1 \qquad \forall i, l, \psi \qquad (3.47)$$

Step 2. Solve the model to obtain resource allocation values x_i^H for each neighborhood.

Step 3. Evaluate the heuristic solution by setting $x_i = x_i^H$ and solving the original model without constraints (3.47).

In Step 1, we fix the number of acquired units from each category in each neighborhood according to the availability rate of each category. Then in Step 2, the total budget is allocated by considering fixed acquisition amounts. As a last step, the model is reevaluated and the acquisition quantities are updated based on the budget allocated.

In the second heuristic simplification (Heuristic-2), we assume that property acquisitions in each scenario will be made proportionally among categories based on the ratios of expected social return over cost, which we refer to as 'marginal social return'. Hence, more acquisitions will be performed from categories with larger marginal social return values. This approach is intuitively and practically reasonable due to the non-profit nature of CDCs and the role of social returns in their decision making. Note that we implicitly assume the availability in each category will be such that the allocation scheme is feasible. The implementation of Heuristic-2 is very similar to the first heuristic, except that the constraints (3.47) to be added are replaced with the following set of constraints: In the second heuristic simplification (Heuristic-2), we assume that property acquisitions in each scenario will be made proportionally among categories based on the ratios of expected social return over cost, which we refer to as 'marginal social return'. Hence, more acquisitions will be performed from categories with larger marginal social return values. This approach is intuitively and practically reasonable due to the non-profit nature of CDCs and the role of social returns in their decision making. Note that we implicitly assume the availability in each category will be such that the allocation scheme is feasible. The implementation of Heuristic-2 is very similar to the first heuristic, except that the constraints (3.47) to be added are replaced with the following set of constraints:

$$h_{il}^{\psi} \leq \frac{\frac{\mu_{\psi}^{il}/c_{\psi}^{il}}{\sum_{l=1}^{|\mathcal{L}|}\mu_{\psi}^{il}/c_{\psi}^{il}} x_i}{c_{\psi}^{il}} \qquad h_{il}^{\psi} \geq \frac{\frac{\mu_{\psi}^{il}/c_{\psi}^{il}}{\sum_{l=1}^{|\mathcal{L}|}\mu_{\psi}^{il}/c_{\psi}^{il}} x_i}{c_{\psi}^{il}} - 1 \qquad \forall i, l, \psi \tag{3.48}$$

These heuristics imply simple and practical rules for CDCs in their budget allocation decisions. CDCs can easily determine the amount of budget to allocate to different neighborhoods in an approximate way by looking at the relative ratios of availability rates or returns.

As part of the adaptation of the above modifications into FHAP-G, first the same constraints are defined for period one. In addition, similar constraints are also included for period two by updating the notation of the acquisition and allocation variables, as well as the uncertain parameter realizations, with their corresponding second period counterparts.

3.4 Numerical Tests and Analyses Based on a Real-life Implementation

In this section, we implement our models in a real-life decision making situation based on data obtained from a CDC located in the city of Boston, Massachusetts. The data was collected through records kept by the CDC as well as through interviews with CDC staff. In addition, property value information used in the calculations were obtained from the authors of Johnson et al. (2013). This CDC has expressed an interest in decision aids to help them improve their capacity for longer-term strategy design related to foreclosure housing acquisition and redevelopment. In this study, we apply the models we have formulated to data provided by the CDC with the aim of generating strategies that could potentially help this and other CDCs in achieving their goals. Hence, our analysis involves both policy implications for the results obtained from the solutions of the models, as well as some computational issues related to the optimization models.

3.4.1 Description of Data

The CDC in consideration has two alternative decision frameworks for strategic resource allocation, which involve different geographical representations of their service area. More specifically, the two alternatives assume that the CDC's service area can be split into either two or four distinct geographical regions. In addition to the geographical split, these regions also reflect different levels of poverty in the corresponding neighborhoods. The CDC is interested in an equitable and effective strategy so that overall welfare in the service area is maximized. In order to achieve this objective, the organization will be acquiring and redeveloping foreclosed properties in each neighborhood to be sold to owner occupants eventually. Similar to the alternative geographical representations, we assume two alternative categorizations for the types of properties to be acquired. In one case, the potential properties are categorized into two groups, while in the other alternative four distinct categories of properties are defined. We describe this categorization scheme in detail in the next paragraph. Overall, the two alternative decision frameworks are defined by letting $i = 1, 2$ and $l = 1, 2$ in one implementation, and $i = 1, 2, 3, 4$ and $l = 1, 2, 3, 4$ in another implementation. We refer to these as "Case 2x2" and "Case 4x4", respectively. The geographical representations of the two cases, along with sample foreclosed property availability counts, are shown in Figure 3.6. In addition to its practical relevance, this structure also allows for a better analysis of computational efficiency from a methodological perspective.

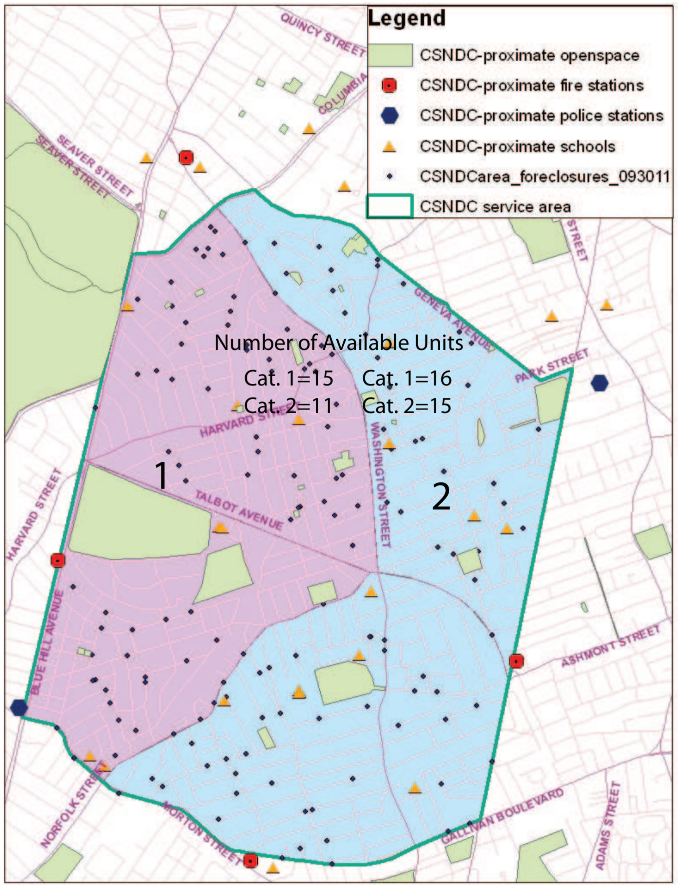

(a) Service area and sample foreclosed property availability information with two neighborhoods and two categories

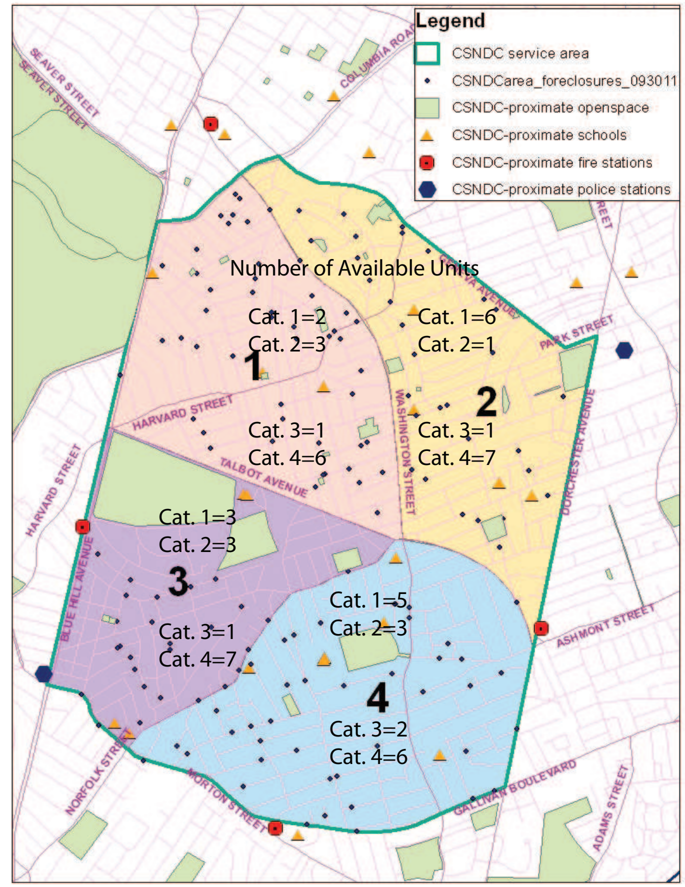

(b) Service area and sample foreclosed property availability information with four neighborhoods and four categories

Figure 3.6. Categorization of CDC's service area based on distinct geographical regions. Sample foreclosed property availability information for each region and property category is also shown on the maps.

A key issue in the modeling framework is the categorization of properties. We assume that properties in each category have similar characteristics which are stochastic and dependent on external market environments. While any type of classification scheme can be used, i.e. based on cost, size or proximity to a specific location, a practical categorization can be based on the property value impacts. As noted previously, PVI corresponds to the expected impacts on proximate property values from a single foreclosure. Hence, PVI reflects a relative measure over the properties available for potential acquisition, where it is natural to assume that the closer the PVI values for given properties, the likelier it is for them to have similar attribute values, such as returns and costs. For example, properties with high PVIs are typically located in central and more desirable locations which imply higher acquisition costs and potentially higher financial returns. The categorizations of properties in the numerical study have been determined by considering their PVI values.

For both Case 2x2 and Case 4x4, empirical data was gathered to generate the specific problem instances based on available information and expert opinions. Two main data sets were used for this purpose. The first data set, obtained directly from the CDC, consisted of information on properties being considered for potential acquisition by the CDC in 2011. This information involved estimates of acquisition and redevelopment costs for the properties, and estimated financial returns from property sales. The second data set was obtained from the authors of Johnson et al. (2013) and involved property value impact calculations for all the properties available for acquisition in the CDC's service area. Model inputs for the numerical study were then created based on information extracted from these data sets. For each parameter considered, histograms and other data displays were plotted as shown in Appendix A to study the variation and correlation structures in the data sets. Based on these, acquisition and redevelopment costs, total required budget to acquire all properties of a given category in a neighborhood, and social returns (represented by standardizing the PVI values to vary between 0 and 1), were taken as stochastic parameters, while financial returns were treated in a deterministic manner.

To characterize the uncertainty in the random parameters of cost, availability, i.e. total required budget to acquire all properties, and social return for each property category in each neighborhood, two-point probability distributions were used. To this end, low and high realizations were computed as the values of the first and third quartiles for each parameter under consideration. Given their exogenous dependence on the economy, we assume in the implementations that the realizations of a parameter for the same category are at the same level across all neighborhoods. For example, if the cost value of a category l in a given neighborhood i is realized as 'low', then the cost of category l in another neighborhood j is also realized as 'low'. The set of data showing possible cost, availability and return values for Case 2x2 of FHAP-S is included in Table 3.1. The scenarios for the stochastic program were then generated by considering all possible combinations of the different levels of the stochastic parameters in the model. The probability for each scenario was then calculated by taking into account the correlation between c^{il} and θ^{il} values as described in Section 3.1.1, and by assuming that the social return realizations are independent from the realizations of these two parameters, where the low and high values for the latter were assigned an equal probability of occurring. Given that the number of stochastic parameters in each model configuration is different, the number of scenarios and thus the complexity of models varies as well. We describe the number of scenarios in each problem configuration in Section 3.4.6.

A total budget value of $5 million was used in the implementations, which is representative of the resources available to the particular CDC considered, while values for community efficacy were generated by normalizing relative crime rate information in each neighborhood so that the values have a range between 0 and 1. Distances between neighborhoods were estimated through existing Geographic Information Sys-

		Cost (c^{il})		Availability Value (θ^{il})		Social Return (μ^{il})	
		Low	High	Low	High	Low	High
Neigh. 1	Cat.1	$389,000	$575,000	$3,090,000	$ 5,935,000	0.966	0.998
	Cat.2	$405,000	$641,000	$4,090,000	$ 4,450,000	0.886	0.997
Neigh. 2	Cat.1	$303,000	$425,000	$4,574,000	$ 4,990,000	0.947	0.986
	Cat.2	$329,000	$431,000	$4,314,000	$ 4,675,000	0.895	0.997

Table 3.1. Data representing possible stochastic parameter realizations for FHAP-S Case 2x2.

tem (GIS) data. Finally, social return function thresholds for FHAP-G were defined based on expert opinions resulting from consultations with CDC staff. The specific values of the deterministic parameters used in the study are summarized in Appendix A for Case 2x2. The computational analysis was based on an equally weighted objective structure. Using this problem setup, optimal budget allocation decisions to different neighborhoods were obtained for the CDC in consideration.

3.4.2 Value of Application of Optimization Models

In this section we study the potential value that can be added to CDC operations by applying the optimization models presented in the study. This is done by comparing the results from the optimization models with the objective levels to be achieved when a resource allocation structure similar to current practice is assumed. We note that our CDC partner did not have a systematic procedure that they implemented in determining resource allocations to different neighborhoods. Rather, it involved an ad hoc process, which typically meant equal resource allocations to different parts of their service area. The allocated amounts were then used to acquire foreclosed properties again through an ad hoc process. Hence, to be able to assess the differences from an optimal strategy, we represent this practical framework by assuming that the available budget is split equally among different neighborhoods. The ad hoc acquisition strategy after resource allocations is studied through three alternative configurations, given that there is no specific system that the CDC utilizes

Obj. Type	Equal Alloc.- Highest Return		Equal Alloc.- Lowest Cost		Equal Alloc.- Optimal Acq.		Opt. Alloc.- Opt. Acq.	
	FHAP-S	-G	FHAP-S	-G	FHAP-S	-G	FHAP-S	-G
Overall	*0.80*	***0.70***	*0.80*	***0.68***	*0.89*	***0.79***	*1.0*	***1.0***
Obj. 1	0.80	**0.88**	0.80	**0.83**	0.80	**0.90**	1.0	**1.0**
Obj. 2	0.88	**0.92**	0.89	**0.90**	0.95	**0.94**	1.0	**1.0**
Obj. 3	0.87	**0.61**	0.87	**0.56**	0.91	**0.61**	1.0	**1.0**
Obj. 4	0.62	**0.35**	0.63	**0.33**	0.90	**0.58**	1.0	**1.0**
Obj. 5	0.63	**0.37**	0.65	**0.36**	0.81	**0.55**	1.0	**1.0**
Obj. 6	0.77	**0.82**	0.78	**0.77**	0.85	**0.94**	1.0	**1.0**
Obj. 7	1.0	**0.99**	1.0	**0.99**	1.0	**1.0**	1.0	**1.0**
Obj. 8	-	**1.0**	-	**1.0**	-	**1.0**	-	**1.0**

Table 3.2. Comparison of standardized objective values for the equal budget allocation strategy, which represents the current practice, and the optimal allocations for FHAP-S and FHAP-G Case 2x2.

for this purpose. We refer to the resulting cases as equal allocation-highest return, equal allocation-lowest cost, and equal allocation-optimal acquisition.

In equal allocation-highest return, we assume that after the budget is allocated equally among neighborhoods, individual acquisition decisions prioritize properties with the higher return values. In other words, first the highest return properties are aimed for acquisition, followed by the next highest if budget still remains, etc. The equal allocation-lowest cost strategy assumes that the prioritization is based on costs of properties, and lower cost properties are acquired first. Finally, equal allocation-optimal acquisition configuration assumes that the acquisition decisions are determined optimally based on the objective structure in the models. Note that the equal allocation-optimal acquisition strategy would result in the best possible value for the CDC given an equally split budget during the allocation phase. Hence, the difference between the corresponding objective values in this case and the optimal solutions constitutes a lower bound for the value of application of optimization models developed.

In Table 3.2 we show a comparison of the standardized objective values for each policy described above under FHAP-S and FHAP-G implementations. The objec-

Policy	Financial Gain		Social Gain	
	FHAP-S	FHAP-G	FHAP-S	FHAP-G
Equal Alloc.-Highest Return	$0	$4,694	$0	$18,905
Equal Alloc.-Lowest Cost	$2,208	$0	$44,973	$0
Equal Alloc.-Optimal Acq.	$60,521	$55,302	$242,602	$252,877
Optimal Alloc.-Optimal Acq.	$80,871	$144,150	$489,710	$853,813

Table 3.3. Comparison of gains in financial and social returns as modeled through Objectives 4 and 5 under different policy implementations.

tive values have been standardized so that the optimal solutions correspond to an objective value of 1.0. As highlighted above, the equal allocation cases represent the current practice. For FHAP-S, Optimization through our modeling framework can be observed to result in an increase of between 10-20% in the overall value of foreclosed housing acquisition policies. Of the specific objectives, the most significant impact is on Objectives 4 and 5, which correspond to maximization of financial returns and social utility, respectively.

The value of optimization over the current practice increases for the FHAP-G model. This is expected, as the uncertainty is captured in a more accurate fashion in this implementation. For FHAP-G, a difference of between 20-30% is observed between the current practice and optimal policies. Again, the most significant value is added through the financial and social utility objectives, implying that equity is achieved at a somewhat high level under the current practical implementations. In Table 3.3 we show the differences in financial and social returns under different implementations in terms of dollar values. Each data column in the table displays the difference between the expected return of a given policy and the lowest expected return among all policies. For example, in the last column we see that equal allocation-lowest cost policy would create the lowest social return as measured through the PVI values. By using the optimal policy the CDC can create an additional value of around $600,000 in property value impacts in their service area when compared with the equal allocation-optimal acquisition policy. By the nature of the restricted financial return structure, the gains in financial returns are lower. Overall, however, the gains through optimization can be consistently observed for all cases, especially in terms of social returns. In Section 3.4.3, we describe the implications of the optimal resource allocation decisions and how changes in different problem parameters impact these decisions.

3.4.3 Resource Allocations and Impacts of Model Parameters

In this subsection we investigate the implications of the resource allocation decisions form a practical perspective and how changes in different problem parameters impact these decisions. For the practical implications of the allocation decisions, we note that no detailed quantitative information was available for one to one comparisons with historical budget allocation decisions of the CDC studied. This was because the specific CDC made such decisions through an ad hoc process, which mostly involved equal resource allocations to different parts of their service area. Hence, through consultations with CDC staff, the design of a structured strategic resource allocation process, as well as the implications of using different quantitative measures in that process, were noted to be the relevant issues from a practical perspective. To this end, in this section we try to analyze the structure of our decision models, specifically with respect to their sensitivity to different model parameters, while the latter issue involving implications of different objectives is addressed in Section 3.4.4.

Our sensitivity study is based on three key parameters in the modeling framework, which represent general inputs, as opposed to neighborhood specific parameters. These inputs consist of the available budget to be allocated, and the two threshold parameters τ_1 and τ_2 used in defining the social returns from foreclosed property acquisitions when investment dependent return is modeled. For each parameter, we consider a range of possible values and study how the allocations to different neigh-

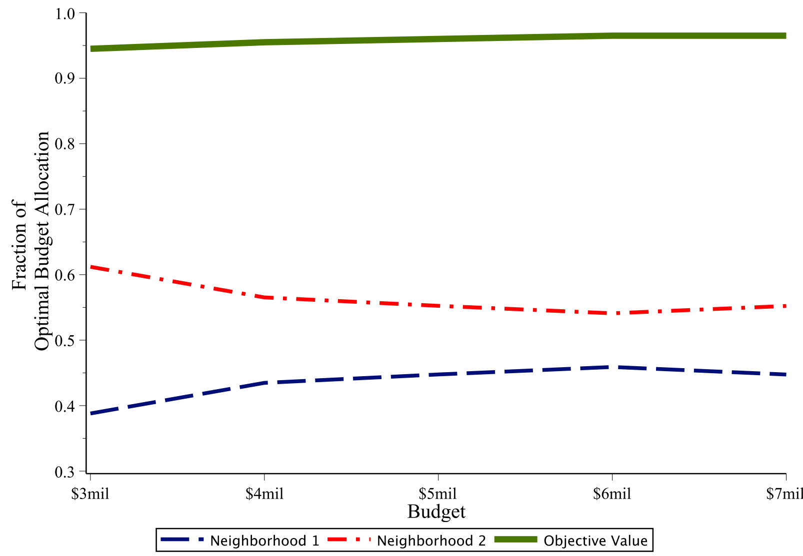

Figure 3.7. Change in optimal resource allocations and objective function value over different budget levels.

borhoods as well as the overall objective function value change over that range. To provide a clearer illustration, the analyses were performed on Case 2x2 of the FHAP-S model with the investment dependent return structure.

In Figure 3.7 we show how the resource allocations and the optimal objective function value vary over a range of budget values. It is observed that the model is quite robust to changes in the budget. First, the increase in the optimal objective function value is minimal as the budget increases. This is likely due to the limitations imposed by the current availability of the foreclosed properties, as well as due to the multi-objective structure of the problem. Even though more properties may be acquired with larger budgets, it does not necessarily mean that these acquisitions would help increase the value of all objectives. While it would increase utility based objectives, it may have a negative impact on the equity objectives. A similar robust structure, although to a smaller extent, is observable in resource allocation decisions as well. For the given empirical setting, a budget split of 55%-45% is optimal for budget amounts larger than $4 million. On the other hand, there is a change towards a 60%-40% split at lower budget levels, which may be due to the decrease in the number of options to balance utility and equity. We also note that these resource allocation decisions have been deemed practically plausible by the CDC considered in the study.

In Figure 3.8 we present the analysis results for the parameters τ_1 and τ_2 used in modeling the social returns. These values were selected for a sensitivity analysis as they are mostly based on expert opinion and few mathematical models exist on such return functions. On the other hand, we observe for both parameters that the optimal objective function value remains mostly the same despite the change in the parameter values, except for lower τ_2 values which enable increased joint return realization without much impact on equity. Optimal budget splits also show a similar pattern.

Overall, *the model solutions are quite robust with respect to increases and minor decreases in the general input parameters of budget and investment dependent return thresholds.* This robustness result is a strengthening argument for the conclusions reached for the given empirical setting, and is likely to hold unless foreclosure rates, which are currently at high levels, increase significantly to result in an even larger number foreclosed properties becoming available for acquisition.

3.4.4 Comparison of Financial vs. Nonfinancial and Equity vs. Utility Based Objective Optimization

As part of our analysis of the impact of using different objectives, which was observed to be of interest to the CDC studied, we consider two trade-off situations in FHAP. These situations deal with financial versus nonfinancial goals, and equity versus utility objectives. These issues are especially relevant and unique to our analysis due to the social dimensions involved in the optimization. We emphasize here that our analyses are numerical and experimental. Hence, any conclusions are based on

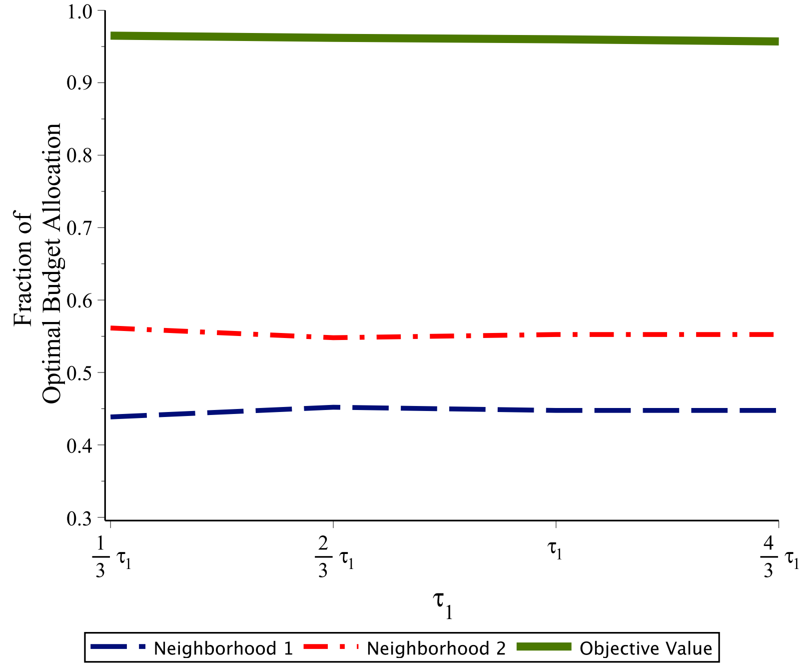

(a) Analysis for parameter τ_1

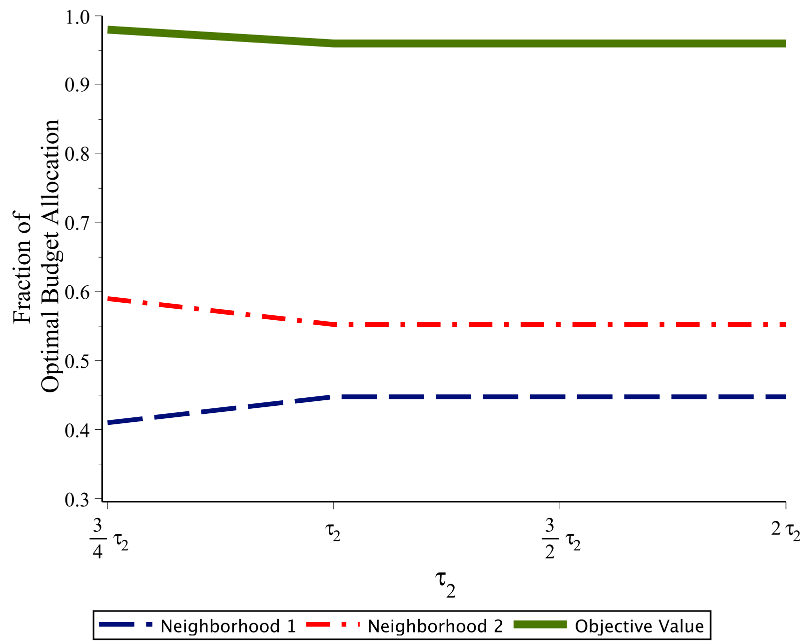

(b) Analysis for parameters τ_2

Figure 3.8. Change in optimal resource allocations and objective function value over different values of parameters τ_1 and τ_2.

the real-world data obtained from the CDC we interacted with. On the other hand, it can potentially be assumed that similar conclusions are likely to be reached for organizations operating in scales similar to this CDC, as there is anecdotal evidence that the CDC studied can be representative of typical CDC operations in other major cities (NeighborWorks, 2009).

We first analyze how financial objective optimization in FHAP relates to nonfinancial objective optimization. In this analysis, the profit objective, i.e. Objective 4, is categorized as financial, while all other objectives are categorized as nonfinancial measures. We apply the constraint method of Collette and Siarry (2003) to these two aggregate objectives, and the result of this analysis is Pareto curves representing the trade-offs between the two categories. Figure 3.9 contains Pareto curves for the base cases of FHAP-S and FHAP-G.

Our main observation is that the trade-off is not so significant and thus inclusion of financial objectives in FHAP do not detract much from the social and equity based objectives. This is especially the case for FHAP-S, where only two decision epochs are involved in the optimization. More specifically, we note that even if purely financial objectives were considered, it would still imply around 92% fulfillment of non-financial objectives for FHAP-S and 87% fulfillment for FHAP-G. We also note that the trade-off is slightly biased towards the nonfinancial objectives in both models, where nonfinancial optimization would imply around 89% fulfillment of financial objectives in FHAP-S, while this rate is 83% for FHAP-G. This is somewhat expected as nonfinancial goals involve several different objectives that the optimization tries to achieve, as opposed to a single objective involving financial profit. While we do not show Pareto plots for alternative configurations of financial and non-financial objectives, the trade-offs in those configurations are also observed to be similar to the base case analysis described above. Overall, *our analysis shows that even if the CDC makes its acquisition decisions purely based on financial returns, it would still imply*

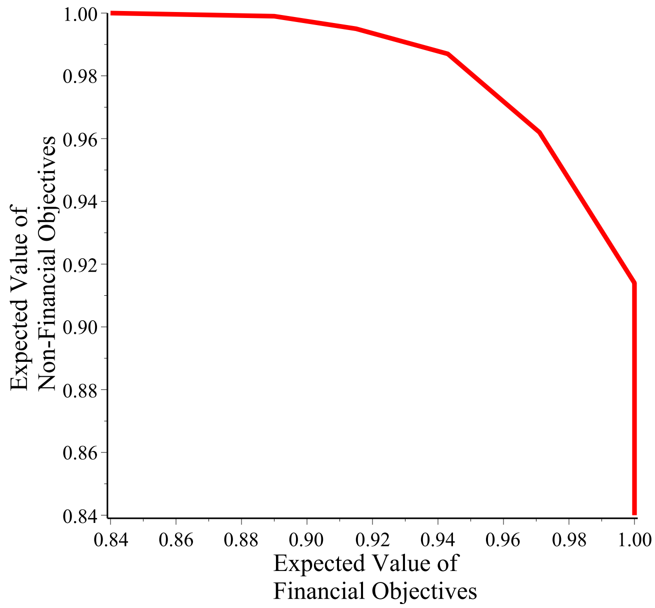

(a) FHAP-S

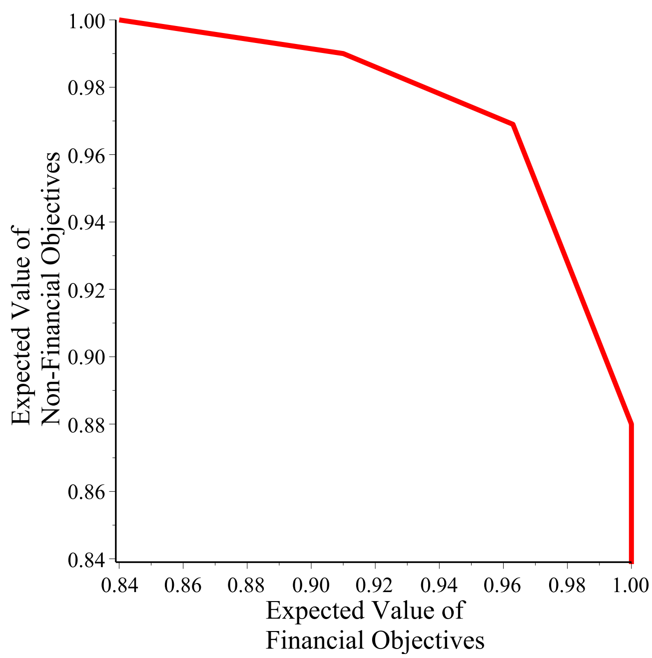

(b) FHAP-G

Figure 3.9. Pareto curves of financial and non-financial objectives for base models of FHAP-S and FHAP-G.

around 90% fulfillment of social objectives. The trade-off between financial profit and non-financial objectives is not so significant and thus inclusion of financial objectives in decision making does not take away much from the social and equity based objectives. In other words, for the service area considered financial and social values of the properties are mostly positively correlated.

An important issue for most nonprofit organizations is how to ensure equity in their services as they try to maximize socio-economic utility. We analyze this issue by categorizing the multiple objectives considered in FHAP as equity versus utility objectives. To this end, we assume that equity related to collective efficacy, allocation rate and owner occupancy, i.e. Objectives 1, 3, and 6, represent the equity related objectives; while the economies of scale, financial return, social utility and efficient use of budget, i.e. Objectives 2, 4, 5, and 6, are utility based objectives. We then perform a Pareto analysis similar to the financial versus nonfinancial objective case above. In Figure 3.10 we display the trade-off curves for equity versus utility objectives for the base cases of the two model types.

We observe that the two models behave somewhat differently with respect to the corresponding values of the two objective types. Overall, utility maximization will achieve around 80% equity, while equity maximization would achieve around 95% of utility in FHAP-S. These rates are around 74% for both cases in FHAP-G. Thus, the two objective types have more of a trade-off when compared with the previous analysis, specifically for FHAP-G. This suggests that, although the magnitude of the trade-offs between the two classes of objectives is not large, for a socially focused organization in this framework the optimization of equity is likely to imply a somewhat less efficient strategic allocation and vice versa. The results for other configurations are also similar, and organizations can choose to balance the emphasis on equity versus utility based on the Pareto representations. For example, it is possible to achieve around 85% equity and same levels of utility through an optimal solution on the

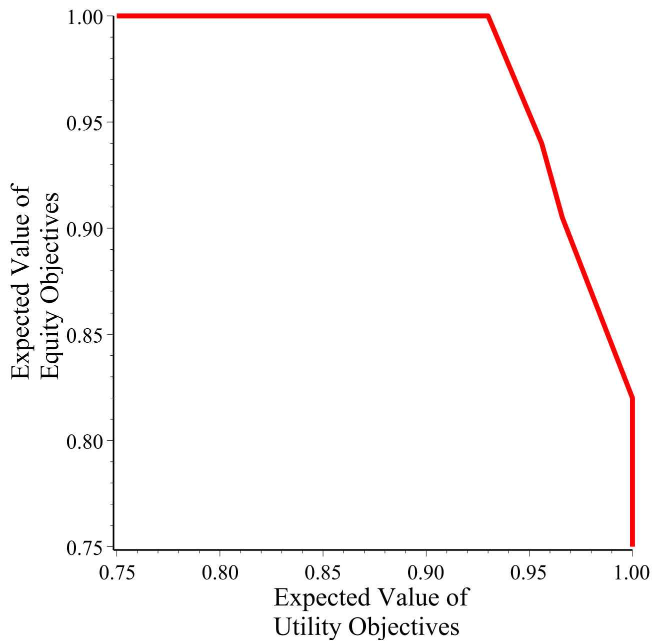

(a) FHAP-S

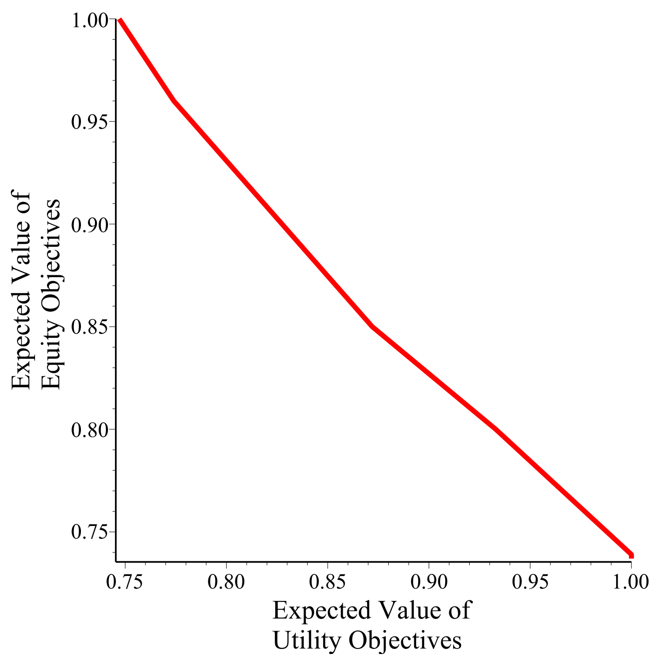

(b) FHAP-G

Figure 3.10. Pareto curves of equity and utility objectives for base models of FHAP-S and FHAP-G.

Pareto curve for FHAP-G. Overall, *we observe that if equity is not considered in CDC acquisition selections, it is expected that these acquisitions will be approximately 20-25% less equitable between different regions than an ideal equitable selection decision.* Such a conclusion can be useful in discussions with community representatives of neighborhoods. We note that we also consider selected trade-offs between individual model objectives, and discuss the resulting conclusions in Section 3.4.5.

3.4.5 Value Path Analysis

In this subsection we consider selected trade-offs between model objectives through value path analyses. Figure 3.11 shows value paths for the equity objectives in the FHAP-S and FHAP-G base configurations. Objectives 1, 3, and 6 correspond to equity objectives related to collective efficacy, allocation rate and owner occupancy, respectively. Each distinct line in the value path represents the performance of a corner point solution to the multiobjective problem according to all objectives. The vertical axis represents the extent to which each model instance achieves the most-desired value for a particular objective. Here we observe a somewhat similar behavior between FHAP-S and FHAP-G base configurations.

When the collective efficacy based equity measure, i.e. Objective 1, is optimized in FHAP-S, all other equity measures are at or close to their minimal levels, implying that different equity objectives are not always synergistic for the neighborhood data considered. A similar observation can also be made for FHAP-G. The pattern is somewhat different when the maximization of the allocation rate and owner occupancy based equity objectives are considered individually. Some positive association is observed between the allocation rate based equity measure and efficacy, as both are typically at high levels when one of these objectives is maximized. Indeed, the optimization of owner occupancy is also synergistic with all other equity objectives, although it is not as strong in FHAP-S where efficacy and allocation rate objectives

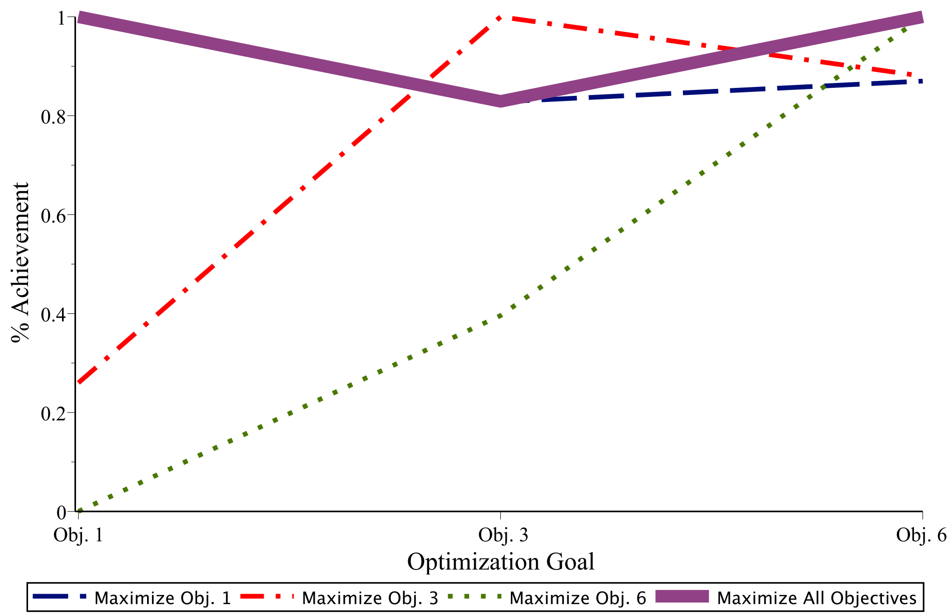

(a) FHAP-S

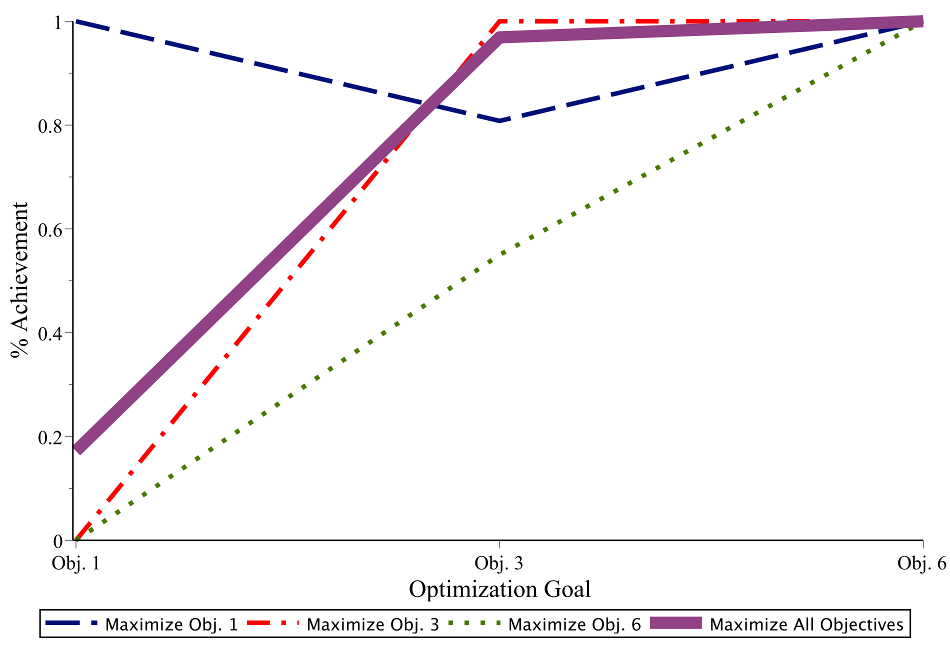

(b) FHAP-G

Figure 3.11. Trade-off graphs for equity objectives of base models of FHAP-S and FHAP-G.

are slightly below their maximum levels when owner occupancy objective is maximized. Overall, *we conclude that maximization of collective efficacy measure by itself would imply some deviation from fulfilling the allocation rate and owner occupancy related equity objectives, while strong synergistic effects exist between the latter two objectives.* On the other hand, it should be noted that due to the potential existence of alternative solutions and the dependency on the data used in the analysis, these insights may not hold at the identified levels for different data or applications.

In Figure 3.12 we display value paths for FHAP-G with investment dependent return and with both investment dependent return and reformulated constraint (3.21). As expected, the former has similarities to the base FHAP-G case. An interesting observation deals with the optimal value of Objective 3, which is related to constraint (3.21), in the overall optimization results shown this figure. Although the difference is not very large, this value is higher than the corresponding value shown for the base FHAP-G case. Hence, it may be concluded that the improved representation of (3.21) impacts the model such that Objective 3 is better defined and maximized at a higher level. On the other hand, *the investment dependent return structure and the reformulated constraint do not have a significant impact on the trade-offs with respect to the equity related objectives*, i.e. the general pattern is similar to the base FHAP-G model.

A similar value path analysis is also performed for utility objectives. In Figure 3.13 we show such curves for the utility objectives, where Objectives 2, 4, 5, 7, and 8 respectively correspond to the economies of scale, financial return, social utility, efficient use of budget, and the reallocation penalty objectives. Here it can be observed that Objectives 2 and 4 do not have significant trade-offs among each other, while Objectives 5 and 7 appear to be negatively correlated with these objectives. Hence, *if objectives related to the economies of scale and financial returns are maximized independently, the efficiency in other utility objectives involving social utility and*

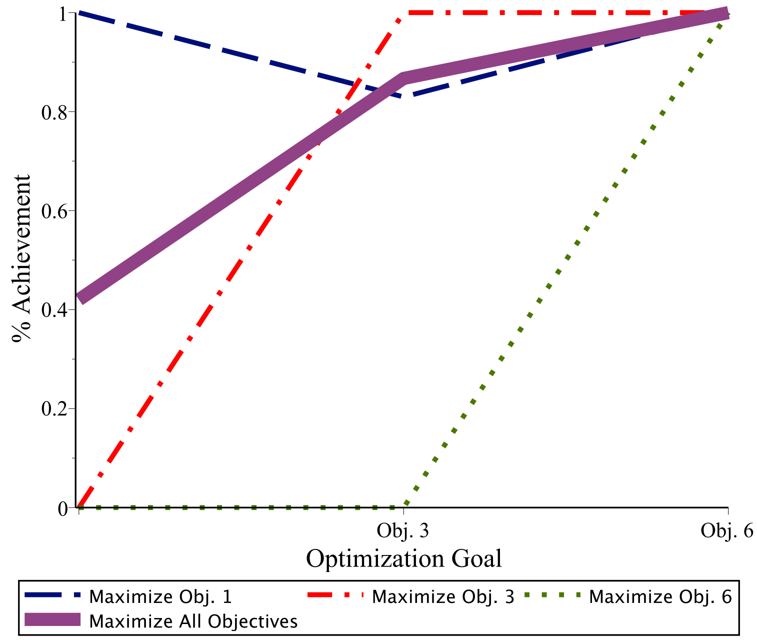

(a) FHAP-G with investment dependent return

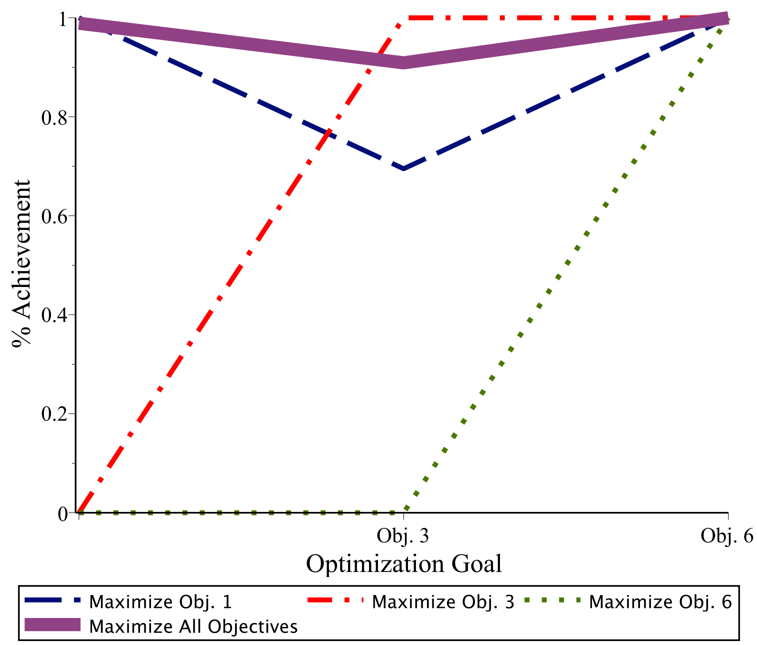

(b) FHAP-G with investment dependent return and reformulated constraint (3.21)

Figure 3.12. Trade-off graphs for equity objectives of investment dependent return extension of FHAP-G with and without reformulation of reallocation constraint (3.21).

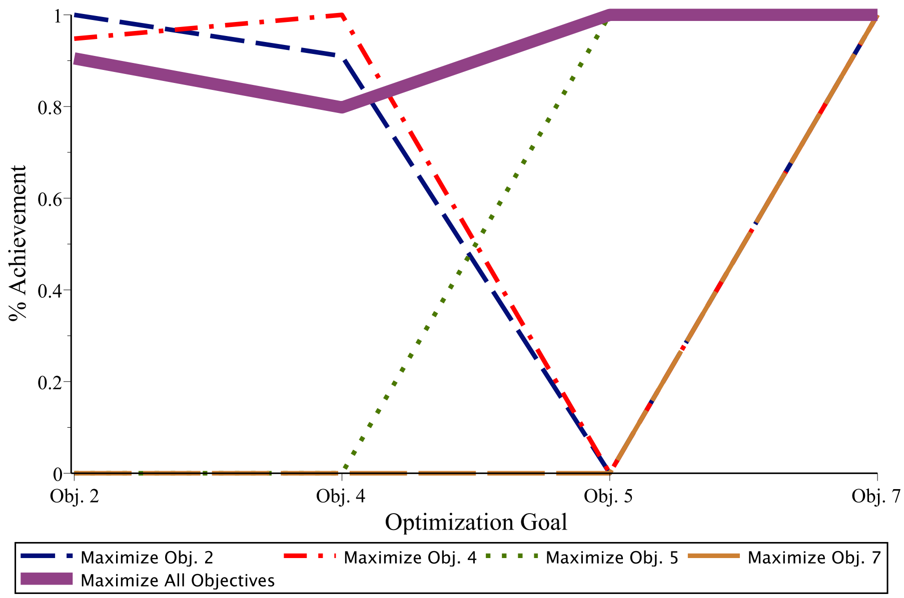

(a) FHAP-S

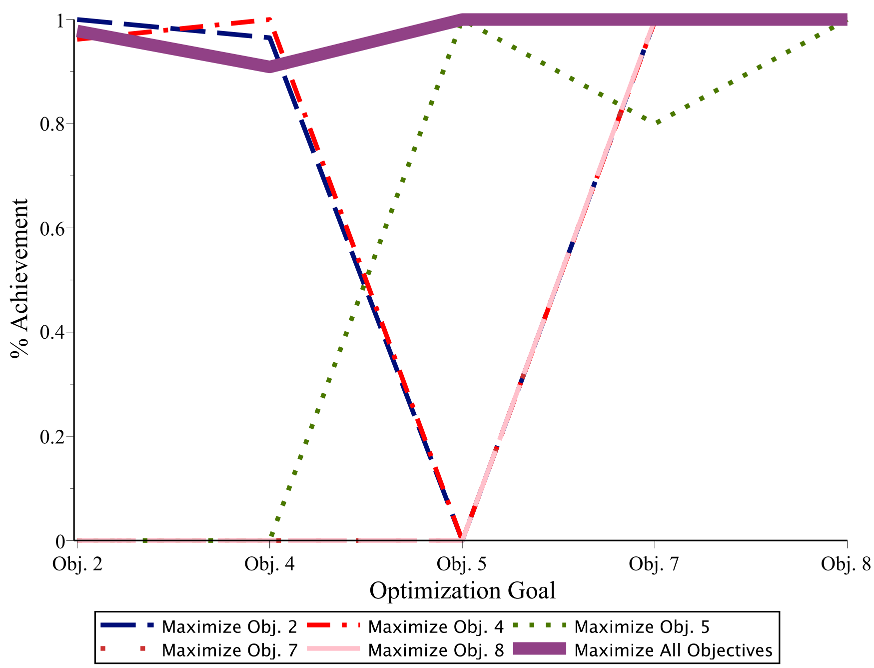

(b) FHAP-G

Figure 3.13. Trade-off graphs for utility objectives of base models of FHAP-S and FHAP-G.

budget utilization is reduced. On the other hand, as expected, the reallocation penalty based goal represented by Objective 8 is synergistic with all other objectives. This behavior is also similar for other configurations of the problem.

3.4.6 Value of Alternative Formulations and Heuristic Approaches

Another analysis that we perform involves the computational aspects of different formulations, specifically to identify lost value if acquisition decisions were to be made according to rule-based heuristics. To this end, we consider the complete stochastic mixed-integer programming (SMIP) solutions of the given formulations, as well as the two simplifying heuristic approaches. We note here that while the problem is a strategic one, where computational times are typically not a significant concern, the proposed decision models are aimed at serving as guides to CDCs in their decision making process. As a result, during the planning stage multiple alternative parameter values can be used and tested from a sensitivity analysis perspective, which would require multiple solutions for the problem. Hence, relatively quick solution generation is likely to have some relevance for practical implementation of the proposed models as well.

The computational results for different instances and versions of FHAP are shown through the tables 3.4 - 3.6 for this study. Computations were performed on a PC with Intel i5 Core processor with 2.3 GHz speed and 4 GB memory. All solutions were obtained using the CPLEX 12 solver, where implementations were performed in the General Algebraic Modeling System (GAMS).

One consideration for our research is that given the implementation challenges of advanced optimization models by CDCs, it may be possible that simplified heuristic approaches, which can be implemented more easily, can be used as decision aids by these organizations. Hence, we are specifically interested in the lost value when such heuristic approximations are used. We first note that the two heuristics proposed are more efficient from a computational perspective, allowing for solutions in reasonably short run times, i.e. much less than one hour. Moreover, the quality of the solutions appear to be quite high for all cases. The overall average computational improvement is around 60% for the two heuristics for FHAP-S, while the corresponding values are even higher, i.e. around 68%, for FHAP-G. Indeed, improvements are much higher for the more complex Case 4x4 configurations. The observed difference in terms of objective function values is around 4% for FHAP-S when averaged over all instances, while this gap is around 2% for FHAP-G. Hence, *it can be concluded that the proposed rule-based heuristic approaches can be chosen as reasonable alternatives to the complete SMIP optimization as the expected difference from optimality is around 4%.* Complete SMIP implementation results in long computational times, especially as larger problem instances are considered. Indeed, the effectiveness of the heuristics increases with computational complexity.

We also compare the computational efficiency of different formulations. More specifically, we compare the computational times for the base and investment dependent return models. We note that the inclusion of investment dependent returns adds significant complexity to the model, as observed in the CPU times of the complete SMIP solutions for both models. For example, FHAP-S can not be solved in the one hour of allocated time when investment dependent return structure is used. Similar observations can also be made for FHAP-G that the computations take more than an hour for all such implementations. Hence, for the complete SMIP models, the computational challenges associated with the inclusion of investment dependent returns should be considered. On the other hand, this issue is not the case for heuristic approaches, as we described above.

As another comparative analysis, we consider the value of the reformulation of constraint (3.21) for FHAP-G based on the information in computational result tables provided as Table 3.5. The base and investment dependent return configurations for this model are based on an approximation of this constraint, which is a more restrictive formulation. Hence, the reformulation allows for potential improvement in the expected utility of the investments. For both the complete SMIP and heuristic formulations, the utility increases about 10% when the reformulation is used. The only trade-off involves the computational complexity added due to the piecewise approximation used as part of the reformulation of (3.21). The results show that the reformulated model performs worse computationally, especially for the complete SMIP approach. In those cases, a deterioration of around 20% is observed in the computational times for FHAP-G, since additional complexity through the SOS2 variables is added to the model.

FHAP-S	Case	# of Scen	Base				Inv. Dep. Ret.			
			Obj. Val.	**Obj. % Gap**	**CPU (sec)**	**CPU % Gain**	**Obj. Val.**	**Obj. % Gap**	**CPU (sec)**	**CPU % Gain**
Complete SMIP	2x2	16	0.934	-	8.7	-	0.96	-	20.1	-
	4x4	256	0.887	-	1340.2	-	0.909	-	5702.5	-
Heuristic-1	2x2	16	0.934	0.0%	6.4	26.3%	0.958	-0.2%	15.2	24.1%
	4x4	256	0.751	-15.3%	83.4	93.8%	0.884	-2.8%	1175.1	79.4%
Heuristic-2	2x2	16	0.934	0.0%	6.2	28.7%	0.96	-0.0%	16.9	15.6%
	4x4	256	0.764	-13.9%	61.7	95.4%	0.885	-2.6%	219.5	96.2%

Table 3.4. Computational results for the base model and investment dependent return extension of FHAP-S.

FHAP-G	Case	# of Scen	Base				Reformulated (3.21)			
			Obj. Val.	**Obj. % Gap**	**CPU (sec)**	**CPU % Gain**	**Obj. Val.**	**Obj. % Gap**	**CPU (sec)**	**CPU % Gain**
Complete SMIP	2x2	1024	0.880	-	245.7	-	0.955	-	325.2	-
	4x4	4096	0.845	-	4527.4	-	0.947	-	5137.8	-
Heuristic-1	2x2	1024	0.873	-0.8%	106.0	56.9%	0.955	-0.0%	197.1	39.4%
	4x4	4096	0.837	-0.9%	802.6	82.3%	0.927	-2.1%	881.4	82.8%
Heuristic-2	2x2	1024	0.875	-0.6%	114.8	53.3%	0.951	-0.4%	127.3	60.9%
	4x4	4096	0.836	-1.0%	638.3	85.9%	0.934	-1.4%	725.9	85.9%

Table 3.5. Computational results for the base model and reformulated allocation rate constraint extension of FHAP-G.

FHAP-G	Case	# of Scen	Inv. Dep. Ret.				Reform. (3.21)- Inv. Dep. Ret.			
			Obj. Val.	**Obj. % Gap**	**CPU (sec)**	**CPU % Gain**	**Obj. Val.**	**Obj. % Gap**	**CPU (sec)**	**CPU % Gain**
Complete SMIP	2x2	1024	0.884	-	284.6	-	0.959	-	426.1	-
	4x4	4096	0.862	-	6444.7	-	0.913	-	7091.9	-
Heuristic-1	2x2	1024	0.861	-2.6%	100.7	64.6%	0.94	-2.0%	215.7	49.4%
	4x4	4096	0.849	-1.5%	698.5	89.2%	0.850	-6.9%	1798.1	74.6%
Heuristic-2	2x2	1024	0.88	-0.5%	183.8	35.4%	0.933	-2.7%	191.5	55.1%
	4x4	4096	0.841	-2.4%	708.4	89.0%	0.898	-1.6%	921.1	87.0%

Table 3.6. Computational results for the investment dependent return extension of FHAP-G with and without reformulation of allocation rate constraint (3.21).

In the computational result tables, the first and second columns indicate the solution method used and the case type for the corresponding version of FHAP, while the third column shows the number of scenarios in each instance. The other columns describe the results obtained for each version by listing the objective function value obtained, its percent difference from the best solution, the computation time and its percent difference from the computation time of the complete SMIP solution. The base configurations correspond to the basic formulations of FHAP-S and FHAP-G as described in Sections 3.1 and 3.2, respectively. The investment dependent return and reformulated (3.21) configurations are the model extensions introduced in Sections 3.3.1 and 3.3.2. Note that reformulation of (3.21) applies only to FHAP-G, where the introduction of gradual uncertainty resolution results in a complexity in the definition of constraint (3.21). The second configuration in the third result table considers both the reformulation structure and investment dependent returns for FHAP-G.

3.4.7 Policy Implications for CDCs

The policy implications of our study arise from our use of real-world based data that represent the strategic decision framework of a particular CDC. While our conclusions specifically apply to this data set, it is possible that the operating environments for many other CDCs are similar in nature, for which some anecdotal evidence exists as noted previously. Hence, we believe that our general findings can be helpful for such organizations in devising strategic investment plans.

CDCs can benefit from the results of this study in two ways. First, as a direct utilization, the optimization models can potentially be implemented to identify a benchmark resource allocation strategy as defined by the model assumptions and inputs. This benchmark strategy can be adjusted based on any other qualitative inputs that may exist, and the adjusted strategy can be used directly to allocate resources to different neighborhoods. As an alternative, the model results can be used to assess or justify the existing resource allocation policy of a given CDC, or to guide other routine activities. Second, as an indirect utilization, the policy related conclusions we reach through our numerical analysis, which is based on a typical CDC operation, can be used for general guidance in strategic resource allocation or property acquisition by CDCs. We specify these general policy implications in the following paragraphs.

For general policy guidelines, first we note that the optimal resource allocation strategy, which involves splitting of the budget among different neighborhoods, is quite robust for different budget levels and return function parameters. Hence, CDCs can adjust the resource allocations proportionally if fund availabilities change during the planning period.

Second set of policy implications deals with the emphasis on different optimization objectives. The results suggest that there is no significant conflict between financial and nonfinancial objectives. While this conclusion is based on the numerical data used for this specific case study, it is likely that if a CDC makes its acquisition decisions solely based on financial returns, it would still imply around 90% fulfillment of social objectives. Hence, CDCs can simply consider only financial objectives in their acquisition policies and this would not result in huge loss of social value.

While still not very significant, the trade-offs are a bit more apparent when equity objectives are considered with respect to utility. Thus, it is important for CDCs to consider equity in their resource allocation and property acquisition processes, as otherwise the resulting social value may be high but unbalanced among different parts of their service area. Optimizing investments based on only social returns may imply some inequity between neighborhoods, corresponding to an observed loss of equity around 20-25%. This conclusion is of course dependent on the distribution of different category properties across the service area. For the case study presented, this distribution is not significantly biased towards a specific subset of neighborhoods.

This relatively even distribution of neighborhood parameters can be expected to be observed in other CDC service areas as well given their typically focused geography. Hence, the results are likely to be applicable to other CDC operations, too.

In addition, CDCs can take into account that the collective efficacy measure is not necessarily synergistic with other equitable allocation objectives such as those involving allocation and owner occupancy ratios in neighborhoods. On the other hand, the latter two equity objectives are strongly correlated implying that focusing on one would also increase the effectiveness level in the other. CDCs should also note that if they try to take advantage of economies of scale by investing mostly in proximate properties, this will have a somewhat significant negative impact on the social utility achieved through such a policy.

A third category of policy implications relate to the use of rule-based heuristics. Given the objective structure presented and assuming that budget allocations to different neighborhoods are done as efficiently as possible, selecting property acquisitions based on relative marginal returns or availabilities over different categories does not result in significant loss of overall utility for CDCs. For most cases, this loss is expected to be less than 4% with respect to an optimal strategy. Hence, in the absence of any optimization implementations, CDCs can consider using such general rule-based acquisition strategies.

3.5 Conclusions

In this chapter, we studied stochastic dynamic models for resource allocation and foreclosed property acquisition to provide some general evidence-based guidance to a specific CDC, with potentially broader implications. To this end we first developed a two-stage stochastic programming formulation, and then expanded this model through a multi-stage structure involving gradual uncertainty resolution. We also studied two variations in these models in order to capture some additional complexities. Finally, an empirical analysis has performed based on real-world data for practical and computational evaluations.

While our conclusions are based on the specific numerical data used, we demonstrate through our analyses that CDCs can benefit from the utilization of the proposed models either through direct implementation for specific strategic guidance, or through the indirect use of several policy results obtained. We further show that two simplistic heuristic improvements result in increased efficiency without a significant optimality gap, indicating the potential practical value of these approaches.

A specific characteristic of our analysis is that we build our models through interactions with a CDC, and use real-world data to test them. As a first stochastic model of its type in this application area, our study is aimed to provide strategic resource allocation guidelines for practitioners through explicit consideration of uncertainty.

CHAPTER 4

TACTICAL SOCIETAL RESOURCE ALLOCATION IN FORECLOSED HOUSING ACQUISITION

In this chapter, we consider a CDC that faces decisions on potential acquisitions of foreclosed properties that become available over time in their service area. By being available, we refer to the case that a property is placed on market for potential sale by a bank or other mortgage holder, and that the property is potentially approvable for acquisition by a funding source. When a foreclosed property is put on sale, an important advantage for CDCs and other similar entities is their priority in making offers on the property. This is due to requirements put in place by most financial institutions through the National First Look Program, which provide owner occupants and public entities that are committed to the community an early opportunity to bid for a foreclosed property. As part of this policy, only offers from owner occupants and buyers using public funds are considered during the first 15 days a property is on the market, and offers from investors are considered only after the first 15 days have passed. This allows for a higher likelihood of a successful offer for CDCs due to the relatively fewer competitors in the process (Axel-Lute and Hersh, 2011). We further describe the details of this decision framework in the following section

4.1 Tactical Foreclosed Acquisition Model

We assume that the availability of foreclosed properties for potential acquisition follows a Poisson process with rate λ as suggested by analysis of historical data. The availability rate λ is typically related to the conditions of the economy and the housing market. A high availability rate implies a poor state of economy where foreclosure rates are high, while low rates would indicate that the economy and the housing market are in better condition. We note here that λ is assumed to be stationary, i.e. we do not model a dynamic environment where the state of the economy fluctuates, due to the long-term dynamics of such fluctuations. On the other hand, we analyze later in the study how optimal policies change for different availability rate levels.

At the beginning of the planning period, CDC has an estimate of the total funding that they can potentially access through various sources during that period. This funding level, which we denote by B, represents the total amount of credit or other funds that the CDC can assume to be potentially available for foreclosed property acquisition. The total amount of accessible funds is typically well estimated by CDCs, as they depend on their existing lines of credit with banks or the fixed grants available through various government programs. Suppose $T \in (0, \infty]$ denotes an expiration time for the available funds, after which any unused funds will have no value. This time limitation typically depends on the funding source. For example, certain government funds have deadlines that they need to be used by, while other resources such as donations may not have any such stipulations, implying that they can be used anytime.

When a foreclosed property is placed on market by the lender, it has an associated asking price, usually based on the price opinion of a broker with experience in the area. In addition, CDCs can also perform a market analysis themselves to estimate the market value of a foreclosed property. Without loss of generality, we assume that the asking price is a lower bound on a foreclosed property's market value, as well as on the amount required for a successful offer. This is quite typical in the regular operation of the real estate market, as banks or other lenders would often have lower asking prices on foreclosed properties due to their desire to sell these properties quickly. Hence, such properties would typically sell at above the asking price, and offers would involve overbids. We let $C \in [\underline{C}, \bar{C}]$ denote the asking price for a foreclosed property, which represents the minimum resource requirement for the acquisition of that property. The asking price of a property is defined by a probability distribution $f(c)$.

Similar to the asking prices, the social-return from a property, denoted by $R \in [\underline{R}, \bar{R}]$, is also stochastic and is characterized by a probability distribution $f(r)$, or $f(r, c)$ if social-returns and the asking prices are correlated. Estimating the social-return from the acquisition and redevelopment of a foreclosed property is clearly difficult. Johnson et al. (2013) highlight this challenge, and develop a measure validated by some CDCs, which is based on the impact of the acquisition of a foreclosed property on the appreciation of the value of nearby properties. As also noted in Chapter 3, more formally, the property value impact (PVI) measure is defined as the expected impact on proximate property values from a given foreclosure. This measure is directly related to the geographical location of a property, and can easily be calculated through the procedure described by Johnson et al. (2013) for each foreclosed property that becomes available for acquisition. In this chapter, we use PVI values that we obtained from Johnson et al. (2013) directly without normalization. Thus, PVI values used in this chapter are in units of dollars. We emphasize here that our focus is on the returns to the society, and hence we do not model any financial returns for the CDC which may be realized due to the rental or sale of an acquired property. The latter involves a much broader scope with a focus towards the overall operation of a CDC, as opposed to foreclosed housing acquisitions. Moreover, several CDCs that were consulted noted the maximization of the impact on property values as being their objective in foreclosed property acquisitions. This is somewhat natural, as most resources such as government funds for foreclosed property acquisition are aimed at appreciation of home prices and stabilization of the housing market.

Observing a foreclosed property entering the market at time $t \in [0, T]$ with an asking price c, a CDC first decides whether they should consult with the funding source and make an offer on the property. If an offer decision is reached, then the next decision involves the determination of the amount to offer. We model the offer amount decision at time t, for a remaining fund level b, through an overbid rate parameter $\delta_{bct} \in [0, \bar{\delta}_c]$, which corresponds to the percent difference between the offer amount and the asking price c. This notation implies that the overbid rate can vary over the planning horizon, and the limits on the overbid rate can differ based on the asking price of a given property. We denote δ_{bct} as a percentage, e.g. $\delta_{bct} = 0.05$ implies that the offer amount is 5% over the asking price. The probability of success for an offer, i.e. the probability of winning a bid, is an increasing function of the overbid rate, and is denoted $p(\delta_{bct})$. As part of our analysis, we assume that $p(\delta_{bct})$ can be any general increasing bounded function.

When an offer is made on a foreclosed property, an overhead cost corresponding to the time and other expenses required to make the offer is incurred by the CDC. This cost is typically a certain percentage G of the offer amount, and can be defined as $g(c, \delta_{bct}) = (c + c\delta_{bct})G$, where $c + c\delta_{bct}$ is the offer amount. While it may not typically hold in practice, a fixed cost assumption is also possible here, in which case the analytical derivations would apply in a simpler way. If the offer is not accepted by the seller, then this cost is sunk. Hence, $g(c, \delta_{bct})$ can be interpreted similar to a penalty cost for not acquiring a property on which the CDC has made an offer.

Given this decision framework, the objective for the CDC is to determine a policy involving offer/no-offer decisions and overbid rates that maximize the expected total social-return accumulated over a given planning horizon. In the following sections, we first summarize the notation used in the model and then describe the model formulation.

4.1.1 Notation Used in the Model

b: Available accessible funds at any given time

B: Available accessible funds at the beginning of the planning period

c: Asking price for a foreclosed property

$\underline{C}, \bar{C}$: Minimum and maximum possible asking price for a property

$f(c)$: Marginal probability distribution of property asking prices

$f(r, c)$: Joint probability distribution of asking prices and property value impacts

$g(c, \delta_{bct})$: Overhead costs representing expenses required to make an offer on a property

G: Rate at which overhead costs are incurred defined as a percentage of the offer amount

$p(\delta_{bct})$: Probability of success for an offer on a property

r: Property value impact of a foreclosed property representing returns from acquisition

$\underline{R}, \bar{R}$: Minimum and maximum possible property value impact of a property

T: Time of budget expiration

$V(b_t)$: Expected total property value impact from an available budget b at time t

$x(\delta_{bct})$: Property value impact threshold used to decide whether an offer should be made on a property

α: Discount rate

δ_{bct}: Overbid rate defined as the percent difference between the asking price and offer amount

λ: Rate that foreclosed properties become available for acquisition

τ: Discretization factor used in the discrete approximations

4.1.2 Model Formulation

Note that when the CDC makes an offer of $c + c\delta_{bct} \leq b$ on a foreclosed property and the offer is accepted, for which the probability is $p(\delta_{bct})$, the property is going to be acquired and a social-return r, defined in terms of the associated PVI, will be realized. If the offer is not accepted, then the overhead expenses $g(c, \delta_{bct})$ are lost. These expenses do not come out of the acquisition funds, but rather from the general operating budget of the CDC, and are considered as lost social value. In addition, the PVI values of different acquisitions, which indirectly capture proximity effects, are additive from a social-return perspective as described in Harding et al. (2009). Given this framework, we let the value function $V\big(b_t\big)$ denote the maximum expected total PVI that can be achieved from time t until T using the remaining funds b, and note that the value function $V\big(b_t\big)$ satisfies the following dynamic programming recursion for $t < T$:

$$\begin{aligned} V\big(b_t\big) = \mathbb{E}_{C,R}\Bigg[\max\Bigg\{V\big(b_t\big), \max_{\substack{\delta_{bCt}\geq 0 \\ C+C\delta_{bCt}\leq b}} \Big\{\big[R + V\big((b - C - C\delta_{bCt})_t\big)\big]p(\delta_{bCt}) \\ + \big[V\big(b_t\big) - g(C, \delta_{bCt})\big]\big[1 - p(\delta_{bCt})\big]\Big\}\Bigg\}\Bigg] \qquad (4.1) \end{aligned}$$

Moreover, we have $V\big(b_T\big) = 0$ for all fund levels b. In the representation above, the two arguments in the first maximum operator correspond to no-offer/offer decisions, while the second maximum operator implies the selection of an overbid rate that would maximize the overall value. Note that the condition $C + C\delta_{bCt} \leq b$ for nonnegative δ_{bCt} in the second maximum operator models the budget constraint and implies that the value function remains the same if accessible funds are not sufficient to acquire a property with a given cost. Defining the expectation based on the distributions of C and R, equation (4.1) can be expressed as:

$$V\big(b_t\big) = \int_{\underline{C}}^{b}\int_{\underline{R}}^{\bar{R}} \max\Bigg\{V\big(b_t\big), \max_{\substack{\delta_{bct}\geq 0 \\ c+c\delta_{bct}\leq b}} \Big\{\big[r + V\big((b - c - c\delta_{bct})_t\big)\big]p(\delta_{bct})$$

$$+ \left[V\big(b_t\big) - g(c, \delta_{bct})\right]\left[1 - p(\delta_{bct})\right]\Big\}\Big\} f(r, c)\mathrm{d}r\mathrm{d}c \qquad (4.2)$$

It can be observed from the recursion that the optimal policy for a foreclosed property that becomes available at time t with an accessible fund level of b would be as follows. The CDC should make an offer on a property with asking price c and property value impact r using an overbid rate of δ^*_{bct} if $c + c\delta^*_{bct} \leq b$ and :

$$\left[r + V^*\big((b - c - c\delta^*_{bct})_t\big)\right] p(\delta^*_{bct}) + \left[V^*\big(b_t\big) - g(c, \delta^*_{bct})\right]\left[1 - p(\delta^*_{bct})\right] \geq V^*\big(b_t\big) \qquad (4.3)$$

where $V^*\big(b_t\big)$ denote the optimal value function, while the optimal overbid rate δ^*_{bct} is formally defined as $\delta^*_{bct} = \text{argmax}_{\delta_{bct}} \Big\{\left[r + V^*\big((b - c - c\delta_{bct})_t\big)\right] p(\delta_{bct}) + \left[V^*\big(b_t\big) - g(c, \delta_{bct})\right]\left[1 - p(\delta_{bct})\right]\Big\}$. Through some algebraic manipulation, condition (4.3) can be expressed as a PVI threshold policy. More specifically, the CDC should make an offer on a foreclosed property available for acquisition if accessible funds are sufficient and the PVI value of the property is greater than a threshold, i.e. if:

$$r \geq V^*\big(b_t\big) - V^*\big((b - c - c\delta^*_{bct})_t\big) + \frac{1 - p(\delta^*_{bct})}{p(\delta^*_{bct})} g(c, \delta^*_{bct}) \qquad (4.4)$$

Hence, to determine the optimal threshold value for fund level b at time t, a priori calculation of the optimal value functions $V^*\big(b_t\big)$ and overbid rates δ^*_{bct} is needed for all $b \in [0, B]$ and $t \in [0, T]$. We describe in the following sections how these values can be determined, and what their implications for CDCs are.

As part of our analysis throughout the rest of the study, we consider two types of practical decision making situations that the CDCs face: (1) an infinite horizon case where the accessible acquisition funds do not expire, i.e. funds can be used anytime, and (2) a finite horizon case where the unused amount of potentially accessible acquisition funds is assumed lost at the end of a fixed planning period such as a fiscal year. We study these two cases separately, and describe results about the optimal value functions and overbid rates for each case.

4.1.3 Optimal Foreclosed Housing Acquisition Policies with No Fund Expiration

A portion of funds potentially accessible by CDCs for foreclosed property acquisitions may not have usage deadlines, such as donations or lines of credit that they might have through private banks or other lenders. Such resources can be considered as funds without any expiration, implying that they can be used over an infinite time horizon. While CDCs would typically try to replace any funds used out of their lines of credit with funds from other sources, it is reasonable that a CDC, like any other similar organization, will do planning every six months or a year to determine an acquisition strategy based on their available lines of credit. In addition, while these lines of credit might involve cash flows due to property sales or other transactions, these can be assumed to be not affecting the acquisition decisions as they can be considered in the next period's planning due to the time delay in the redevelopment and sale of acquired properties. In this section, we address optimal acquisition policies under such conditions, which corresponds to the case with $T = \infty$. We specifically describe procedures for calculating optimal value functions, and characterize optimal policies including overbid rates to be used if an offer decision is made on a foreclosed property.

Given the stationarity of the probability distributions of foreclosed property asking prices, PVI measures, and the availability rates, as observed through analysis of historical data from 2009 to 2012, the value function for the case without fund expiration is independent of time t, and is thus denoted by $V(b)$. Moreover, a continuous discount rate of α is assumed for this case to reflect the time value of available funds and property value impacts of acquisitions. Our first result deals with the calculation of the optimal value functions. We note that under some very general assumptions, it is possible to solve for the optimal values of $V(b)$ through a recursive relationship as follows:

Theorem 1. *If accessible funds for foreclosed housing acquisition for a CDC do not expire, then the optimal expected total PVI for a given fund level b, denoted as $V^*(b)$, is the solution of the following equation:*

$$\begin{aligned}\alpha V^*(b) =& \lambda \int_{\underline{C}}^{b} \max_{\delta_{bc}} \bigg\{ \int_{x(\delta_{bc})}^{\bar{R}} p(\delta_{bc}) \Big(r - \big[V^*(b) - V^*(b - c - c\delta_{bc}) \\ &+ \frac{1 - p(\delta_{bc})}{p(\delta_{bc})} g(c, \delta_{bc}) \big] \Big) f(r, c) \mathrm{d}r \bigg\} \mathrm{d}c \end{aligned} \tag{4.5}$$

where $x(\delta_{bc})$ is the PVI threshold for making an offer and is defined as $x(\delta_{bc}) = V^*(b) - V^*(b - c - c\delta_{bc}) + \frac{1-p(\delta_{bc})}{p(\delta_{bc})} g(c, \delta_{bc})$.

Proof. All proofs are included in Appendix B.2. □

By evaluating the integral in Equation (4.5), the set of corresponding recursive relationships can be numerically solved to determine the optimal expected total PVI for each fund level $b \in [0, B]$, and thus the optimal overbid rates δ^*_{bc} and the PVI thresholds $x(\delta^*_{bc})$. For the optimal overbid rate, it is possible to numerically evaluate the recursion in (4.5) by considering a discrete set of overbid options, and then selecting the rate that results in the maximum expected total PVI. On the other hand, it is also possible to characterize the optimal overbid rate analytically under certain conditions. These characterizations are described through Theorem 2 as follows:

Theorem 2. *Let $\bar{K} = \max_{k \in \{\underline{R}, \bar{R}\}} \{\mathbb{E}(r | r \geq k) - k\}$. In addition, let $L(\delta_{bc}) = Gc\big(1 - p(\delta_{bc}) - \frac{p'(\delta_{bc})}{p(\delta_{bc})}(1 + \delta_{bc})\big)$ with $\bar{L} = \max_{\delta_{bc} \in [0, \bar{\delta}_c]} \{L(\delta_{bc})\}$ and $\underline{L} = \min_{\delta_{bc} \in [0, \bar{\delta}_c]} \{L(\delta_{bc})\}$ for a property with asking price c and PVI value of r.*

If accessible funds for foreclosed housing acquisition for a CDC do not expire, then the optimal overbid rate is approximately independent of the amount of accessible *funds, and the following policies are optimal for overbidding on a foreclosed property for which a CDC will make an offer:*

1. *If the condition $p'(\bar{\delta}_c)\bar{K} - \underline{L} \leq 0$ holds, then the CDC's offer should be at the asking price.*

2. *If the condition $\bar{L} \leq 0$ holds , then the CDC's offer should be at an overbid level of $\bar{\delta}_c$:*

3. *If the probability of success for an offer is a convex function of the overbid rate or if $-p''(\delta_{bc})\big[r - \underline{R} + Gc\big(\delta_{bc} + 1 - \frac{1-p(\delta_{bc})}{p(\delta_{bc})}\big)\big] \leq 2Gcp'(\delta_{bc})$ for all $\delta_{bc} \in [0, \bar{\delta}_c]$, then the CDC's offer should always be either at the asking price or at overbid level $\bar{\delta}_c$.*

An important implication of Theorem 2 is the independence of the optimal overbid rate from the amount of accessible funds, which suggests that $\delta^*_{bc} = \delta^*_c$ for all b. Hence, under some basic assumptions discussed in the proof of the theorem, the same overbid rate is optimal for a property at all fund levels. On the other hand, for the sake of completeness, we continue to use the subscript b when referring to the overbid rate throughout the study. The results in Theorem 2 can be used to help determine the amount to offer for a given property, while at the same time simplifying the solution of Equation (4.5) as the maximization over δ_{bc} will not be needed if any of the first two conditions listed are satisfied. Even when the two conditions do not hold, but the condition in item 3 applies, the solution is still simpler due to the conclusion that $\delta^*_{bc} \in \{0, \bar{\delta}_c\}$ under that case. Moreover, the conclusions can serve as a simple benchmark for offers made using arbitrary overbid rates. Note that if the conditions in Theorem 2 are not satisfied, then the optimal overbid rate can be obtained through enumeration of potential discrete values of δ_{bc}, and solving Equation (4.5) separately for each case.

An indirect result of the analysis in Theorem 2 involves the characterization of the relationship between the optimal overbid rate, the PVI thresholds, and the asking prices of the properties. The following result provides insights about these relationships which has implications about the overbid policy that the CDC should use:

Corollary 1. *For any PVI threshold level k, let $K = \mathbb{E}(r|r \geq k) - k$. The optimal overbid rate that the CDC should use under no fund expiration for a property with asking price c has the following properties:*

1. *The optimal overbid rate that the CDC should use is either 0, $\bar{\delta}_c$, or a solution of the equation $p'(\delta_{bc})K - L(\delta_{bc}) = 0$ for a PVI threshold level k.*
2. *The optimal overbid rate is nonincreasing in K.*
3. *The optimal overbid rate is nondecreasing in c.*

Given the dependence of optimal overbid rates and PVI threshold levels, item 1 in Corollary 1 indicates that for any threshold level k the optimal overbid rate can be obtained by solving the equation $p'(\delta_{bc})K - L(\delta_{bc}) = 0$. A solution lying in the range $[0, \bar{\delta}_c]$ would correspond to the optimal overbid rate. If all solutions are outside the range, then the optimal overbid rate is one of the boundary values. This result might also be helpful when an arbitrary PVI threshold is used. More specifically, it may be the case that the CDC uses a PVI threshold based on previous experience of the staff or based on existing organizational policies, and the results above would provide insights about the offer amounts to be made. Item 2 in Corollary 1 describes how the optimal overbid rate changes as a function of K, which depends on the distribution of the PVI values. A more direct result is item 3, which indicates that CDCs typically should use higher overbid rates for higher cost properties. This is likely due to the overhead costs being higher for those properties. In Figures 4.1(a) and 4.1(b), we demonstrate as an example how the optimal overbid rates vary as a function of K and c for a concave increasing function of probability of success in an offer.

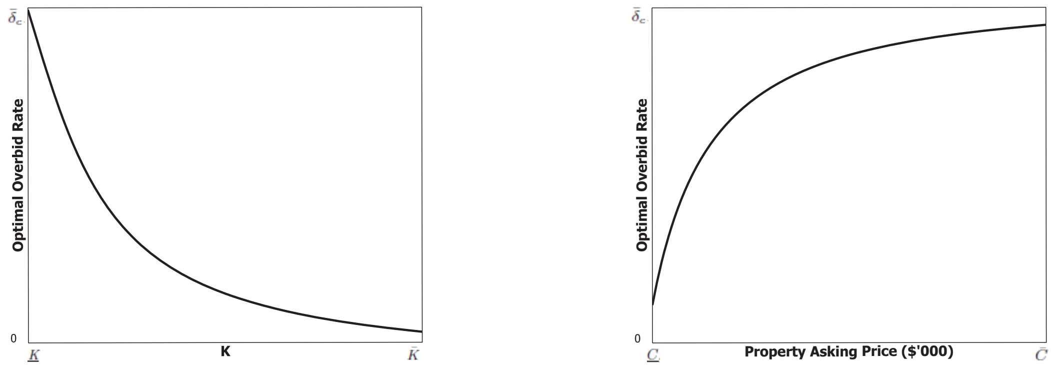

(a) Change in optimal overbid rate as a function of K

(b) Change in optimal overbid rate as a function of the property asking price

Figure 4.1. Demonstration of how optimal overbid rate changes as a function of K and property asking price for a PVI threshold k, when the probability of success in an offer is a concave increasing function of overbid rate.

Using the discussion above, it can be shown that for the case with uniformly distributed returns the optimal overbid policy can be expressed in a more compact form. We summarize this through the following corollary:

Corollary 2. *If the returns in the foreclosed housing acquisition problem are uniformly distributed, then the following policies are optimal on the overbid rate for a property with asking price c under no fund expiration:*

1. *If the condition $p'(\bar{\delta}_c)(\bar{R} - \underline{R}) - 2\underline{L} \leq 0$ holds, then the CDC's offer should be at the asking price.*

2. *The optimal overbid rate that the CDC should use is either 0, $\bar{\delta}_c$, or a solution of the equation $p'(\delta_{bc})(\bar{R} - k) - 2L(\delta_{bc}) = 0$ for a PVI threshold level k.*

Through further analysis, we also note some qualitative characteristics related to the optimal acquisition policy under the no fund expiration case. As part of this analysis we introduce two measures of practical relevance, which we refer to as the "critical fund level" and "critical time". The critical fund level is defined as the specific funding level such that the optimal policy for funds larger than that level is to make offers to all available properties that satisfy a minimum return requirement. Similarly, the critical time is the time period such that the optimal policy after that time period is to make offers to all available properties satisfying the minimum return requirement. For the no fund expiration case, the optimal thresholds are constant over time, so the critical time is either 0 or ∞. Hence, this measure becomes more relevant when the funds expire at a certain time, which we discuss later. Given these additional definitions, we summarize some important characteristics for the optimal foreclosed housing acquisition policy as follows:

Theorem 3. *The following conditions always hold for the foreclosed housing acquisition problem with no fund expiration:*

1. *The larger the amount of accessible funds, the higher the expected total PVI value to be realized from foreclosed property acquisitions.*

2. *The higher the availability rate of foreclosed properties, the higher the optimal PVI thresholds that a CDC should use.*

3. *The marginal value of accessible funds decreases as the fund amounts get larger, if optimal PVI thresholds are decreasing in the amount of accessible funds.*

4. *Let $\dot{\delta}_{bc}$ be a solution to the equation $p(\delta_{bc})\big(1 - p(\delta_{bc})\big) - p'(\delta_{bc})(1 + \delta_{bc}) = 0$. If there is a unique solution $\dot{\delta}_{bc} \in [0, \bar{\delta}_c]$ or if $\dot{\delta}_{bc} > \bar{\delta}_c$, then for all $\delta_{bc} \in [0, \dot{\delta}_{bc}]$, the higher the PVI threshold used by the CDC, the higher the overbid rate should be. For all, $\delta_{bc} \in [\dot{\delta}_{bc}, \bar{\delta}_c]$ or if $\dot{\delta}_{bc} < 0$, the higher the PVI threshold used by the CDC, the lower the overbid rate should be.*

5. *If optimal PVI thresholds are increasing in overbid rate, then the higher the overbid rate used, the higher the critical fund level.*

6. *The critical fund level and the marginal value of accessible funds are constant over time.*

The first result is an intuitive conclusion that the higher the amount of accessible funds, the more value they have in terms of the total PVI that can be achieved from acquired properties. Similarly, item 2 in Theorem 3 is also somewhat intuitive, as it indicates that a CDC should be more selective if acquisition options arrive at a higher rate. The third conclusion is due to the concavity of the total expected PVI value from acquisitions under the stated condition of being less selective when operating with larger funding levels. In that case, the marginal value of available funds will be higher as the remaining amount of accessible funds gets lower. The property described in the fourth item in Theorem 3 implies that the relationship between PVI thresholds and overbid rates vary over the range of overbid rates. If a CDC has a policy to overbid at a rate lower than $\dot{\delta}_{bc}$, then they should use higher overbid rates only when an offer is made on a property with a larger PVI value. However, if the CDC's policy is to offer above $\dot{\delta}_{bc}$, then they can use higher overbid rates for properties with lower PVI values. As the fifth item, we note that if the CDC uses high overbid rates and high thresholds, then the critical fund level will get higher as the overbid rate increases. In other words, usage of higher overbid rates would result in the CDC stopping being selective earlier. Finally, given that the no fund expiration case assumes an infinite planning horizon, the optimal threshold policy and thus the critical fund level and the marginal value of accessible funds are the same at all times.

4.1.4 Optimal Foreclosed Housing Acquisition Policies with Fund Expiration

Another important case for CDCs' foreclosed housing acquisition process is when they face deadlines for utilizing the potentially accessible acquisition funds. This is typically the case when the providers of the funds stipulate that they are used within a given time frame. For example, the funds that were made available to CDCs by the federal government as part of the Neighborhood Stabilization Program over the last few years required that these funds were used by the end of 2012 Stable Communities (2012).

Utilizing a similar structure as the infinite horizon case, in this section we characterize the optimal foreclosed housing acquisition policies for CDCs when they have time-based limitations for using the accessible funds, which we broadly refer to as foreclosed property acquisition under fund expiration. This introduces a time-dependent decision structure, where the optimal offer decisions depend on the remaining time before expiration. We first note through Theorem 4 below that the optimal expected total PVI at a given time for different remaining fund levels can be found by recursively solving a set of differential equations:

Theorem 4. *If accessible funds for foreclosed housing acquisition for a CDC expire at a finite time T, then the optimal expected total PVI for a given funding level b at time t, denoted as $V^*\big(b_t\big)$, is the solution of the following differential equation:*

$$\frac{\partial V^*\big(b_t\big)}{\partial t} = -\alpha V^*\big(b_t\big) + \lambda \int_{\underline{C}}^{b} \max_{\delta_{bct}} \Bigg\{ \int_{x(\delta_{bct})}^{\bar{R}} p(\delta_{bct}) \Big(r - \big[V^*\big(b_t\big) - V^*\big((b - c - c\delta_{bct})_t\big) + \frac{1 - p(\delta_{bct})}{p(\delta_{bct})} g(c, \delta_{bct}) \big] \Big) f(r, c) \mathrm{d}r \Bigg\} \mathrm{d}c \tag{4.6}$$

where the PVI threshold $x(\delta_{bct})$ is defined as $x(\delta_{bct}) = V^*\big(b_t\big) - V^*\big((b - c - c\delta_{bct})_t\big) + \frac{1-p(\delta_{bct})}{p(\delta_{bct})} g(c, \delta_{bct})$.

Note that in the representation above we slightly abuse the notation, and show the time dependence of the value function through the subscript t in the budget notation b_t. Our utilization of a discount factor in the fund expiration case is mostly due to completeness in capturing the time value of available funds over the planning horizon which might be long enough to justify discounting. Moreover, we note that the funds with expiration are typically government grants and are not paid back. Equation (4.6) represents a set of ordinary differential equations which can not be solved analytically. Thus, these equations need to be solved numerically as a system, possibly in a recursive way. On the other hand, a discretization approach is possible for improved computational efficiency in the numerical analysis. In addition to its computational implications, the discrete-time based approach also approximates the actual decision process of CDCs whose acquisition related decisions are periodic. As part of the discrete time approximation, let τ be the discretization factor such that the minimum time between two consequent decisions is defined by T/τ. Based on this representation, equation (4.6) can be approximated by:

$$\begin{aligned} V^*(b_{t-T/\tau}) =&(1-\alpha)V^*\big(b_t\big) + \frac{T}{\tau}\lambda \int_{\underline{C}}^{b} \max_{\delta_{bct}} \Bigg\{ \int_{x(\delta_{bct})}^{\bar{R}} p(\delta_{bct})\Big(r - \big[V^*\big(b_t\big) \\ &- V^*\big((b-c-c\delta_{bct})_t\big) + \frac{1-p(\delta_{bct})}{p(\delta_{bct})} g(c,\delta_{bct})\big]\Big) f(r,c)\mathrm{d}r \Bigg\} \mathrm{d}c \qquad (4.7) \end{aligned}$$

where the solutions converge to the actual optimal value functions as $\tau \to \infty$.

While the optimal total PVI for a given fund level at a given time can be calculated through Theorem 4, the identification of the optimal overbid rates adds to the complexity of the problem as discussed in Section 4.1.3, as it would typically involve enumeration over a discrete set of overbid rates. On the other hand, we show through Theorem 5 below that similar results as in the no fund expiration case apply to the fund expiration case as well:

Theorem 5. *For the foreclosed housing acquisition problem with fund expiration, the optimal overbid rate is approximately independent of time and the amount of accessible funds, and thus the optimal policy for overbidding on a foreclosed property for which a CDC will make an offer is same as the case with no fund expiration.*

More specifically, Theorem 5 states that the introduction of a time dimension would have a negligible impact on the optimal overbid policy, and that the same results as those described in Theorem 2, Corollary 1 and Corollary 2 apply to the fund expiration case as well. These properties can help identify the optimal overbid rate for a CDC or simplify the solution of (4.6). In addition, further practical implications for the foreclosed housing acquisition problem with fund expiration can also be derived on the value functions and threshold levels, which we summarize through Theorem 6 as follows:

Theorem 6. *The following conditions always hold for the foreclosed housing acquisition problem with fund expiration:*

1. *Results 1, 2, 3, 4, and 5 in Theorem 3 apply to the foreclosed housing acquisition problem with fund expiration.*
2. *The expected total PVI value of accessible funds decreases over time.*
3. *The marginal value of accessible funds decreases over time.*
4. *Optimal PVI thresholds decrease over time.*
5. *The critical fund level decreases over time.*
6. *If optimal PVI thresholds are increasing in overbid rate, then the higher the overbid rate used, the later the critical time.*
7. *If optimal PVI thresholds are decreasing in the amount of accessible funds, then the larger the amount of accessible funds, the earlier the critical time.*

The first statement in Theorem 6 indicates that some structural characteristics of the no fund expiration case also apply to the problem with fund expiration, and thus their interpretations are the same as those described in Section 4.1.3. Items 2 and 3, on the other hand, imply that the value of available funding decreases over time if not used, and moreover the rate of change is higher as it gets closer to the fund expiration date. The fourth item is related to the PVI threshold levels and indicates that a CDC would be better off by gradually being more aggressive, i.e. less selective, in making offers to foreclosed properties as time progresses towards fund expiration. Similarly, other results in Theorem 6 help estimate the behavior of the optimal policy as well. More specifically, item 5 states that as a CDC becomes less selective in acquisitions over time, the critical fund level indicating an offer decision for all available properties above the minimum return requirement also decreases over time. In item 6, we note that usage of high overbid rates by a CDC would imply that they should begin making offers to all properties above the minimum return requirement at a later time than if they were to use lower overbid rates. Finally, result 7 suggests that for any two different fund levels, it should be expected that, under the stated condition, the larger funds would imply an earlier switch to making offers to all available properties above the minimum return requirement.

4.2 Real-Life Implementation and Policy Implications of the Models in Foreclosed Housing Acquisition

The optimal policies described in Section 4.1 are quite general and address different types of problem configurations. In this section, we use these general results to identify policies that apply to the decision framework *currently* faced by many CDCs. To this end, we utilize real numerical data as input to our models to provide guidelines for the foreclosed housing acquisition process of a typical CDC, which is considered to be reflective of CDCs operating in similar urban neighborhoods.

4.2.1 Description of Data

Data based implementation and analysis of the foreclosed housing acquisition problem was performed in close coordination with the CDC located in the city of Boston, Massachusetts. This CDC was also involved in the model building phase of the study. While there is no comprehensive quantitative information that compares the operating framework for this CDC to that of other CDCs, there is anecdotal evidence that the CDC studied can be representative of typical CDC operations in other major cities (NeighborWorks, 2009; Gass, 2010). This is also supported by the

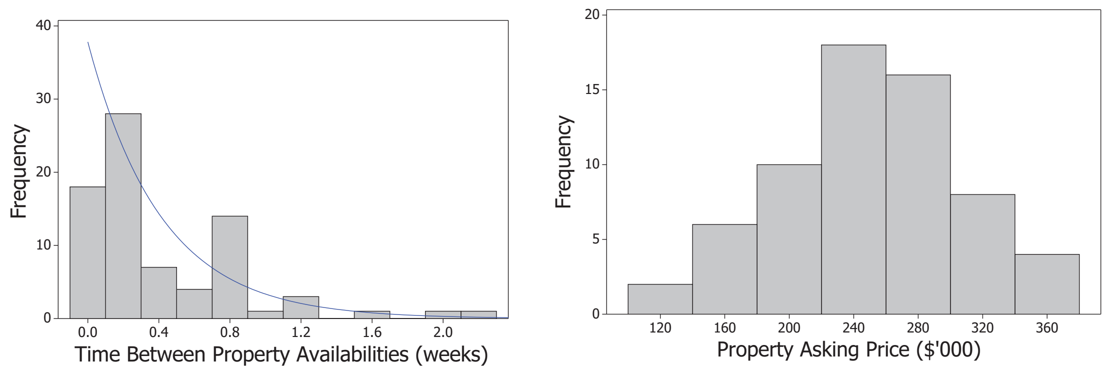

(a) Distribution of availability times for acquisition

(b) Distribution of asking prices

Figure 4.2. Distributions of asking price and market entry times of foreclosed properties in the CDC's service area.

fact that PVI distributions calculated for a different CDC in an entirely different area of Boston, Massachusetts reflect similar characteristics as those obtained for the service area studied in this study Johnson et al. (2013).

The decision making situation faced by this CDC involves managing funds that they can potentially access for acquiring foreclosed properties in their service area. Similar to our categorization of the two problem types, these funds differ in their usage requirements. The acquisition process for the CDC starts with their notification of a property becoming available for acquisition in their service area. The CDC then gathers information about the property, specifically with respect to the asking price and the potential returns to be realized if the property is acquired and redeveloped. Given such information, the CDC decides whether to work with a funder to make an offer on the property and how much to offer.

To characterize the actual decision problem parameters, as well as the uncertainty in property costs and returns, data based on recent historical foreclosed property availabilities and acquisitions were used. This data was directly obtained from the records of the CDC that we worked with and is available upon request. Based on this data, an average of approximately 10 properties were observed to be entering the market each month following a Poisson distribution, which corresponds to an average availability rate of 2.5 properties/week. A histogram showing the distribution of the time between property availabilities is included in Figure 4.2(a). While this number is likely to fluctuate based on the conditions of the economy and the housing market, it reflects a practical quantity for the current state of the economy. On the other hand, our analysis later in this section involves a sensitivity study around this availability rate value. In Figure 4.2(b), we show the asking price distribution for the properties considered in the data set, which implies a triangular distribution with parameters of 120, 250 and 380 thousand dollars.

The distribution of the PVI values for the same data set, as calculated through the methodology described in Johnson et al. (2013), is shown in Figure 4.3(a). The best fitting distribution for the PVI values is uniform between 60 and 120 thousand dollars. Moreover, the PVI values of the properties are found to be independent of their asking prices as reflected in the scatter plot in Figure 4.3(b), which also includes a regression line. Hence, we assume independent distributions for asking prices and the PVI measures. This independence structure is likely because lower cost properties can have higher impacts on the values of nearby properties, especially if they are located in dense neighborhoods. Similarly, a higher priced property does not necessarily imply higher social value from a CDC's perspective, e.g. in the case of a property with few proximate properties.

The overhead costs for the CDC for each offer that they make on a property are calculated to be around 1.5% of the amount offered on the property. As discussed in the model description, the probability of acquisition after an offer on a property depends on the overbid rate used for a given asking price. Using data from previous acquisitions, and also based on consultations with the CDC staff, we define this probability as $p(\delta_{bct}) = 0.22\delta_{bct} + 0.37$. Note that this probability assumes that the CDC's offer is competing only with owner occupants and public entities as part of the

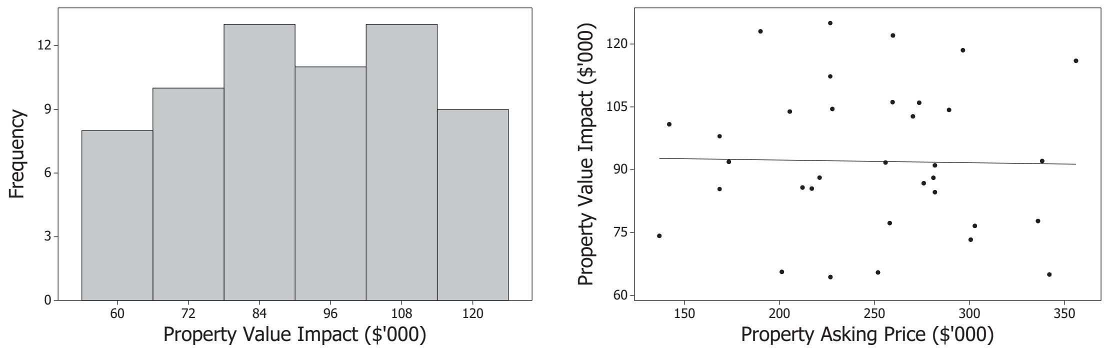

(a) Distribution of PVI values

(b) Relationship between asking prices and PVI values

Figure 4.3. Distribution of PVI values and their dependency on asking prices for foreclosed properties in the CDC's service area.

early opportunity to bid for a foreclosed property. The structure of this probability of success function is also consistent with the discussions and function descriptions by Holt and Sherman (2000) and Aobdia and Caskey (2012) for similar settings.

Given this framework, the CDC needs to decide on how to utilize the funds that they can potentially access with and without fund expiration conditions. Since the grant based funds are prioritized in making the acquisitions, the decisions for the two sources do not need to be considered together. Based on available information, we assume a $4 million fund level for both finite and infinite horizon implementations, but we also analyze the optimal policies for other fund levels.

4.2.2 Implementation and Analysis under No Fund Expiration

Our first implementation and analysis are for the case without fund expiration, which refers to the usage of resources that do not have certain deadlines. Using the numerical data provided, we specifically try to develop numerical insights on the policies that should be used by the CDC.

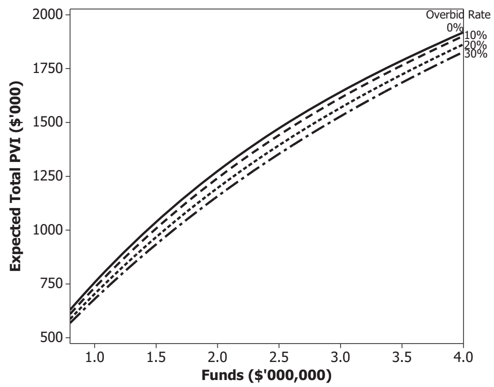

(a) The change in the expected total PVI as a function of accessible funds for different overbid rates

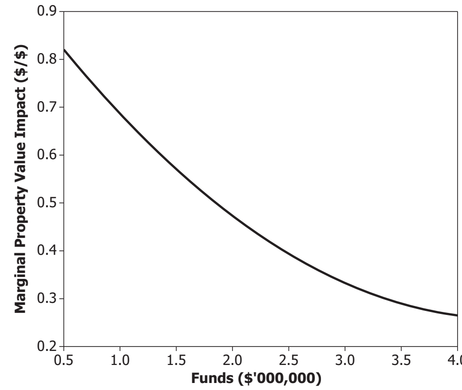

(b) The change in the marginal value of accessible funds

Figure 4.4. Optimal expected total PVI for different funding levels and the marginal value of funds under no fund expiration.

4.2.2.1 Optimal Expected Property Value Impact

For a fund level of $4 million without an expiration deadline, the current expected PVI to be realized through the foreclosed property acquisitions by the CDC is around 1.9 million dollars. Note that the expected PVI is independent of time due to the funds not expiring and only being subject to discounting. This value decreases for lower fund levels as shown in Figure 4.4(a) through the top curve corresponding to an overbid rate of 0%. It can be observed that the optimal expected value is a nondecreasing concave function of the remaining amount of funds. While we discuss the optimal overbid rates and their implications later in this section, as some additional information, Figure 4.4(a) also includes the impact of using different overbid rates on the optimal value function under the assumption that the same overbid rate is used for all properties. Although the differences are not that large, the value function can be observed to be decreasing as the overbid rate is increased.

Clearly, the value of the accessible funds for a CDC, in terms of its potential PVI based returns, is constant over time given an infinite horizon setting. On the other hand, a relevant question involves the marginal value of these resources. For

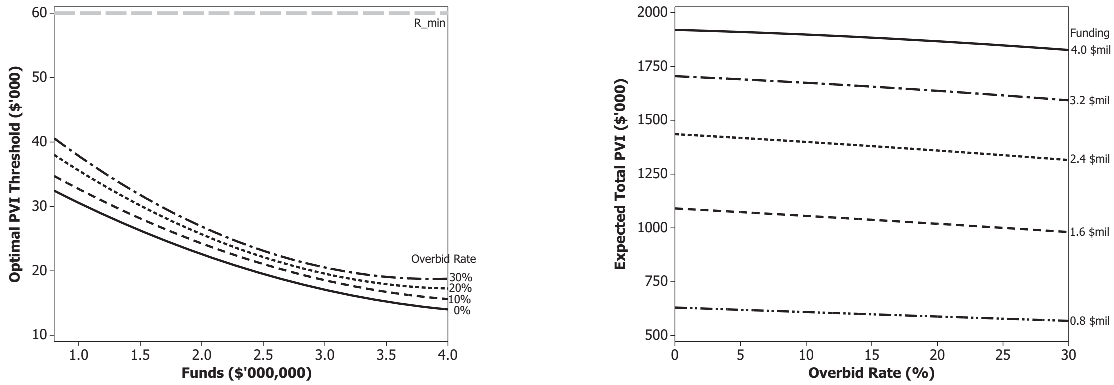

(a) The change in the optimal PVI thresholds as a function of available funds for different overbid rates

(b) The change in expected total PVI as a function of overbid rate for different funding levels

Figure 4.5. Optimal PVI thresholds and the change in expected total PVI for different funding levels and overbid rates under no fund expiration.

example, the marginal impact of a reduction in the acquisition funds can play a role when a CDC faces a decision on whether to use part of their available line of credit for purposes other than foreclosed property acquisition. As can be seen in Figure 4.4(a), the marginal return decreases as the fund level is increased. In Figure 4.4(b) we quantify this change over fund levels, which can be used by CDCs for budgeting purposes. *While each dollar of accessible funds is expected to result in about \$0.8 of PVI at a fund level of \$0.5 million, this marginal PVI impact reduces to around \$0.3/dollar at the \$4 million fund level.*

4.2.2.2 Optimal PVI Thresholds for Offer/No-Offer Decisions

A policy implication for the infinite horizon problem is that, assuming a discount rate and no time limitation for using the accessible funds, the CDC should work with the funding source and make an offer on all properties that satisfy the minimum PVI level, which is \$60 thousand for the given data. Indeed, this threshold is much lower, around \$20 thousand for a general implementation. This is based on the analysis of the optimal PVI thresholds as illustrated in Figure 4.5(a) where the lighter dashed horizontal line in the plot represents the minimum possible PVI of any acquired property. Hence, a PVI threshold less than this value implies that all properties in the market should be made an offer. It can be observed that even at lower funding levels the optimal policy is not selective, i.e. an offer is made on all properties with PVI values of at least $30 thousand. Given that the current numerical setup is likely to be reflective of most urban neighborhoods, specifically with respect to the PVI distributions as shown through a numerical study, this result might be applicable to a large number of CDCs. Such a result might be due to the interaction between property availability rates and the discounting effects. The value of the current funds will decrease over time based on a standard discount rate, and the CDC might be better off by acquiring properties early before the present value of the funds decreases. Moreover, the current average availability rate of 2.5 properties per week, while quite high historically, is still not significant enough to justify a highly selective policy. We later describe a sensitivity analysis that shows how increases in availability rates impact these optimal policies .

We note that in general the marginal change in the PVI thresholds decreases as a function of the funding level as observed in Figure 4.5(a). In other words, having access to larger amount of funds implies less selectivity in making offers to foreclosed properties in the market. In Figure 4.5(a), we also illustrate that the optimal PVI threshold is a nonincreasing convex function of the remaining funds, and that the threshold value is higher if a high overbid rate were to be used for the offers. In addition, as also mentioned in Section 4.1.3, a critical fund level can be identified such that at that funding level the threshold drops below the minimum realizable PVI values. Hence, for any remaining fund level that is greater than the critical fund level, the CDC would make offers to all available properties satisfying the minimum PVI level of $60 thousand, while a more selective policy can be used for fund levels that are less than the critical fund level based on the optimal PVI thresholds. On the other hand, while not shown explicitly, we observe through Figure 4.5(a) that the critical fund level for this numerical setup is very small, i.e. much less than \$0.5 million.

4.2.2.3 Optimal Overbid Rates

The optimal overbid rate for the types of CDCs studied is at the minimum possible level for all properties, i.e. the CDC should not offer more than the asking price for any foreclosed property. This result implies a different policy than what is used in practice, and is a result of the characteristics of the current data. We show in Theorem 2 the ranges of cases where the optimal overbid rate is not zero. In Figure 4.5(b), we illustrate the changes in the optimal expected PVI as a function of the overbid rate for different remaining amounts of accessible funds. These representations visually show the optimal overbid rate to be zero. On the other hand, the differences in value and threshold levels are not huge for different overbid rates. In general, it can be observed that the optimal expected PVI is a decreasing function of the overbid rate, while the threshold is increasing in the overbid rate. This result is consistent with both our analytical findings and the expert views from the CDC staff. One potential reason for this conclusion is that the overhead costs are not that significant when compared with other costs such as the losses due to discounting, while at the same time there exist a relatively large number of foreclosures in the CDC's service area. The result holds even when the overhead costs are increased to higher levels than 1.5% of the asking price. Therefore, even if the CDC's offer is not successful, it is likely that there will be other properties with comparable PVI values that will become available. This also implies that the shape of the PVI distribution might have an impact on the overbid rate decisions, and thus our finding may be a result of the distribution observed in practice. We also note that the optimal overbid rate values can serve as a benchmark such that they could be the maximum to be accepted in a negotiation.

4.2.3 Implementation and Analysis under Fund Expiration

In this section we analyze the optimal policies for the case where any accessible but unused funds have no value after a finite expiration date. As noted previously, this is typically the case for grants that the CDC can receive for foreclosed housing acquisitions, which may have stipulations such that they need to be expended within a certain time frame. Our analysis follows a similar structure as in the infinite horizon case.

4.2.3.1 Optimal Expected Property Value Impact

For an accessible funding level of $4 million to be used within a year, the optimal expected total PVI due to foreclosed property acquisitions by the CDC is approximately $1.8 million under the optimal policy. As observed in Figure 4.6(a), this value decreases over time if the funds remain unused. For higher fund levels the *rate of reduction in value when accessible funds are not used is mostly linear at an average rate of $7,000 per week until around the last three months of the year.* After that point, the expected total PVI decreases sharply. Hence, the CDC should try to utilize their accessible funds earlier rather than later. Moreover, the marginal value of accessible funds does not significantly diminish for higher fund levels, or rather the rate of decrease is very slow, especially in the first three quarters of the planning year. Hence, higher levels of accessible funds are likely to result in proportionally higher total PVI. We quantify these observations in Figure 4.6(b) by displaying the change in marginal PVI values over fund levels and time. *Per dollar PVI returns of potentially accessible acquisition funds decrease from $0.6 at a fund level of $0.5 million to $0.4 at a fund level of $4 million.* This difference is less than that of the case without fund expiration, where both the marginal values and their rate of change over fund levels are higher. It can also be observed that the behavior of the marginal

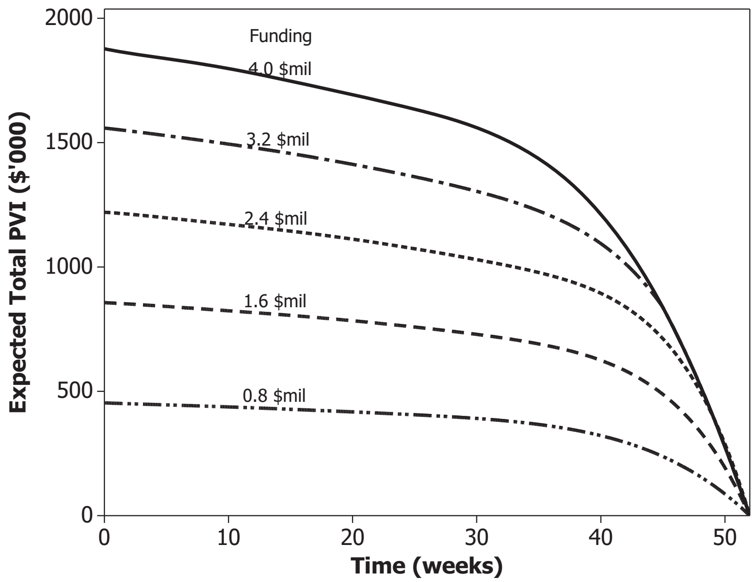

(a) The change in expected total PVI over time for different funding levels

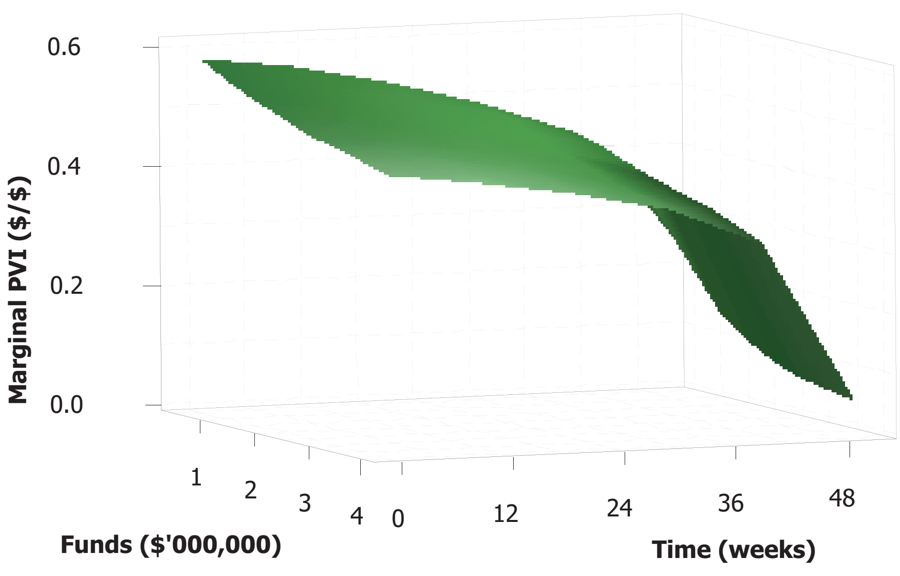

(b) The change in the marginal value of accessible funds over time

Figure 4.6. Optimal expected total PVI for different funding levels and the marginal value of accessible funds over time under fund expiration.

values at different fund levels over time is similar with a slow rate of decrease until the last three months of the planning period, followed by a sharp decline afterwards.

4.2.3.2 Optimal PVI Thresholds for Offer/No-Offer Decisions

For low annual accessible fund levels, i.e. less than around \$1.5 million, the CDC should employ a selective strategy based on the optimal PVI thresholds shown in Figure 4.7(a). For example, for accessible funds of around \$1 million, initially offers should be made only to those properties with a PVI value greater than \$65 thousand. In addition, we note that the marginal change in the PVI thresholds decreases as a function of the amount of accessible funds. In other words, selectivity increases significantly at lower fund levels. On the other hand, at higher levels of accessible funds and for the given foreclosure rates, the optimal policy for the CDC is to make offers to all available foreclosed properties above the minimum PVI level of \$60 thousand when a finite planning horizon of one year is assumed. As can be seen in Figure 4.7(a), for these funding levels the optimal PVI threshold is always below the minimum PVI level. This is another demonstration of the impact of the available funds in the acquisition decisions, where larger funds enable more aggressive acquisition policies.

We also perform a sensitivity analysis over different availability rates, and observe how the optimal PVI thresholds change as the availability rate increases. The case where availability rates decrease is not so interesting, as it would imply even lower threshold levels which will be further less than the minimum possible PVI level. In Figure 4.7(b) we display the optimal PVI threshold graph for an average availability rate of 5 properties per week, which represents foreclosure rates twice the current levels. In this case, a highly selective policy is optimal at all fund levels until around the last quarter of the planning period. This indicates that under the given numerical setting *CDCs should become highly selective in acquisitions only if foreclosure rates*

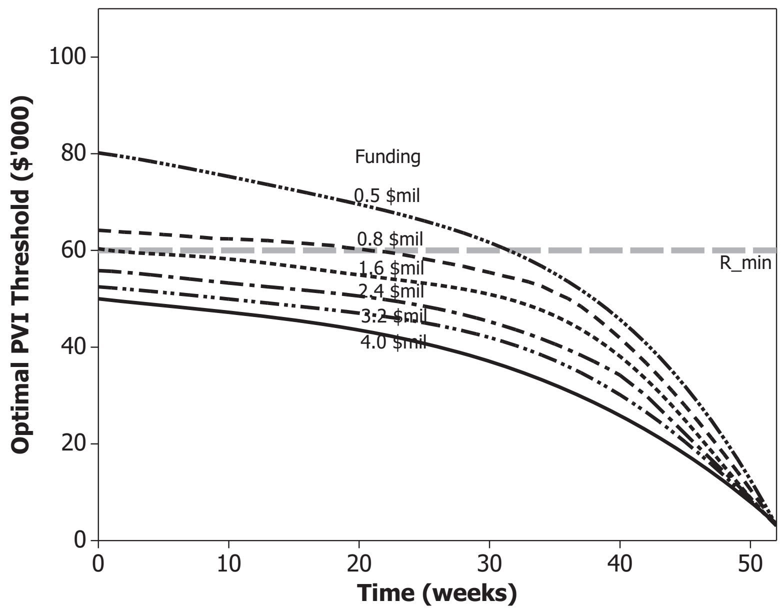

(a) Optimal PVI thresholds over time for an average availability rate of 2.5 properties/week

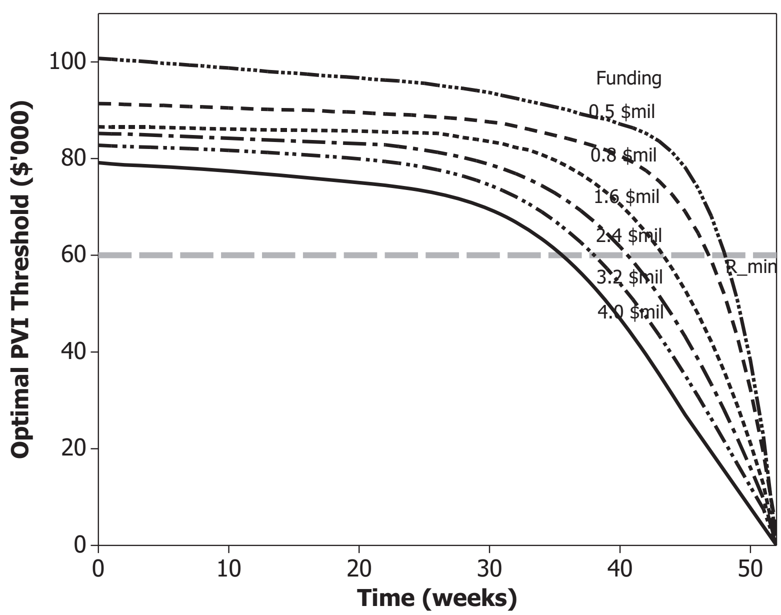

(b) Optimal PVI thresholds over time for an average availability rate of 5 properties/week

Figure 4.7. The change in optimal PVI thresholds over time for different availability rates.

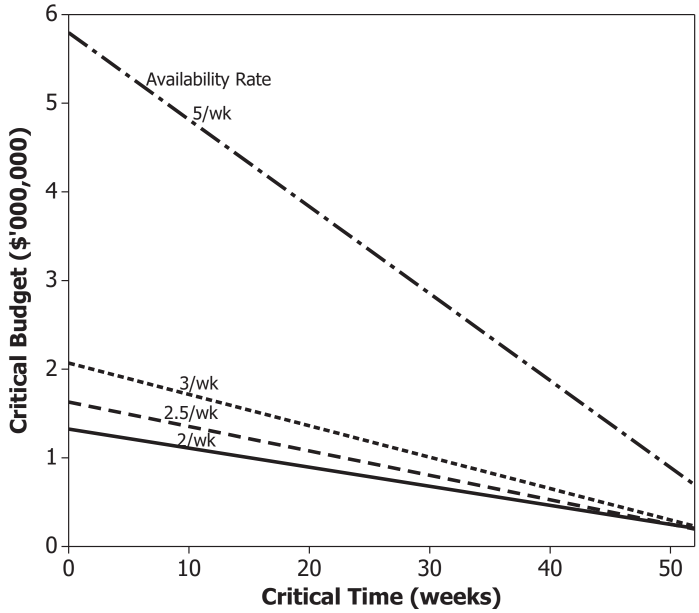

Figure 4.8. The change in critical fund level over time for different availability rates

become worse than the current levels. Related to this analysis, Figure 4.8 contains information about the critical time and critical fund level levels for different availability rates for an initial funding level of $4 million. This diagram can be used to identify the critical fund level for a given time or the critical time for a given budget for the given availability rate. For example, if the average availability rate is 5 properties/week, then the CDC should not be as selective and make offers to all properties with PVI values above $60 thousand when the current time and available budget combination falls in the region above the dashed line corresponding to 5 properties/week. As another example, the CDC should start making offers to all such properties in the 20th week of a budget period if the potentially accessible funds at that time are greater than $4 million, while this critical level is $1 million for an availability rate of 2 properties/week. Overall, based on the slopes of the lines in Figure 4.2.3.1, we note that critical fund level increases significantly at high availability rates. Similarly, critical time for a given fund level decreases with a higher rate for high availability rates.

4.2.3.3 Optimal Overbid Rates

We conclude that, contrary to the current practice, for the given numerical setting the *CDC does not need to overbid on foreclosed properties and should typically offer the asking price*. This result is similar to the infinite horizon case, and is again possibly due to relatively lower overhead costs and the variance of the PVI values of properties. Figure 4.9 shows the changes in optimal expected PVI and PVI thresholds as a function of overbid rates for different amounts of remaining funds. The optimal expected total value can be seen to be a nonincreasing, almost linear function of overbid rate. On the other hand, the PVI threshold is a nondecreasing function of overbid rate, implying that selectivity increases for higher overbid rates.

4.2.4 Value of Optimal Policies

In this section we describe a comparative study aimed at demonstrating the value of the optimal policies with respect to current practice and other simplistic heuristic procedures. The analysis is based on historical bidding and acquisition data obtained from the CDC that has been collaborated with. This data consists of information on a set of properties which were considered for potential acquisition and an offer/no offer decision was made. In Table 4.1 we show part of this information, which includes the asking price and the estimated PVI value for each property, whether an offer was made on the property and the overbid rate used. Current practices used by the CDC when considering an offer decision do not involve a systematic structure, and are mostly based on qualitative and subjective expert opinions. An important observation is that the CDC is selective in making offers, and almost always overbids on the properties for which an offer decision is reached. Contrary to this implementation, the optimal policy suggests that an offer decision should be made on all candidate properties, and that there is no need for overbidding. For our comparative study, we assume an accessible funding level of $1 million and calculate the expected total discounted

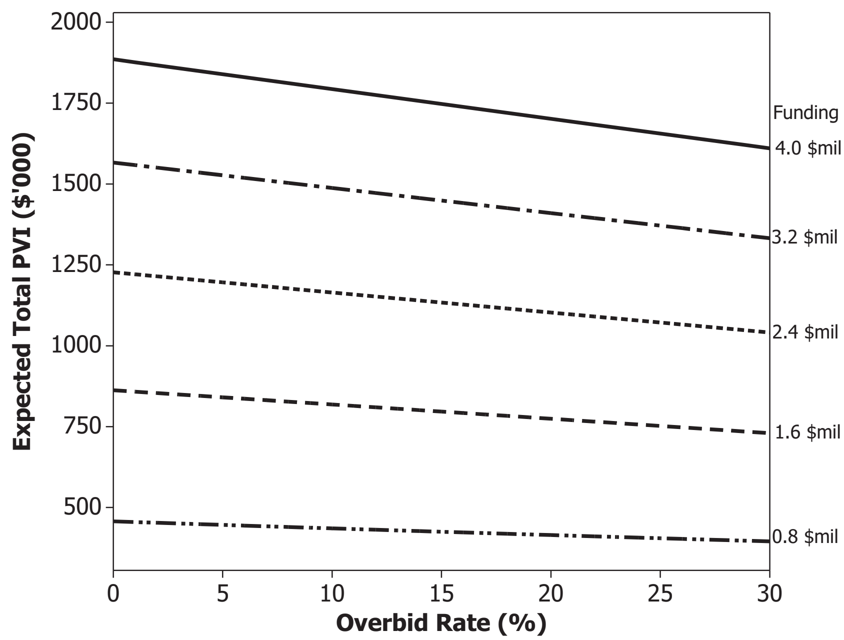

(a) The change in expected total PVI

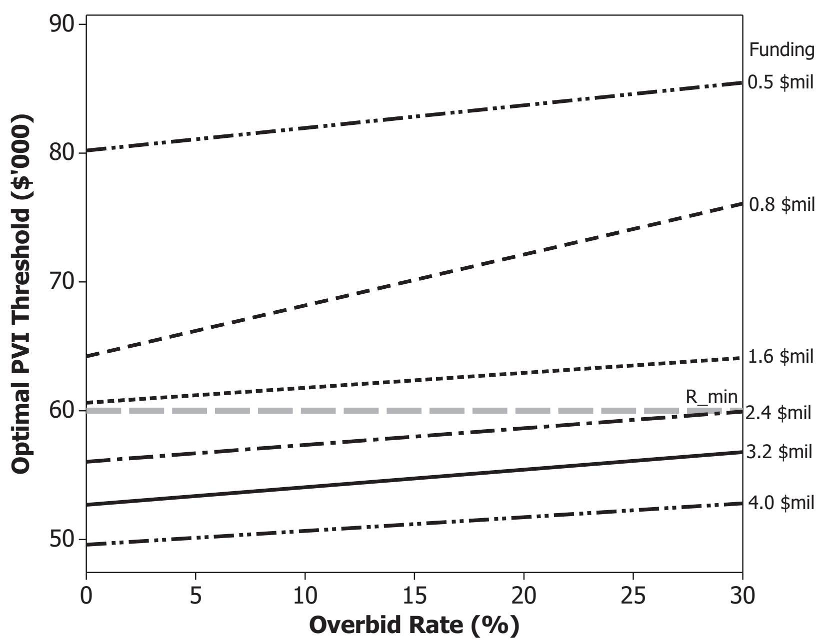

(b) The change in optimal PVI thresholds

Figure 4.9. Optimal expected PVI values and PVI thresholds as a function of overbid rate for different funding levels under fund expiration.

ID	Asking Price	Estimated PVI	Offer Made?	Overbid Rate	Outcome
1	$164,500	$85,401	Yes	4.6%	Lost
2	$170,360	$91,896	Yes	5.6%	Acquired
3	$201,250	$75,628	Yes	4.5%	Lost
4	$205,400	$103,884	Yes	9.6%	Lost
5	$221,100	$88,122	No	-	-
6	$226,700	$112,285	No	-	-
7	$227,800	$104,507	No	-	-
8	$212,100	$85,767	No	-	-
9	$214,000	$85,513	Yes	5.2%	Acquired
10	$190,000	$105,989	Yes	0%	Acquired
11	$142,000	$100,850	Yes	7.2%	Lost
12	$259,700	$122,034	No	-	-
13	$259,500	$106,138	No	-	-
14	$296,500	$108,519	Yes	3.2%	Acquired
15	$338,200	$92,093	Yes	3.5%	Lost
16	$226,800	$64,390	No	-	-
17	$125,000	$75,620	No		-
18	$150,000	$88,765	Yes	6.7%	Lost
19	$184,900	$93,487	Yes	5.4%	Lost

Table 4.1. Summary information on a set of properties considered for potential acquisition by the CDC.

PVI that would have been achieved if the optimal policy were implemented on the properties in the data set. This value is then compared with the total discounted PVI achieved through the actual offer and acquisition decisions. Similarly, we test the efficiency of two heuristic selection criteria by calculating the corresponding expected total PVI values if they were to be implemented for the sample data set. The two heuristics have a somewhat similar setup. In the first heuristic, an offer decision is reached if the standardized marginal return of a given property is greater than 0.5, while the offer price is selected as the asking price. In the second heuristic, offer/no-offer decisions are made similarly, but the overbid rate used is assumed to be the average overbid rate in current practice, i.e. 5%. In Table 4.2 we show the differences in expected total discounted PVI values based on multiple simulated bid outcomes for the four cases, as well as the average time it takes to use the accessible funds of $1 million for each case.

	Expected Total Discounted PVI	% Difference from Implemented	Fund Usage Time (months)
Implemented Policy	$380,159	-	2.5
Optimal Policy	$445,727	17.2%	1
Heuristic-1 Policy	$415,478	9.3%	5
Heuristic-2 Policy	$399,886	5.2%	4

Table 4.2. Comparison of different policies based on historical property availability data.

Based on the results of this comparative analysis, it can be observed that the optimal policy improves the expected total PVI of a funding level of $1 million by about 17%, when compared with the PVI levels realized from the historically implemented offer/no-offer decisions. The superiority of the optimal policy is also visible over the heuristic policies that were based on marginal returns of properties. Similarly, it can be noted through a comparison of the two heuristics that overbidding still does not add value when it is used as part of a less aggressive strategy such as the marginal return based heuristic evaluated. Overall, we observe that a systematic approach to acquisition decisions of a CDC through the simple optimal policy results is likely to be of value in terms of the societal response to the foreclosure problem through property value impact reduction.

4.3 Conclusions

In this chapter we developed, implemented and evaluated a dynamic and stochastic decision model that aims to assist community-based organizations to choose foreclosed properties for potential acquisition in the service of community stabilization and revitalization, specifically in response to the increase in foreclosures due to economic decline. We considered two practical planning situations based on whether the potentially accessible funds need to be used by a certain deadline or not. For both cases, we derived analytical results for calculating optimal return thresholds that a

CDC can use to determine which properties they should work with their funders on and make an offer. We also determined policies for overbidding on a property given that probability of success for an offer depends on the amount offered on that property. The policies were implemented in a numerical setting based on operational data from a CDC, which is considered to be reflective of the operating conditions of many other CDCs in major cities. General policy guidelines have been suggested based on this numerical study, where it is estimated that a potential increase of around 17% can be achieved in expected total PVI through optimal policy implementations, when compared with historical acquisition data.

We conclude that CDCs should be more selective in making offers on foreclosed properties if they operate with lower funding levels accessible for acquisition. If the funds will expire at the end of the planning period, then they should initially make offers on properties with higher expected returns. Increased selectivity is also optimal if foreclosed property availability is higher. On the other hand, for the current data, which is expected to be reflective of conditions in urban neighborhoods, we conclude that it is optimal to make offers on all properties with property value impacts greater than the minimum of $60 thousand, when the accessible funds are greater than about $1.5 million. Moreover, the optimal policy is always to make offers at the asking price and not to overbid. These results change and return thresholds become more active, only when availability rates reach almost twice the current high levels, or when the PVI values of potential acquisitions are very low, which typically is the case in low population density neighborhoods. Hence, unless the foreclosure crisis is significantly worsened, the proposed guidelines can be expected to be valid for urban areas in major cities. We also find that cost of making an offer on a property has a negligible impact on the optimal policy, and CDCs should continue with a given optimal strategy even if the overhead costs might vary from initial levels. In general, most policy results are similar for the cases with and without fund expiration, especially before the last several periods of the finite horizon case. Given the expiration of the funds, the acquisition policies get aggressive in using the remaining funds towards the end of the planning horizon.

Overall, the presented models and guidelines can potentially aid CDCs and other similar organizations in making investment decisions with social returns, as in foreclosed housing acquisition and redevelopment. Given the absence of any such optimization based analysis tool for this type of nonprofit decision making, our results can help in improving the efficiency and effectiveness of the decisions by these nonprofit organizations, thus helping improve the value to the society. We believe that the presented research contributes to nonprofit operations management literature by studying a new and important decision problem with many implications for a sustainable economy and society.

CHAPTER 5

TEAM-BASED RESOURCE ALLOCATION IN ROBOTIC SURGERY

Consider a hospital making surgical team configuration decisions to maximize operating room efficiency and effectiveness in advance of a planning horizon for robotic surgical operations. It is assumed that the team allocation decisions will be made at the beginning of the planning horizon and performance information on the teams will become available over the planning periods as teams work together on different surgeries. Future team allocation decisions will be made based on this realized information, as well as probabilistic information on performance values further into the future, as compatibility of team members become more clear.

A more specific representation of this general decision process is depicted in Figure 5.1, which can be described as follows. The decision maker, i.e. the scheduling office, decides on possible multiple team configurations for a given period by considering potential individual and dependent performances of each team member according to their experiences. Subsequently, the assigned surgeries are performed and independent/dependent performances of each team member become known. Once this

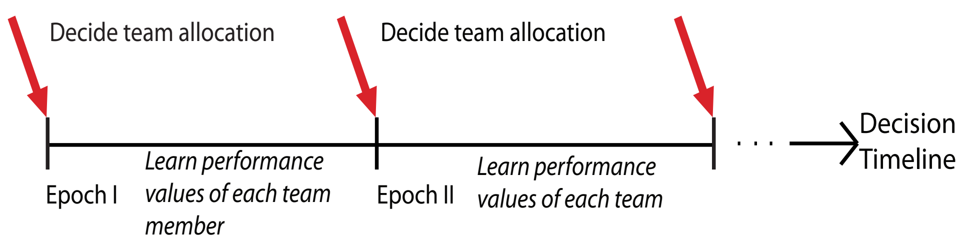

Figure 5.1. General decision process for robotic surgery team allocation problem

information is available, the new team allocation decisions are made by considering realized performance measures. The process can continue for multiple periods where team reallocations can take place based on any information that becomes available. In many cases, these assignments could take place every 1-3 months.

An important process in modeling this decision framework involves the definitions of team performance, and identification of mappings between team member experiences and performances. We first describe this input generation process in the following section, and then introduce our stochastic programming model which we use to determine optimal team configurations under performance uncertainty.

5.1 Modeling and Analysis of Team Performance Functions Using Operational Data

In this section, we analyze available data and obtain an input to our stochastic optimization model to identify policies that apply to the decision framework currently faced by many hospitals in determining surgery teams.

Data based implementation and analysis of robotic surgery team allocation problem was performed in close coordination with a hospital located in Massachusetts. Hospital staff were also involved in the model building phase of the study. Our data focused on robotic sacrocolpopexy operations, i.e. urologic and pelvic surgeries. The available information spanned the period between March 2008 and April 2012, consisting of a sample of approximately 400 surgeries. This data involves confidential patient information, and is not publicly available.

We perform some statistical data analyses to study the characteristics of different attributes within the decision framework, and to obtain experience and performance metrics for use in our stochastic model. For analysis purposes, we apply factor analysis, regression analysis and one way analysis of variance (ANOVA), which we describe in detail in the following subsections.

5.1.1 Factor Analysis

We use factor analysis to develop a more detailed description of the role of the relevant robotic surgery procedures for use in model building. More specifically, factor analysis is used to group numerous factors in robotic surgery performance into a few critical factors that explain most of the variability in the data by taking into account the parameter relationships.

For this analysis, we filtered our data to obtain standardized robotic sacrocolpopexy instances with similar characteristics. We included patient information and surgery team member experiences as variables into the factor analysis model, while redundant measurements and dimensions that were deemed irrelevant to the analysis (i.e. race, length of stay, etc.) were eliminated. The patient characteristics considered in the analysis are patient's age, body mass index (BMI), menopausal status, gravida (the number of times a woman has been pregnant), pathology result, and measures related to the severeness of the patient's condition. This filtered database includes 150 patient records, each containing 10 variables or factors. Once these variables were selected, factor analysis using varimax rotation was performed which allows for an easier interpretation (McLain, 2010). A varimax rotation is a change of coordinates that maximizes the sum of the variances of the squared loadings. Thus, all the coefficients will be either large or near zero, with few intermediate values. The goal is to associate each variable with at most one factor that had the highest weighted value. The factor analysis results are summarized in Table 5.1. In this table, the components with eigenvalue values greater than 1 are shown in bold and accounted as one factor. It can be observed that there would be a small benefit in adding more factors and that four factors explain around 60 percent of the total variance for the surgery data. These four factors are then used to form a factor loading matrix.

Table 5.2 shows this factor loading matrix, which is a varimax rotated matrix of variables and factors that shows the amount of influence a variable has on each

	Initial Eigenvalues		
	Total	% of Variance	Cumulative %
1	**2.903**	**22.858**	**22.858**
2	**2.118**	**16.677**	**39.535**
3	**1.396**	**10.992**	**50.528**
4	**1.146**	**9.024**	**59.551**
5	0.947	7.457	67.008
6	0.899	7.079	74.087
7	0.857	6.748	80.835
8	0.741	5.835	86.669
9	0.653	5.142	91.811
10	0.496	3.906	95.717
11	0.338	2.661	98.378
12	0.206	1.622	100

Table 5.1. Factor analysis table showing all the components included.

	Component			
	1	2	3	4
Surgeon Experience	-0.794	0.007	-0.204	-0.026
Anaesthetist Experience	-0.493	0.055	-0.037	0.123
ST Experience	-0.472	0.236	-0.189	0.079
CN Experience	-0.748	0.016	-0.208	-0.093
PA Experience	-0.482	-0.275	0.197	-0.462
Age of Patient	0.004	0.901	0.104	-0.031
BMI	-0.002	-0.24	-0.111	0.685
Menopausal Status	0.076	0.867	0.088	-0.129
Gravida	0.266	0.206	0.201	0.64
Pathology Report Result	0.179	-0.345	-0.018	-0.135
Severity Measure-1	-0.004	0.049	0.904	-0.026
Severity Measure-2	0.074	0.134	0.846	0.008

Table 5.2. Rotated component matrix.

factor. The first factor explains about 23% of total variance and there are 5 variables in factor one, corresponding to the experience levels of the surgeon, PA, ST, CN, and the nurse anaesthetist. Since all the variables in this factor are related to the surgery team experience, factor one is called the experience factor. Based on this, it can be further concluded that experience of each team member has crucial importance in robotic surgery. Factor two consisted of 3 variables related to patient's health status: age of patient, menopausal status, pathology report result. This factor accounts for approximately 17% of total variance. The severeness measure variables are grouped in the third factor where they explain 11% of total variability. Finally, the last factor is composed of two variables, namely BMI and gravida, which are related to the demographic information about the patient. Overall, there are four main factors which have significant influence on the surgery and it is sufficient to consider these four factors instead of all variables. We also highlight again that the experience factor plays an important role in robotic surgery based on our analysis.

After reducing the dimension of categories, regression analysis is then used to extrapolate the data onto the remaining variables to predict total operating time in the following subsection.

5.1.2 Regression Analysis

Using the results that we obtained from the factor analysis study, we perform a multiple nonlinear regression analysis to develop a model for predicting robotic surgery operating room time based on each team member's experience levels and some primary patient characteristics. In order to obtain better predictions, we split the total operating room time in three categories: preparation time (phase 1), surgery time (phase 2), and patient awakening/out time (phase 3). In phase 1, every team member has a role except the scrub tech, while all team members without exception are involved in phase 2. For patient awakening/out time, the circulating nurse and the nurse anesthetist are the active participants. Using this setup, we obtain the regression equation (5.1) to predict the total operating room time t based on identified factors. We include in our regression model the patient age a, the measure of severeness m, and the experience of each team member, denoted by e_i for $i = Doc, PA, ST, AN$, and CN. Note that Doc refers to the surgeon, while AN refers to the nurse anaesthetist.

$$
\begin{aligned}
t = &-.15(a) - 2.10(m) - 0.05(e_{CN})^2 - .14(e_{AN})^2 + 0.03(e_{PA})^2 - 0.02(e_{Doc})^2 \\
&+ 22.30(e_{AN}) \ln(e_{AN}) + 10.99(e_{CN}) \ln(e_{CN}) + 9.40(e_{Doc}) \ln(e_{Doc}) \\
&- 8.33(e_{PA}) \ln(e_{PA}) + 140.27 \ln(e_{CN}) - 51.71(e_{CN}) - 166.98 \ln(e_{PA}) + 41.62(e_{PA}) \\
&- 102.22(e_{AN}) + 343.26 \ln(e_{AN}) - 50.99(e_{Doc}) + 239.11 \ln(e_{Doc}) + 71600.6 \\
&+ 1.92(e_{ST})^2 - 753.31(e_{ST}) \ln(e_{ST}) + 4191.03(e_{ST}) - 35393.8 \ln(e_{ST})
\end{aligned} \tag{5.1}
$$

In order to assess the validity of our regression model we perform cross validation, which is an evaluation method that is typically better than simply looking at the residuals. To this end, we split our data into two sets called training and testing sets. We perform the analysis on the training set, and validate the analysis on the testing set. We find that there is no significant difference between training and testing data sets, implying a validation of our model.

Using the regression analysis results, we obtain the "optimal" experience level for each team member that would minimize the total operation time assuming independence between individual experiences and joint experiences of team members. To find this optimal level, we calculate the first order derivative of the regression function with respect to each team member's experience level, again by assuming all the other parameters as constant. We further validate our result by comparing it with those obtained by single regression models for each parameter. This is achieved by building a nonlinear regression model for each experience level to predict operating

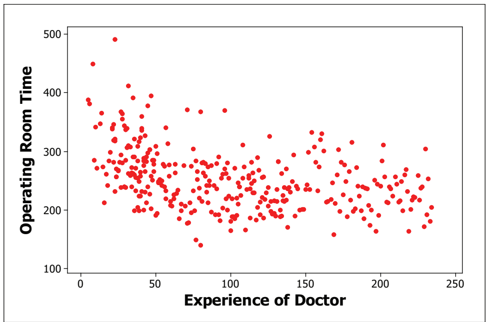

(a) Operating room time over doctor experience.

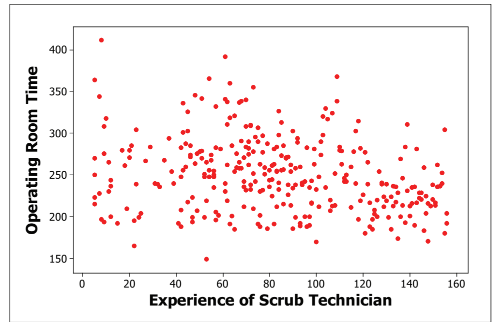

(b) Operating room time over scrub technician experience.

Figure 5.2. Operating room time as a function of team member experiences.

	Doctor		PA		Anesthetist		ST		CN	
	Exp.	Per.	Exp.	Per.	Exp.	Per.	Exp.	Per.	Exp.	Per.
Low	13	0.295	3	0.23	10	0.217	52	0.788	5	0.089
Medium	24	0.545	7	0.538	24	0.522	59	0.894	34	0.607
High	44	1	13	1	46	1	66	1	56	1

Table 5.3. Categorization of experience and independent performance levels of each team member in robotic surgery based on number of surgeries performed.

room time, and then by comparing our findings of full and single regression models for each experience level separately. We also categorize the experience levels for each team member as being low, medium, or high, according to the 33^{rd}, 66^{th} percentiles and optimum levels of experience data. These experience levels are summarized in Table 5.3 where "high" refers to the optimum experience level. We note that we use the single regression model function to find optimum experience level for doctor since it provides a better prediction based on our interactions with hospital.

In Figure 5.2 we provide sample graphs for operating room time as a function of experiences of the surgeon (doctor) and scrub technician. These graphs can also be used to develop a single regression model for each team member separately. We use this single regression model to validate the optimal experience levels that we obtained from the full regression model. The optimal value is expected to be around 50 for the surgeon, while this value is expected to be between 55-65 for the scrub technician.

By using these experience levels we calculate individual standardized performance measures for each team member as summarized in Table 5.3 by dividing the corresponding experience level by the optimum level. Moreover, we calculate dependent performance measures where we assume that performance of a team member might be effected from other team members' performances. To calculate dependent performance values we use our predicted regression function and vary the given experience levels by keeping the others as constant. For example, to calculate the dependent performance value when the doctor and the PA are both with low experience levels, we plug in low experience values of doctor and PA, shown in Table 5.3, into equation 5.1 and keep other experience values at their optimum levels. We note that in our study we only consider dual dependency, as higher degree dependencies have much less implications and are also harder to quantify based on existing samples of data.

In our joint performance analysis we find that the anesthetist has the lowest impact on robotic surgery performance compared to other team members. We also note that the scrub technician has a key role in robotic surgery, specifically as the low performance of a scrub tech has a significant affect on the team performance. As expected, the roles of the surgeon and the PA are also very significant.

5.1.3 Analysis of Variance (ANOVA)

In this subsection we use analysis of variance to evaluate the differences in operating room times as a function of various parameters for practical implications. Since we analyze variability across one factor categorically, we implement a one-way ANOVA analysis.

We first analyze the effect of the time of the surgery on total operating time. Based on our interactions with the hospital staff, it was hypothesized that surgeries that are held in afternoon typically take longer, when compared to morning surgeries,

ANOVA					
Operation Starting Time					
	Sum of Squares	df	Mean Square	F	Sig.
Between Groups	11403.549	1	11403.549	4.262	.040
Within Groups	904322.507	338	2675.510		
Total	915726.056	339			

Table 5.4. ANOVA results for surgery starting time.

Multiple Comparisons ANOVA						
Dependent Variable:Operating Room Time Tukey HSD						
Proc Type		Mean Difference	Std. Error	Sig.	95% Confidence Interval	
					Lower Bound	Upper Bound
1.00	2.00	54.535*	8.779	.000	33.87	75.20
	3.00	53.304*	8.705	.000	32.81	73.80
2.00	1.00	-54.535*	8.779	.000	-75.20	-33.87
	3.00	-1.230	5.676	.974	-14.59	12.13
3.00	1.00	-53.304*	8.705	.000	-73.80	-32.81
	2.00	1.230	5.676	.974	-12.13	14.59

*. The mean difference is significant at the 0.05 level.

Table 5.5. ANOVA results for different types of surgeries.

as a shift change occurs in the afternoon. So we divide our data into two groups, e.g. surgeries starting before 11am and surgeries starting after 11am. The ANOVA results are shown in Table 5.4, which validate the hypothesis that there is significant difference between the morning and afternoon surgeries, based on the F-test results.

As a second analysis, we compare different *types* of surgeries with respect to operating room time and provide the ANOVA results in Table 5.5. In this table, surgery types 1, 2 and 3 refer to surgery types robotic supracervical hysterectomy with sacrocolpopexy, total robotic hysterectomy with sacrocolpopexy and robotic sacrocolpopexy, respectively. Based on these results, it is concluded that surgery types 1 and 2, as well as 1 and 3 have significant differences between each other in terms of operating room time. However, no significant difference can be observed between surgery types 2 and 3.

We also analyze the operating room time across the number of scrub technicians attending the surgery to see whether taking a break during the surgery would effect

Multiple Comparisons						
Dependent Variable: Operating Room Time Tukey HSD						
Number of STs Attended		Mean Difference	Std. Error	Sig.	95% Confidence Interval	
					Lower Bound	Upper Bound
1.00	2.00	-4.529	6.014	.732	-18.69	9.63
	3.00	.290	11.615	1.000	-27.06	27.64
2.00	1.00	4.529	6.014	.732	-9.63	18.69
	3.00	4.819	11.743	.911	-22.83	32.47
3.00	1.00	-.290	11.615	1.000	-27.64	27.06
	2.00	-4.819	11.743	.911	-32.47	22.83

Table 5.6. ANOVA results for different number of STs attended

the operating time, since multiple scrub technicians may exchange roles during the surgery to take breaks. The results are represented in Table 5.6. It can be concluded that taking breaks do not have a significant effect on operating times because no significant difference could be observed between surgeries with a higher number of scrub techs attending the surgery.

5.1.4 Stochastic Characterization of the Performances

We include stochasticity into our model through a representation of the uncertainty in the realized performance levels for each team member and experience level combination. To this end, we define exogenous random performance variables and associate them with a probability distribution based on analysis of existing data.

Let ϵ be a vector of random variables corresponding to performances of each team member with different experience levels. The components of this vector are denoted by ϵ_{ij}, where i refers to the team member, and j refers to the experience level of the team member. We assume two possible realizations for each random parameter, e.g. low ϵ_{ij}^{low}, and high ϵ_{ij}^{high}. In order to quantify these realizations, we first calculate the difference between the highest and lowest possible performance values for each type of performance measure. We then divide it by 6 by assuming that lowest and highest values are 6 standard deviations away from the average. To calculate ϵ_{ij}^{low} and ϵ_{ij}^{high}, we add and subtract a single standard deviation from the observed performance levels, respectively. The same procedure is used for dependent performance measures as well, where the notation in this case involves $e^{low}_{iji'j'}$ and $e^{high}_{iji'j'}$, where i and i' correspond to two different team members, while j and j' are their respective experience levels.

The probability distributions for these realizations are determined through the analysis of historical data. For each team member with a given experience level, we calculated the likelihood of having low or high performance based on the frequency of the observations. For example, an experienced doctor is assumed to perform well if the total operating room time is lower than the overall average time, while it would imply a low performance if the observed time is higher than the average time. Looking at the frequency of historical occurrences of such cases, a discrete probability can be assigned for each outcome.

5.2 Stochastic Programming Model

In this section we develop a two stage stochastic programming approach and utilize it to determine optimal team configurations for robotic surgery, based on different levels of experience that each team member can have. Assume that there are $\mathcal{K}$ categories of team members that need to be present in the surgery, e.g. surgeon, scrub tech, etc., and each category has $\mathcal{J}$ different experience levels, e.g. low, medium, and high. It is further assumed that, during the given period it is required to set up a $|\mathcal{M}|$ teams for surgical operations, where $\mathcal{M}$ is the set of all teams. Since the performance of team members are uncertain and become known after a set of surgeries is completed, the problem is stochastic and analyzed for different realizations $\psi \in \Psi$, which represent scenarios with corresponding probabilities π_ψ. Each scenario corresponds to one possible combination of performance outcomes over all team members.

Given this setting, we first define a binary variable $x^{j\psi}_{skm}$ such that it is 1 if a member in group $k \in \mathcal{K}$ at performance level of $j \in \mathcal{J}$ is assigned to be in team $m \in \mathcal{M}$ at stage $s = 1, 2$ in scenario ψ, and 0 otherwise. The individual performance value of each member in group k at level j in period s is represented by p^j_{sk} while the dependent performance of a member in group k at level j with member in group n at level l for scenario ψ in period s is represented by parameter $\rho^{jl\psi}_{skn}$. Another binary variable $z^{jl\psi}_{sknm}$ is also defined such that it is equal to 1 if both the member of group k at level j and group n level l is assigned to team m in time period s under scenario ψ. We first summarize the notation used in the model as follows:

Variables Used in the Model

$x^{j\psi}_{skm}$: Binary variable such that it is 1 if a team member in group $k \in \mathcal{K}$ at performance level of $j \in \mathcal{J}$ is assigned to be in team $m \in \mathcal{M}$ at stage $s = 1, 2$ in scenario $\psi \in \Psi$, and 0 otherwise.

$z^{jl\psi}_{sknm}$: Binary variable such that it is equal to 1 if both member of group $k \in \mathcal{K}$ at level $j \in \mathcal{J}$ and group $n \in \mathcal{K}$ level $l \in \mathcal{J}$ is assigned to team $m \in \mathcal{M}$ in time period $s \in \mathcal{S}$ under scenario $\psi \in \Psi$, and 0 otherwise.

$c^{j\psi}_{km}$: Auxiliary variable used to define team change cost in the second period

Parameters Used in the Model

$p^{j\psi}_{sk}$: The individual performance value of each member in group $k \in \mathcal{K}$ at level $j \in \mathcal{J}$ in period $s \in \mathcal{S}$

$\rho^{jl\psi}_{skn}$: Dependent performance of a member in group $k \in \mathcal{K}$ at level $j \in \mathcal{J}$ with member in group $n \in \mathcal{K}$ at level $l \in \mathcal{J}$ for scenario $\psi \in \Psi$ in period $s \in \mathcal{S}$

π_ψ : Probability value of scenario $\psi \in \Psi$

$\lambda^{j\psi}_{km}$: First lagrangian multiplier for the first set of nonanticipativity constraints

$\mu^{jl\psi}_{knm}$: Second lagrangian multiplier for the second set of nonanticipativity constraints

Using these variable definitions, the two stage stochastic programming formulation is as follows:

$$\mathbf{F}(\mathbf{x},\mathbf{z},\mathbf{\Psi}) = \max \quad \min_{m\in\mathcal{M}} \Bigg\{ E_\psi \Bigg[\sum_{s\in\mathcal{S}} \sum_{k\in\mathcal{K}} \sum_{n\in\mathcal{N}} \sum_{j\in\mathcal{J}} \sum_{l\in\mathcal{L}} \frac{\left(p^{j\psi}_{sk} x^{j\psi}_{skm} - |x^{j\psi}_{1km} - x^{j\psi}_{2km}|\right)}{5} + \frac{\rho^{jl\psi}_{skn} z^{jl\psi}_{sknm}}{10} \Bigg] \Bigg\} \tag{5.2}$$

s.t

$$z^{jl\psi}_{sknm} \leq x^{j\psi}_{skm} \qquad \forall k\in\mathcal{K}\ \forall n\in\mathcal{K}-k\ \forall j\in\mathcal{J}\ \forall m\in\mathcal{M}\ \forall s\in\mathcal{S}\ \forall l\in\mathcal{J}-j\ \forall\psi\in\Psi-\psi' \tag{5.3}$$

$$z^{jl\psi}_{sknm} \leq x^{j\psi}_{snm} \qquad \forall k\in\mathcal{K}\ \forall n\in\mathcal{K}-k\ \forall j\in\mathcal{J}\ \forall m\in\mathcal{M}\ \forall s\in\mathcal{S}\ \forall l\in\mathcal{J}-j\ \forall\psi\in\Psi-\psi' \tag{5.4}$$

$$\sum_{m\in\mathcal{M}} x^{j\psi}_{skm} = 1 \qquad \forall k\in\mathcal{K}\ \forall j\in\mathcal{J}\ \forall s\in\mathcal{S}\ \forall l\in\mathcal{J}-j\ \forall\psi\in\Psi \tag{5.5}$$

$$\sum_{j\in\mathcal{J}} x^{j\psi}_{skm} = 1 \qquad \forall k\in\mathcal{K}\ \forall m\in\mathcal{M}\ \forall s\in\mathcal{S}\ \forall l\in\mathcal{J}-j\ \forall\psi\in\Psi \tag{5.6}$$

$$\sum_{k\in\mathcal{K}} \sum_{j\in\mathcal{J}} x^{j\psi}_{skm} = 5 \qquad \forall m\in\mathcal{M}\ \forall s\in\mathcal{S}\ \ \forall\psi\in\Psi \tag{5.7}$$

$$x^{j\psi}_{1km} = x^{j\psi'}_{1km} \quad \forall k\in\mathcal{K}\ \forall n\in\mathcal{K}-k\ \forall j\in\mathcal{J}\ \forall m\in\mathcal{M}\ \forall s\in\mathcal{S}\ \forall l\in\mathcal{J}-j\ \forall\psi\in\Psi-\psi' \tag{5.8}$$

$$z^{jl\psi}_{1knm} = z^{jl\psi'}_{1knm} \quad \forall k\in\mathcal{K}\ \forall n\in\mathcal{K}-k\ \forall j\in\mathcal{J}\ \forall m\in\mathcal{M}\ \forall s\in\mathcal{S}\ \forall l\in\mathcal{J}-j\ \forall\psi\in\Psi-\psi' \tag{5.9}$$

$$x^{j\psi}_{skm}, z^{jl\psi}_{sknm} \in \{0,1\} \quad \forall k\in\mathcal{K}\ \forall n\in\mathcal{K}-k\ \forall j\in\mathcal{J}\ \forall m\in\mathcal{M}\ \forall s\in\mathcal{S}\ \forall l\in\mathcal{J}-j\ \forall\psi\in\Psi \tag{5.10}$$

where $\mathbf{F}(\mathbf{x},\mathbf{z},\mathbf{\Psi})$ is a scalar value and represents value of objective function. Equation (5.2) refers to the objective function which maximizes the minimum expected total performance value of team configuration decisions at all stages, which includes a penalty for team changes in the second period. More specifically, individual and dependent performance values in each period are summed, and then a penalty cost for team changes in the second period is included into the objective function. We divide performance values by 5 and 10, since there are 5 individual and 10 dependent performance values to be summed up for each team configuration. Note that the nonlinearity due the absolute value term at the objective function can be linearized by replacing the term with $c_{km}^{j\psi}$ and adding the following constraints in the formulation:

$$c_{km}^{j\psi} \leq x_{1km}^{j\psi} - x_{2km}^{j\psi} \tag{5.11}$$

$$c_{km}^{j\psi} \leq -x_{1km}^{j\psi} + x_{2km}^{j\psi} \tag{5.12}$$

where $c_{km}^{j\psi}$ refers to a team change cost for the second period.

Constraint (5.3) and (5.4) relate $z_{knm}^{sjl\psi}$ and $x_{skm}^{j\psi}$ variables and linearize a nonlinear constraint structure which is originally stated as $z_{knm}^{sjl\psi} \leq x_{skm}^{j\psi} x_{snm}^{j\psi}$. More specifically, $z_{knm}^{sjl\psi} = 1$ if both $x_{skm}^{j\psi}$ and $x_{snm}^{j\psi}$ are equal to 1, and $z_{knm}^{sjl\psi} = 0$ if any or both of them are equal to 0. Constraint (5.5) ensures that each team member at each performance level should be assigned to one team exactly while constraint (5.6) is used to assign exactly one member from each group to each surgical team. The total number of team members is at most $|\mathcal{K}|$ and this is defined by constraint (5.7). Constraint (5.8) and (5.9) are stated as nonanticipativity constraints where the first stage variables should be equal to each other. Finally, Constraint (5.10) states that decision variables of the model are binary variables.

5.3 Solution Approach and Numerical Analysis

In this section, we perform a numerical analysis through the stochastic programming model to seek insights for the general team allocation problem. More specifically, we try to determine whether general rules of thumb for team composition decisions exist, which might aid hospitals for determining optimal team combinations. In our analysis, we also address computational issues related to the stochastic programming model, which runs into tractability issues. To this end, we propose a Lagrangian decomposition method as a solution algorithm, as explained in the following subsection.

5.3.1 Solution through a Lagrangian Decomposition Procedure

Model (5.2)-(5.10) is linked in scenarios through the nonanticipativity constraints (5.8) and (5.9). Let $g_\psi(x,z)$ represent the objective function (5.2). Then by subjecting the nonanticipativity conditions to Lagrangian relaxation, we form the following Lagrangian

$$\begin{aligned} L(x,y,\lambda,\mu) = & g_\psi(x,z) + \sum_{k\in\mathcal{K}}\sum_{j\in\mathcal{J}}\sum_{m\in\mathcal{M}}\sum_{\psi\in\Psi} \pi_\psi \lambda_{km}^{j\psi}\big(x_{1km}^{j\psi} - x_{1km}^{j\psi'}\big) \\ & + \sum_{k\in\mathcal{K}}\sum_{n\in\mathcal{N}}\sum_{j\in\mathcal{J}}\sum_{l\in\mathcal{L}}\sum_{m\in\mathcal{M}}\sum_{\psi\in\Psi} \pi_\psi \mu_{knm}^{jl\psi}(z_{1knm}^{jl\psi} - z_{1knm}^{jl\psi'}) \end{aligned} \tag{5.13}$$

where $\lambda_{km}^{j\psi}$ and $\mu_{knm}^{jl\psi}$ are the Lagrange multipliers. Notice that the formulation of the nonanticipativity constraints (5.8) and the multiplication of the relaxed constraints (5.9) by π_ψ in the above Lagrangian account for the scenario probabilities, and prevent the ill-conditioning in the Lagrangian dual as discussed by Louveaux and Schultz (2003). This procedure is similar to the decomposition method described by Carøe and Schultz (1999). We adapt this procedure and express the resulting Lagrangian as:

$$\begin{aligned} L(x,y,\lambda,\mu) = & g_\psi(x,z) + \sum_{k\in\mathcal{K}}\sum_{j\in\mathcal{J}}\sum_{m\in\mathcal{M}}\sum_{\psi\in\Psi} \big\{\lambda_{km}^{j\psi}\big(-x_{1km}^{j\psi}\big) + \sum_{\psi'\in\Psi} + \pi_\psi \lambda_{km}^{j\psi'} x_{1km}^{j\psi}\big\} \\ & + \sum_{k\in\mathcal{K}}\sum_{n\in\mathcal{N}}\sum_{j\in\mathcal{J}}\sum_{l\in\mathcal{L}}\sum_{m\in\mathcal{M}}\sum_{\psi\in\Psi} \big\{\mu_{knm}^{jl\psi}\big(-z_{1knm}^{jl\psi}\big) + \sum_{\psi'\in\Psi} \pi_\psi \mu_{knm}^{jl\psi'} z_{1km}^{j\psi}\big\} \end{aligned} \tag{5.14}$$

Problem (5.14) is a nonsmooth convex minimization problem, and can be solved by subgradient optimization methods (Hiriart-Urruty and Lemaréchal, 1996). Notice that this method reduces to solving $|\Psi|$ problems of manageable size, each of which corresponds to a single scenario.

The overall procedure to solve the stochastic team allocation problem is summarized below.

Step 1. Perform Lagrangian relaxation on the problem, decomposing the problem into individual scenario subproblems.

Step 2. Use subgradient algorithm to obtain an upper bound for the problem.

Step 2a. Solve the LP relaxation of constraints (5.2)-(5.10), and set the corresponding dual values as the initial Lagrangian multipliers. Use a rounding heuristic to obtain an initial lower-bound on the problem.

Step 2b. At each iteration j of the algorithm, determine a lower-bound for the scenario subproblems by calculating the corresponding Lagrangian and selecting the minimum.

Step 2c. Use the best lower-bounds for the scenario subproblems as the starting solution for the subproblems at iteration $j + 1$.

Step 3. Calculate the duality gap upon convergence of the subgradient algorithm. If the gap is less than or equal to the minimum acceptable level, stop. Else, if computationally feasible, use branch and bound to close the duality gap, by branching on the nonanticipativity conditions.

5.3.2 Numerical Results and Optimal Policy Insights

Our numerical analysis in this section utilizes the stochastic programming model to seek insights for the surgical team allocation problem. More specifically, we try to determine whether general rules of thumb for allocation decisions can be observed that might aid hospitals for the optimal allocation of team members.

	CN	ST	Surgeon	Anesthetist	PA
Team-1	Medium	High	Medium	Medium	Medium
Team-2	High	Low	Low	Low	High
Team-3	Low	Medium	High	High	Low

Table 5.7. First stage team allocation decisions representing best team configurations.

Computational tests based on the available data set were conducted using the developed solution procedure. The performance data was extracted through the regression analysis described in detail in Section 5.1. We implemented our model for 1024 scenarios where low and high realizations are used for each stochastic parameter. Computations were performed on a PC with an Intel i7 Quad processor with 2.4 GHz speed and 8 GB of internal memory, using IBM ILOG CPLEX Version 12.1. Although the computational studies were conducted on a single computer, the proposed solution procedure can easily be parallelized by solving the scenario subproblems on multiple machines to improve the solution times significantly. We obtained a converged solution for 1024 scenarios in approximately 10 hours of time. The percent gap between best upper and lower bounds was around 0.14% at convergence. Optimal team allocation decisions for the fist stage are represented in Table 5.7, where low, medium, and high refers to different experience levels for each team member as defined in Section 5.1.

In Table 5.7 we present the optimal team configuration for the first decision epoch. These results reflect the "ideal" configurations such that the maximum expected operating room time is minimized over the three teams. Note that the problem setup assumes the existence of team members from each possible experience level, and seeks to identify the best team structures if all team members are to be utilized.

These results suggest some relevant practical insights for hospital schedulers. First, it can be concluded that if a doctor has low experience, it is generally better to match him/her with a more experienced PA. Similarly, if a doctor has high experience, it is fine to match him with a less experienced PA or scrub tech. These findings also support the general observation that the surgeon and the PA are the key actors and have primary control on robotic surgery, as both of them can perform robot docking, positioning and anything that relates to the coordination of robot's activities during a surgery. Hence, the surgeon and the PA can generally substitute each other, and at least one of them should have higher levels of experience for improved performance in the surgery. We also note that if the scrub tech has low experience in a surgical team, then either the surgeon or the PA should be more experienced. Independent from other team member experiences, it is not recommended to include low experienced ST, PA and surgeon in the same team. In the case that both the surgeon and PA are not as experienced, then it is better to match them with an experienced scrub tech. These results are also supportive of our observations that ST plays an important role in surgery and sometimes could replace the PA if there is no PA available. Another relationship exists between the CN and the anesthetist. It can be observed that if the anesthetist has more experience, it is fine to have a less experienced CN in the team, however if anesthetist has less experience, he/she should be matched with a more experienced CN. This relationship between CN and the anesthetist is also reasonable since both of them mostly work together during the surgery room preparation and patient awakening phase. Given that the surgeon is also sometimes active in the preparation process we can observe from the results that a low experienced CN should be matched with an experienced surgeon or vice versa.

Besides first stage allocation decisions, for demonstration purposes we also provide second stage allocation decisions for some selected scenarios in Table 5.8. These are recourse decisions that would be implemented if it turns out that the observed performances differ significantly from their expected levels. As it can be generally observed, similar conclusions as above can be derived for the surgeon, PA and the ST in the recourse decisions as well.

		Team Members				
Sample Scenario Index	Teams	CN	ST	Surgeon	Anesthetist	PA
1	Team-1	Low	High	Medium	Medium	High
	Team-2	Medium	Low	High	Low	Low
	Team-3	High	Medium	Low	High	Medium
2	Team-1	High	Low	Low	Low	High
	Team-2	Low	High	Medium	High	Medium
	Team-3	Medium	Medium	High	Medium	Low
3	Team-1	High	Low	Medium	High	Low
	Team-2	Low	Medium	High	Medium	Medium
	Team-3	Medium	High	Low	Low	High
4	Team-1	Low	Medium	High	High	Low
	Team-2	High	Low	Medium	Medium	Medium
	Team-3	Medium	High	Low	Low	High
5	Team-1	High	Low	Medium	Medium	Medium
	Team-2	Medium	High	High	Low	Low
	Team-3	Low	Medium	Low	High	High

Table 5.8. Second stage team allocations for sample scenarios.

5.4 Conclusions

In this chapter, we investigated dynamic portfolio management approaches for optimization of surgical team compositions in robotic surgeries. For this problem, we developed stochastic dynamic model to identify policies for optimal team configurations, where optimality is defined based on the minimum experience level required to achieve the maximum attainable performance over all ranges of feasible experience measures. We derived individual and dependent performance values of each surgical team member by using data on operating room time and team member experience, and then used them as inputs to a two-stage stochastic programming based framework that we developed. In our analysis, we also addressed computational issues related to the stochastic programming model, which runs into tractability issues. To this end, we proposed a Lagrangian decomposition method as a solution algorithm. Finally, we performed a numerical analysis based on real-world data for practical insights.

Although, our conclusions are based on the specific numerical data used, we believe that hospitals can benefit from the proposed models either through direct implementation for specific guidance, or through the indirect use of several policy results obtained. In our results we show that operation starting time and different operations could affect operating room time while the breaks that STs and CNs use during the surgery do not have significant effects on the overall operating room time. We further obtain dependent and independent performance levels for each team member by finding optimal experience levels for each case. By using these findings as an input to our stochastic model we derive further insights related to the team configuration decisions. An important characteristic of our study is that we build our models by using real-world data through interactions with a hospital. As a first stochastic model of its type in this application area, we aim to provide surgical team allocation guidelines for hospitals through explicit consideration of uncertainty. As future work, this problem could be combined with a staffing problem by considering time, costs, experiences, and performances of individuals, rather than team member categories.

CHAPTER 6

CONCLUSIONS AND FUTURE RESEARCH

In this dissertation, we study specific types of resource allocation problems where social benefits and non-quantitative objectives are specifically considered in resource allocation decisions. Two applications of stochastic dynamic models on societal resource allocation are described throughout the thesis. In the first application, we present strategic and tactical aspects involving the acquisition of foreclosed properties by nonprofits, while in the second application, we propose a two-stage stochastic programming model for allocating team members to surgeries to minimize operating room times.

In Chapters 1 and 2, we provide general introduction and literature review information describing the background for the problems investigated in the study. In Chapter 3, the strategic dimension of the foreclosed housing acquisition problem is described in detail, where we consider long term budget allocation decisions along with acquisition decisions. We model the strategic foreclosed housing acquisition problem as a two stage stochastic programming model and then expand this model through a multi-stage structure involving gradual uncertainty resolution. We include some further variations to reflect potential real life cases to obtain better practical insights for CDCs and practitioners in their long term decisions. Some computational analyses are also performed to demonstrate the applicability of the proposed models.

In Chapter 4, the tactical dimension of the foreclosed housing acquisition problem is discussed where we mainly consider short term acquisition decisions in our modeling framework. We investigate two practical planning situations based on whether the potentially accessible funds have an expiration date or not. Analytical results are obtained for both cases. In addition, we describe policies to determine optimal overbid rates to use when targeting a property for potential acquisition. We implement our model and policies in a numerical setting by using operational data obtained from a CDC. Based on this analysis, we observe a potential increase of around 17% in expected total property value impacts, if the optimal policies were to be implemented by the CDC that the data was obtained from.

In Chapter 5, we develop a data-based optimization model to identify policies for surgical team compositions in robotic surgeries. As part of this analysis, we derive individual and dependent performance values of each surgical team member by using operational data obtained from a hospital. By using these performance values, we develop a stochastic optimization model to obtain general insights that can be used as decision guidelines. In our analysis, we also address computational issues related to the stochastic programming model, which runs into tractability issues. To this end, we propose a Lagrangian decomposition method as a solution algorithm for the problem.

As potential future research, we note for the foreclosed housing acquisition problem that as in any model, accurate quantification of relevant measures is crucial for the validity of implementations involving the presented approaches. Hence, in addition to the consideration of the variances of objectives and priorities between different CDCs, future work may involve assessments of the accuracy of expert opinions used in quantitative measurements with respect to their impacts on the optimization models. The observed real life implications of the proposed models on CDCs would also constitute an important extension to our study in terms of its practical significance.

One additional issue that relates to foreclosed housing acquisition problem involves the role of private investors as competitors to nonprofit CDCs. This becomes relevant under stable market conditions, where prioritization of CDCs in acquiring properties is not implemented by funding agencies or lenders. Since acquisitions in such cases will involve game theoretical aspects, it is possible that a game theory based analysis approach is likely to be more valid for that problem setting. On the other hand it is still possible to use the tactical decision framework in Chapter 4 by modifying the probability of success function to account for the increased competition in bidding for properties.

For future research in robotic surgery team composition problem, it is likely to be of value to analyze staffing and scheduling policies by taking into account the individual and joint experiences of team members. Current staffing and scheduling policies are mostly done in an ad hoc fashion based on random assignments. Hence, if such assignments were to be performed based on expected performance levels, it is likely that overall surgery times can be reduced.

While there are certain tractability issues, one alternative approach to optimal surgical team composition problem involves a Markov decision process based analysis where analytical policies can potentially be derived. On the other hand, the combinatorial nature of the problem might make it necessary to use simplifying assumptions in such an approach, and this might take away from the validity of the model.

APPENDIX A

APPENDIX FOR STRATEGIC SOCIETAL RESOURCE ALLOCATION

A.1 Stochastic Parameters

Acquisition and redevelopment costs

Social returns

Total required budget to acquire all properties of a given category in a neighborhood

A.2 Deterministic Parameters

Available budget

Financial returns

Collective efficacy measure of a given neighborhood

Probability that a given category property will be sold within a certain time frame

Current number of owner occupied properties in a given neighborhood

Total number of properties in a given neighborhood

Distance between two neighborhoods

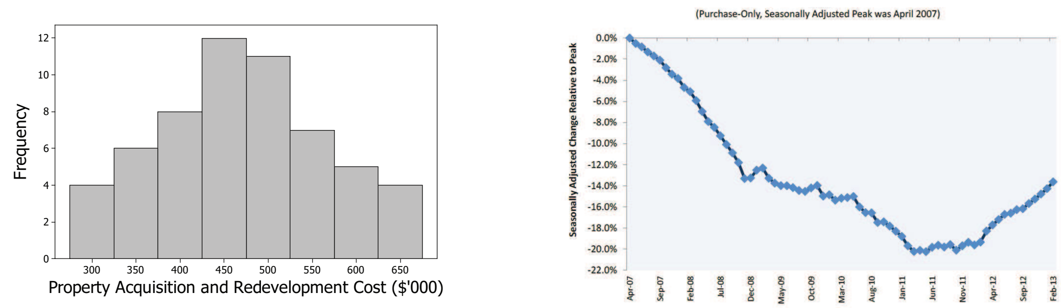

(a) Histogram showing the observed variation in acquisition and redevelopment costs

(b) Change in U.S. residential property prices over time Russell and Johnson (2013)

Figure A.1. Supporting information for the stochastic treatment of acquisition and redevelopment costs.

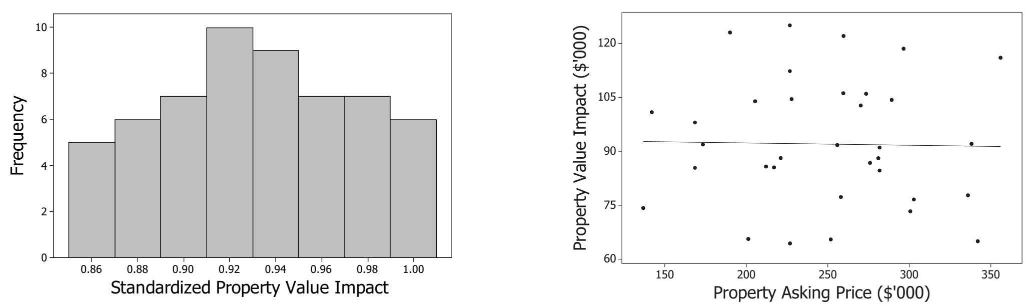

(a) Histogram showing the observed variation in social returns as represented through PVI values

(b) Relationship between property acquisition and redevelopment costs and PVI values

Figure A.2. Supporting information for the stochastic treatment of social returns.

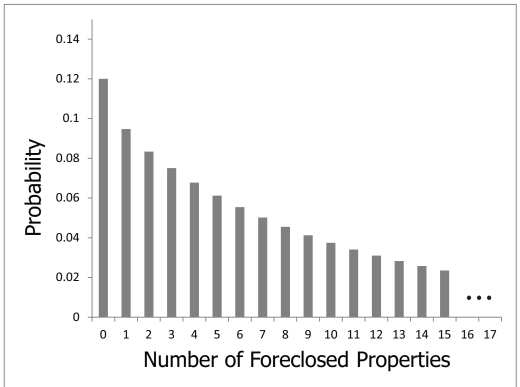

(a) Sample probability distribution defining the number of foreclosed properties in the next period, derived through transition probabilities described in Johnson et al. (2013)

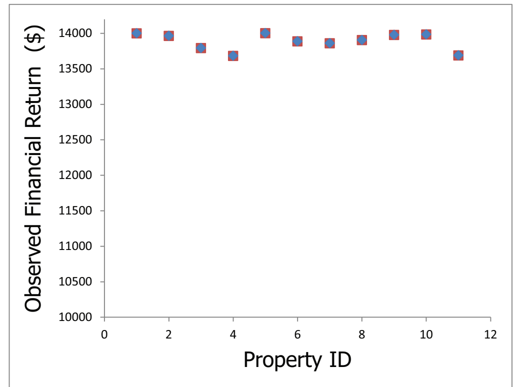

(b) Plot of observed financial returns from a set of acquired, redeveloped and sold properties

Figure A.3. Supporting information for the stochastic treatment of total required budget for acquiring all properties and deterministic treatment of financial returns.

A.3 Values of Parameters used in Numerical Analysis for Case 2x2

A.3.1 Deterministic Parameter Values

Budget :	\$5 million
Distance between neighborhoods:	0.9 miles
Standardized neighborhood efficacies:	0.3; 0.5
Current number of properties in neighborhoods:	2,640; 4,335
Current number of owner occupied properties:	1492; 2795
Probability of sale for categories:	0.5; 0.6
Expected financial returns:	\$13,960 and \$15,780 for neighborhood 1; \$22,350 and \$25,410 for neighborhood 2

APPENDIX B

APPENDIX FOR TACTICAL SOCIETAL RESOURCE ALLOCATION

B.1 Proofs of Analytical Results

Proof of Theorem 1

Kleywegt and Papastavrou (2001) note that for any given policy in the stochastic dynamic knapsack problem, the value of the policy can be calculated by conditioning on the availability time A_k after time t of a property k, its asking price C_k and PVI value R_k as follows, where the availability rate λ and discount rate α are also included. Given this, we have that:

$$\begin{aligned} V\big(b_t\big) = \int_{\underline{C}}^{b}\int_{\underline{R}}^{\bar{R}}\int_{t}^{\infty} \lambda e^{-\lambda(a_k-t)}\mathbb{E}\Bigg[\sum_{i:A_i>t} e^{-\alpha(A_i-t)} \max\Big\{V\big(b_{A_i}\big), \max_{\delta_{bC_iA_i}}\Big\{\big[R_i \\ + V\big((b-C_i-C_i\delta_{bC_iA_i})_{A_i}\big)\big]p(\delta_{bC_iA_i}) + \big[V\big(b_{A_i}\big) - g(C_i,\delta_{bC_iA_i})\big] \\ \big[1-p(\delta_{bC_iA_i})\big]\Big\}\Big\}\Bigg| A_k = a, R_k = r, C_k = c\Bigg] \mathrm{d}a f(r,c)\mathrm{d}r\mathrm{d}c \qquad \text{(B.1)} \\ = \int_{\underline{C}}^{b}\int_{\underline{R}}^{\bar{R}}\int_{t}^{\infty} \lambda e^{-\lambda(a-t)}\Big\{e^{-\alpha(a-t)}\Bigg[\max\Big\{V\big(b_a\big), \\ \max_{\delta_{bca}}\Big\{\big[r + V\big((b-c-c\delta_{bca})_a\big)\big]p(\delta_{bca}) \\ + \big[V\big(b_a\big) - g(c,\delta_{bca})\big]\big[1-p(\delta_{bca})\big]\Big\}\Big\} \\ + \mathbb{E}\Bigg[\sum_{i:A_i>a} e^{-\alpha(A_i-a)} \max\Big\{V\big(b_{A_i}\big), \max_{\delta_{bC_iA_i}}\Big\{\big[R_i \\ + V\big((b-C_i-C_i\delta_{bC_iA_i})_{A_i}\big)\big]p(\delta_{bC_iA_i}) \\ + \big[V\big(b_{A_i}\big) - g(C_i,\delta_{bC_iA_i})\big]\big[1-p(\delta_{bC_iA_i})\big]\Big\}\Big\} \end{aligned}$$

$$
\begin{aligned}
&\qquad\qquad \bigg| A_k = a, R_k = r, C_k = c \bigg]\bigg]\bigg\} \mathrm{d}a f(r,c) \mathrm{d}r \mathrm{d}c \\
&= \frac{\lambda}{\alpha+\lambda}\Bigg[\int_{\underline{C}}^{b} \max_{\delta_{bca}} \bigg\{ \int_{x(\delta_{bca})}^{\bar{R}} r p(\delta_{bca}) - g(c,\delta_{bca})\big(1-p(\delta_{bca})\big) f(r,c)\mathrm{d}r \bigg\} \mathrm{d}c \Bigg] \\
&\quad + \int_{\underline{C}}^{b} \max_{\delta_{bca}} \Bigg\{ \int_{\underline{R}}^{x(\delta_{bca})} \int_{t}^{\infty} \lambda e^{-(\alpha+\lambda)(a-t)} \mathbb{E}\Bigg[\sum_{i:A_i>a} e^{-\alpha(A_i-a)} \\
&\quad \max\bigg\{ V\big(b_{A_i}\big), \max_{\delta_{bC_iA_i}} \Big\{ \big[R_i + V\big((b - C_i - C_i\delta_{bC_iA_i})_{A_i}\big)\big] p(\delta_{bC_iA_i}) \\
&\quad + \big[V\big(b_{A_i}\big) - g(C_i,\delta_{bC_iA_i})\big]\big[1-p(\delta_{bC_iA_i})\big] \Big\}\bigg\} \\
&\quad \bigg| A_k = a, R_k = r, C_k = c \bigg] \mathrm{d}a f(r,c)\mathrm{d}r \Bigg\} \mathrm{d}c \\
&\quad + \max_{\delta_{bca}} \Bigg\{ \int_{\underline{C}}^{b-c-c\delta_{bca}} \int_{x(\delta_{bca})}^{\bar{R}} \int_{t}^{\infty} \lambda e^{-(\alpha+\lambda)(a-t)} \mathbb{E}\Bigg[\sum_{i:A_i>a} e^{-\alpha(A_i-a)} \\
&\quad \max\bigg\{ V\big(b_{A_i}\big), \max_{\delta_{bC_iA_i}} \Big\{ \big[R_i + V\big((b - C_i - C_i\delta_{bC_iA_i})_{A_i}\big)\big] p(\delta_{bC_iA_i}) \\
&\quad + \big[V\big(b_{A_i}\big) - g(C_i,\delta_{bC_iA_i})\big]\big[1-p(\delta_{bC_iA_i})\big] \Big\}\bigg\} \\
&\quad \bigg| A_k = a, R_k = r, C_k = c \bigg] \mathrm{d}a f(r,c)\mathrm{d}r \Bigg\} \mathrm{d}c \qquad \text{(B.2)}
\end{aligned}
$$

Given that the planning horizon is infinite and that the distribution of asking prices and PVI values are stationary, we have $V\big(b_t\big) = V\big(b\big)$. This implies that equation (B.2) can be expressed as:

$$
\begin{aligned}
V\big(b\big) &= \frac{\lambda}{\alpha+\lambda}\Bigg[\int_{\underline{C}}^{b} \max_{\delta_{bc}} \bigg\{ \int_{x(\delta_{bc})}^{\bar{R}} r p(\delta_{bc}) - g(c,\delta_{bc})\big(1-p(\delta_{bc})\big) f(r,c)\mathrm{d}r \bigg\} \mathrm{d}c \Bigg] \\
&\quad + \frac{\lambda}{\alpha+\lambda}\Bigg[\int_{\underline{C}}^{b} \max_{\delta_{bc}} \bigg\{ \int_{\underline{R}}^{x(\delta_{bc})} V\big(b\big) f(r,c)\mathrm{d}r \bigg\} \mathrm{d}c \\
&\quad + \int_{\underline{C}}^{b} \max_{\delta_{bc}} \bigg\{ \int_{x(\delta_{bc})}^{\bar{R}} V\big(b - c - \delta_{bc}\big) f(r,c)\mathrm{d}r \bigg\} \mathrm{d}c \Bigg] \qquad \text{(B.3)} \\
&= \frac{\lambda}{\alpha+\lambda}\Bigg[\int_{\underline{C}}^{b} \max_{\delta_{bc}} \bigg\{ \int_{x(\delta_{bc})}^{\bar{R}} r p(\delta_{bc}) - g(c,\delta_{bc})\big(1-p(\delta_{bc})\big) f(r,c)\mathrm{d}r \bigg\} \mathrm{d}c
\end{aligned}
$$

$$+\int_{\underline{C}}^{b}\int_{\underline{R}}^{\bar{R}} V\big(b\big)f(r,c)\mathrm{d}r\mathrm{d}c - \int_{\underline{C}}^{b}\max_{\delta_{bc}}\Big\{\int_{x(\delta_{bc})}^{\bar{R}} V\big(b\big)f(r,c)\mathrm{d}r\Big\}\mathrm{d}c$$
$$+\int_{\underline{C}}^{b}\max_{\delta_{bc}}\Big\{\int_{x(\delta_{bc})}^{\bar{R}} V\big(b-c-\delta_{bc}\big)f(r,c)\mathrm{d}r\Big\}\mathrm{d}c\Bigg] \tag{B.4}$$
$$= \frac{\lambda}{\alpha+\lambda}\int_{\underline{C}}^{b}\max_{\delta_{bc}}\Big\{\int_{x(\delta_{bc})}^{\bar{R}}\Big[rp(\delta_{bc}) - g(c,\delta_{bc})\big(1-p(\delta_{bc})\big) - V\big(b\big)$$
$$+V\big(b-c-\delta_{bc}\big)\Big]f(r,c)\mathrm{d}r\Big\}\mathrm{d}c + \frac{\lambda}{\alpha+\lambda}V\big(b\big) \tag{B.5}$$

When a countable state space is assumed, the results of Yushkevich and Feinberg (1979) or Kleywegt and Papastavrou (2001) can be used along with equation (B.5) above to conclude that, after some simple algebraic manipulation, the value of the optimal policy can be calculated using the equation:

$$\alpha V^*(b) = \lambda\int_{\underline{C}}^{b}\max_{\delta_{bc}}\Big\{\int_{x(\delta_{bc})}^{\bar{R}} p(\delta_{bc})\Big(r - \big[V^*(b) - V^*(b-c-c\delta_{bc})$$
$$+\frac{1-p(\delta_{bc})}{p(\delta_{bc})}g(c,\delta_{bc})\big]\Big)f(r,c)\mathrm{d}r\Big\}\mathrm{d}c \tag{B.6}$$

□

Proof of Theorem 2

For results 1 and 2, we note that based on Equation (4.5) in Theorem 1, optimal overbid rate δ_{bc}^* for a given asking price c can be expressed as:

$$\delta_{bc}^* = \operatorname*{argmax}_{\delta_{bc}}\Big\{\int_{x(\delta_{bc})}^{\bar{R}} p(\delta_{bc})\big(r - x(\delta_{bc})\big)f(r,c)\mathrm{d}r\Big\} \tag{B.7}$$

We first analyze when the function is on the right hand side is increasing or decreasing with respect to δ_{bc}. Considering the derivative of the function with respect to δ_{bc}, we get:

$$\frac{\partial}{\partial\delta_{bc}}\int_{x(\delta_{bc})}^{\bar{R}} p(\delta_{bc})\big(r - x(\delta_{bc})\big)f(r,c)\mathrm{d}r = \int_{x(\delta_{bc})}^{\bar{R}}\frac{\partial}{\partial\delta_{bc}}\Big[p(\delta_{bc})\big(r-x(\delta_{bc})\big)f(r,c)\Big]\mathrm{d}r$$

$$+ \Big[p(\delta_{bc})\big(\bar{R} - x(\delta_{bc})\big) f(\bar{R}, c)\Big] \frac{\partial \bar{R}}{\partial \delta_{bc}} - \Big[p(\delta_{bc})\big(x(\delta_{bc}) - x(\delta_{bc})\big) f(x(\delta_{bc}), c)\Big] \frac{\partial x(\delta_{bc})}{\partial \delta_{bc}} \tag{B.8}$$

where the relationship is due to the property that

$$\frac{d}{dy} \int_{g(y)}^{h(y)} f(x, y) \mathrm{d}x = \int_{g(y)}^{h(y)} \frac{\partial f(x, y)}{\partial y} \mathrm{d}x + f(h(y), y) \frac{\mathrm{d}h(y)}{\mathrm{d}y} - f(g(y), y) \frac{\mathrm{d}g(y)}{\mathrm{d}y} \tag{B.9}$$

Given that the second and third terms on the right hand side of Equation (B.8) are zero, it follows that:

$$\begin{aligned}
\frac{\partial}{\partial \delta_{bc}} \int_{x(\delta_{bc})}^{\bar{R}} p(\delta_{bc})\big(r - x(\delta_{bc})\big) f(r, c) \mathrm{d}r &= \int_{x(\delta_{bc})}^{\bar{R}} \frac{\partial p(\delta_{bc})}{\partial \delta_{bc}} r f(r, c) \mathrm{d}r \\
&\quad - \int_{x(\delta_{bc})}^{\bar{R}} \frac{\partial p(\delta_{bc}) x(\delta_{bc})}{\partial \delta_{bc}} f(r, c) \mathrm{d}r \\
&= \int_{x(\delta_{bc})}^{\bar{R}} \frac{\partial p(\delta_{bc})}{\partial \delta_{bc}} r f(r, c) \mathrm{d}r - \int_{x(\delta_{bc})}^{\bar{R}} \frac{\partial p(\delta_{bc})}{\partial \delta_{bc}} x(\delta_{bc}) f(r, c) \mathrm{d}r \\
&\quad - \int_{x(\delta_{bc})}^{\bar{R}} p(\delta_{bc}) \frac{\partial x(\delta_{bc})}{\partial \delta_{bc}} f(r, c) \mathrm{d}r && \text{(B.10)} \\
&= p'(\delta_{bc}) \int_{x(\delta_{bc})}^{\bar{R}} r f(r, c) \mathrm{d}r - p'(\delta_{bc}) x(\delta_{bc}) \int_{x(\delta_{bc})}^{\bar{R}} f(r, c) \mathrm{d}r \\
&\quad - p(\delta_{bc}) x'(\delta_{bc}) \int_{x(\delta_{bc})}^{\bar{R}} f(r, c) \mathrm{d}r && \text{(B.11)} \\
&= p'(\delta_{bc}) \mathbb{E}[r | r \geq x(\delta_{bc})] P(r \geq x(\delta_{bc})) - p'(\delta_{bc}) x(\delta_{bc}) P(r \geq x(\delta_{bc})) \\
&\quad - p(\delta_{bc}) x'(\delta_{bc}) P(r \geq x(\delta_{bc})) && \text{(B.12)}
\end{aligned}$$

Note that $x'(\delta_{bc}) \approx \frac{\partial}{\partial \delta_{bc}} \left(\frac{(1 - p(\delta_{bc})) g(c, \delta_{bc})}{p(\delta_{bc})} \right)$ under the assumption that $\frac{\partial (V(b) - V(b - c - c\delta_{bc}))}{\partial \delta_{bc}}$ is small enough to be ignored. This implies that $p(\delta_{bc}) x'(\delta_{bc})$ in the last term of equation (B.10) above can be expressed as $L(\delta_{bc}) = Gc(1 - p(\delta_{bc}) - \frac{p'(\delta_{bc})}{p(\delta_{bc})}(1 + \delta_{bc}))$. It follows that:

$$\frac{\partial}{\partial \delta_{bc}} \int_{x(\delta_{bc})}^{\bar{R}} p(\delta_{bc})\big(r - x(\delta_{bc})\big) f(r, c) \mathrm{d}r = p'(\delta_{bc}) P(r \geq x(\delta_{bc})) \Big(\mathbb{E}[r | r \geq x(\delta_{bc})]$$

$$- x(\delta_{bc}) - \frac{L(\delta_{bc})}{p'(\delta_{bc})}\Big) \tag{B.13}$$

Clearly, the function maximized in equation (B.7) will be decreasing in δ_{bc}, if equation (B.13) is negative, i.e. if $\mathbb{E}[r|r \geq x(\delta_{bc})] - x(\delta_{bc}) - \frac{L(\delta_{bc})}{p'(\delta_{bc})} \leq 0$. Given that this function depends on $x(\delta_{bc})$ which is a variable itself, a condition based on an upper bound for the expression can be used to determine whether the function will be decreasing in δ_{bc} for all possible threshold levels. To this end, let $\bar{K} = \max_{k \in \{\underline{R}, \bar{R}\}}\{\mathbb{E}(r|r \geq k) - k\}$. In addition, let $\bar{L} = \max_{\delta_{bc} \in [0, \bar{\delta}_c]}\{L(\delta_{bc})\}$ and $\underline{L} = \min_{\delta_{bc} \in [0, \bar{\delta}_c]}\{L(\delta_{bc})\}$. Given this notation and that $p(\delta_{bc})$ is increasing in δ_{bc}, an upper bound for the left hand side of the condition can be expressed to get the condition $p'(\bar{\delta}_c)\bar{K} - \underline{\mathrm{L}} \leq 0$. If this condition holds, then the optimal overbid rate is zero, regardless of the threshold policy used by the CDC.

Similarly, a lower bound for the right hand side is when $\{\mathbb{E}(r|r \geq k) - k\} = 0$, which implies that if $\underline{L} \leq 0$, then the derivative function is increasing in δ_{bc} for all threshold levels. If so, the optimal overbid rate is the maximum possible value for δ_{bc}, which is defined as $\bar{\delta}c$.

For result 3, we show when the function on the right hand side is convex in δ_{bc}, which implies that the optimal overbid rate should be at the boundaries of the range for δ_{bc}. The function to maximize over δ_{bc} is as follows.

$$\int_{x(\delta_{bc})}^{\bar{R}} p(\delta_{bc})\Big(r - \Big[V(b) - V(b - c - c\delta_{bc}) + \frac{1 - p(\delta_{bc})}{p(\delta_{bc})} g(c, \delta_{bc})\Big]\Big) f(r, c)\mathrm{d}r \tag{B.14}$$

$$= \int_{x(\delta_{bc})}^{\bar{R}} p(\delta_{bc})\Big(r - \Big[V(b) - V(b - c - c\delta_{bc}) + \frac{1}{p(\delta_{bc})} Gc + \frac{1}{p(\delta_{bc})} Gc\delta_{bc}$$

$$- Gc - Gc\delta_{bc}\Big]\Big) f(r, c)\mathrm{d}r \tag{B.15}$$

$$= \int_{x(\delta_{bc})}^{\bar{R}} \Big[p(\delta_{bc})r - p(\delta_{bc})\Big(V(b) - V(b - c - c\delta_{bc})\Big) - Gc - Gc\delta_{bc} + Gcp(\delta_{bc})$$

$$+ Gc\delta_{bc}p(\delta_{bc})\Big] f(r, c)\mathrm{d}r \tag{B.16}$$

We now show when the expression inside brackets in equation (B.16) is convex. We consider the second derivative of the function as follows:

$$\frac{\partial^2}{\partial \delta_{bc}^2}\Big(p(\delta_{bc})r - p(\delta_{bc})\Big(V(b) - V(b-c-c\delta_{bc})\Big) - Gc - Gc\delta_{bc} + Gcp(\delta_{bc})$$

$$+ Gc\delta_{bc}p(\delta_{bc})\Big) \tag{B.17}$$

$$= p''(\delta_{bc})r - \frac{\partial}{\partial \delta_{bc}}\Big[p'(\delta_{bc})\Big(V(b) - V(b-c-c\delta_{bc})\Big)$$

$$+ \frac{\partial\Big(V(b) - V(b-c-c\delta_{bc})\Big)}{\partial \delta_{bc}}p(\delta_{bc})\Big] + \frac{\partial}{\partial \delta_{bc}}\Big[-Gc + Gcp'(\delta_{bc})$$

$$+ Gc\delta_{bc}p'(\delta_{bc}) + Gcp(\delta_{bc})\Big] \tag{B.18}$$

$$= p''(\delta_{bc})r - \Big[p''(\delta_{bc})\Big(V(b) - V(b-c-c\delta_{bc})\Big) + p'(\delta_{bc})\frac{\partial\Big(V(b) - V(b-c-c\delta_{bc})\Big)}{\partial \delta_{bc}}$$

$$+ p'(\delta_{bc})\frac{\partial\Big(V(b) - V(b-c-c\delta_{bc})\Big)}{\partial \delta_{bc}} + p(\delta_{bc})\frac{\partial^2\Big(V(b) - V(b-c-c\delta_{bc})\Big)}{\partial \delta_{bc}^2}\Big]$$

$$+ \Big[Gcp''(\delta_{bc}) + Gcp'(\delta_{bc}) + Gc\delta_{bc}p''(\delta_{bc}) + Gcp'(\delta_{bc})\Big] \tag{B.19}$$

$$= p''(\delta_{bc})\Big[r + Gc\delta_{bc} + Gc - \Big(V(b) - V(b-c-c\delta_{bc})\Big)\Big] + 2Gcp'(\delta_{bc}) \tag{B.20}$$

which is based on the assumption that $\frac{\partial\left(V(b)-V(b-c-c\delta_{bc})\right)}{\partial \delta_{bc}} \approx 0$. Given that the multiplier of $p''(\delta_{bc})$ is positive by the definition of PVI threshold and integration preserves convexity, the function being maximized over δ_{bc} is convex, if $p''(\delta_{bc}) \geq 0$; i.e. when $p(\delta_{bc})$ is convex in δ_{bc}, which implies that δ_{bc}^* is at the boundary of the range of δ_{bc} values.

Moreover, the function being maximized is also convex when the expression in (B.20) is negative for concave probability of success functions. Hence, if $p''(\delta_{bc}) < 0$, the maximized function is convex when the following condition holds for all $\delta_{bc} \in [0, \bar{\delta_c}]$:

$$-p''(\delta_{bc})\Big[r + Gc\delta_{bc} + Gc - \Big(V(b) - V(b-c-c\delta_{bc})\Big)\Big] \leq 2Gcp'(\delta_{bc}) \tag{B.21}$$

Note that by the definition of the PVI threshold we have that $r \geq \Big(V(b) - V(b-c-c\delta_{bc})\Big)$ and a lower bound on $V(b) - V(b-c-c\delta_{bc})$ is $\underline{R} + \frac{1-p(\delta_{bc})}{p(\delta_{bc})}Gc$. It follows that for convexity :

$$-p''(\delta_{bc})\Big[r + Gc\delta_{bc} + Gc - \underline{R} - \Big(\frac{1-p(\delta_{bc})}{p(\delta_{bc})}\Big)Gc\Big] \leq 2Gcp'(\delta_{bc}) \tag{B.22}$$

$$\Rightarrow -p''(\delta_{bc})\Big[r + Gc\Big(\delta_{bc} + 1 - \frac{1-p(\delta_{bc})}{p(\delta_{bc})} - \underline{R}\Big)\Big] \leq 2Gcp'(\delta_{bc}) \tag{B.23}$$

□

Proof of Corollary 1

For result 1, we note that the function in equation (B.7) is either convex or concave depending on the problem parameters as defined by (B.23). If it is convex, then the optimal overbid rate $\delta^*_{bc} \in \{0, \bar{\delta}_c\}$ as discussed in the proof of Theorem 2. If the function is concave, then per equation (B.13), the maximizer for the function has to satisfy the condition that $p'(\delta_{bc})K - L(\delta_{bc}) = 0$ for a PVI threshold level k. Note that if the solution of this equation does not lie within the range $[0, \bar{\delta}_c]$, then the optimal overbid rate is either 0 or $\bar{\delta}_c$ depending on whether the function is increasing or decreasing in that range.

For results 2 and 3, the optimal overbid rate corresponds to a root of a polynomial defined by $p'(\delta_{bc})K - L(\delta_{bc}) = 0$, which can expressed as $Gc(1 - p(\delta_{bc}) - \frac{p'(\delta_{bc})}{p(\delta_{bc})}(1 + \delta_{bc})) - Kp'(\delta_{bc}) = 0$. Thus as the polynomial function is nonincreasing in K and nondecreasing in c, the solution for the optimal overbid rate is also nonincreasing in K and nondecreasing in c. □

Proof of Corollary 2

For result 1, we can express equation (B.12) for the uniformly distributed PVI values as follows:

$$p'(\delta_{bc})\int_{x(\delta_{bc})}^{\bar{R}} r\frac{1}{\bar{R}-\underline{R}}\mathrm{d}r - p'(\delta_{bc})x(\delta_{bc})\frac{\bar{R}-x(\delta_{bc})}{\bar{R}-\underline{R}} - L(\delta_{bc})\frac{\bar{R}-x(\delta_{bc})}{\bar{R}-\underline{R}} \tag{B.24}$$

If this derivative is negative, then $\delta_{bc}^* = 0$. Hence, we have that:

$$p'(\delta_{bc})\frac{\bar{R}^2-x(\delta_{bc})^2}{2(\bar{R}-\underline{R})} - p'(\delta_{bc})x(\delta_{bc})\frac{\bar{R}-x(\delta_{bc})}{\bar{R}-\underline{R}} - L(\delta_{bc})\frac{\bar{R}-x(\delta_{bc})}{\bar{R}-\underline{R}} \leq 0 \tag{B.25}$$

$$\Rightarrow \quad p'(\delta_{bc})(\bar{R}-x(\delta_{bc}))(\bar{R}+x(\delta_{bc})) - 2p'(\delta_{bc})x(\delta_{bc})(\bar{R}-x(\delta_{bc}))$$

$$- 2L(\delta_{bc})(\bar{R}-x(\delta_{bc})) \leq 0 \tag{B.26}$$

$$\Rightarrow \quad p'(\delta_{bc})(\bar{R}+x(\delta_{bc})) - 2p'(\delta_{bc})x(\delta_{bc}) - 2L(\delta_{bc}) \leq 0 \tag{B.27}$$

$$\Rightarrow \quad p'(\delta_{bc})(\bar{R}-x(\delta_{bc})) - 2L(\delta_{bc}) \leq 0 \tag{B.28}$$

An upper bound for the expression on the left hand side is when $\delta_{bc} = \bar{\delta}_c$, $x(\delta_{bc}) = \underline{R}$, and $L(\delta_{bc}) = \underline{L}$. Hence, the function is decreasing in δ_{bc} and $\delta_{bc}^* = 0$, if the condition $p'(\bar{\delta}_c)(\bar{R}-\underline{R})-2\underline{L} \leq 0$ holds. Similarly, $\delta_{bc}^* = \bar{\delta}_c$ if the derivative is positive, and in that case result 2 in Theorem 2 applies.

For result 2, we use the derivative function given on the left hand side of (B.28), along with the observation that in case of convexity the optimal overbid rate is either 0 or $\bar{\delta}_c$. If the function being maximized is concave in δ_{bc} and a threshold k is used, then $p'(\delta_{bc})(\bar{R}-k)-2L(\delta_{bc}) = 0$ should hold for the optimal overbid rate. If, however, none of the solutions of the equation lie within the range $[0, \bar{\delta}_c]$, then again optimal overbid rate is either 0 or $\bar{\delta}_c$. □

Proof of Theorem 3 Item 1

The result implies that the optimal expected total PVI value is nondecreasing in the amount of accessible funds. Note that for a given overbid rate δ_{bc}, the value function can be represented as follows:

$$\alpha V(b) = \lambda \int_{\underline{C}}^{b} \max_{\delta_{bc}} \Bigg\{ \int_{x(\delta_{bc})}^{\bar{R}} p(\delta_{bc})\Bigg(r - [V(b) - V(b-c-c\delta_{bc})$$

$$+ \frac{1-p(\delta_{bc})}{p(\delta_{bc})} g(c,\delta_{bc})]\Big) f(r,c)\mathrm{d}r \Big\}\mathrm{d}c \tag{B.29}$$

Note that upper limit on the first integral is b. Moreover, PVI values are accumulated additively for every property that can be acquired with the current amount of accessible funds. Hence, if the same acquisition policy is used for two fund levels b_1 and b_2 such that $b_1 > b_2$, then the definition of $V(b)$ in (B.29) implies $V(b_1) \geq V(b_2)$. $\square$

Proof of Theorem 3 Item 2

This result implies that optimal PVI thresholds are nondecreasing in availability rate λ. Note that the optimal PVI threshold $x(\delta^*_{bc})$ is defined based on

$$x(\delta_{bc}) = V(b) - V(b-c-c\delta_{bc}) + \frac{1-p(\delta_{bc})}{p(\delta_{bc})} g(c,\delta_{bc}) \tag{B.30}$$

Per the result in Theorem 1, for any fund level the value function is defined as follows:

$$V(b) = \frac{\lambda}{\alpha}\int_{\underline{C}}^{b}\int_{x(\delta_{bc})}^{\bar{R}} p(\delta_{bc})\Big(r - \big[V(b)-V(b-c-c\delta_{bc}) + \frac{1-p(\delta_{bc})}{p(\delta_{bc})} g(c,\delta_{bc})\big]\Big) f(r,c)\mathrm{d}r\mathrm{d}c \tag{B.31}$$

which implies that expected total PVI is nondecreasing in the availability rate λ. Considering that this would apply both to $V(b)$ and $V(b-c-c\delta_{bc})$, and given the fact that $V(b) \geq V(b-c-c\delta_{bc})$, it follows that $V(b)-V(b-c-c\delta_{bc})$ is nondecreasing in λ. This in turn implies that optimal PVI thresholds are nondecreasing in availability rate λ. $\square$

Proof of Theorem 3 Item 3

Note that the statement implies the concavity of $V^*(b)$ if and only if the optimal PVI thresholds $x(\delta^*_{bc})$ are nonincreasing in the amount of accessible funds b for any property with asking price c. $V^*(b)$ is concave in b when the following holds for any $b_1 \geq b_2$.

$$V^*(b_1) - V^*(b_1 - c - c\delta^*_{b_1c}) \leq V^*(b_2) - V^*(b_2 - c - c\delta^*_{b_2c}) \tag{B.32}$$

$$\Leftrightarrow \quad V^*(b_1) - V^*(b_1 - c - c\delta^*_{b_1c}) + \frac{1 - p(\delta^*_{b_1c})}{p(\delta^*_{b_1c})} g(c, \delta^*_{b_1c}) \leq V^*(b_2) - V^*(b_2 - c - c\delta^*_{b_2c}) + \frac{1 - p(\delta^*_{b_2c})}{p(\delta^*_{b_2c})} g(c, \delta^*_{b_2c}) \tag{B.33}$$

$$\Leftrightarrow \quad x(\delta^*_{b_1c}) \leq x(\delta^*_{b_2c}) \tag{B.34}$$

where the inequality in (B.33) is due to the approximate independence of the optimal overbid rate δ^*_{bc} and the fund level, i.e. due to having $\delta^*_{bc} = \delta^*_c$ for all fund levels b. □

Proof of Theorem 3 Item 4

Note that the optimal PVI threshold $x(\delta^*_{bc})$ is defined based on

$$x(\delta_{bc}) = V(b) - V(b - c - c\delta_{bc}) + \frac{1 - p(\delta_{bc})}{p(\delta_{bc})} g(c, \delta_{bc}) \tag{B.35}$$

Hence, to determine whether PVI thresholds will decrease or increase as a function of δ_{bc}, we approximate the derivative of $x(\delta_{bc})$ for given b and c as:

$$\frac{\partial x(\delta_{bc})}{\partial \delta_{bc}} \cong \frac{\partial}{\partial \delta_{bc}} \left(\frac{1 - p(\delta_{bc})}{p(\delta_{bc})} (Gc + Gc\delta_{bc}) \right) \tag{B.36}$$

$$= -\left(\frac{p'(\delta_{bc})[Gc + Gc\delta_{bc}]}{p(\delta_{bc})} + \frac{1 - p(\delta_{bc})[Gc + Gc\delta_{bc}]p'(\delta_{bc})}{p^2(\delta_{bc})} \right) + \frac{(1 - p(\delta_{bc}))Gc}{p(\delta_{bc})} \tag{B.37}$$

By setting expression (B.37) equal to zero, we get

$$-\frac{p'(\delta_{bc})[Gc + Gc\delta_{bc}]}{p(\delta_{bc})} \left(1 + \frac{1 - p(\delta_{bc})}{p(\delta_{bc})} \right) + \frac{(1 - p(\delta_{bc}))Gc}{p(\delta_{bc})} = 0 \tag{B.38}$$

$$\Rightarrow \quad -p'(\delta_{bc})[Gc + Gc\delta_{bc}] + (1 - p(\delta_{bc}))Gcp(\delta_{bc}) = 0 \tag{B.39}$$

$$\Rightarrow \quad Gc(-p'(\delta_{bc}) - \delta_{bc}p'(\delta_{bc})) + Gc(p(\delta_{bc}) - (p(\delta_{bc}))^2) = 0 \tag{B.40}$$

$$\Rightarrow \quad p(\delta_{bc}) - p(\delta_{bc})^2 - p'(\delta_{bc}) - \delta_{bc}p'(\delta_{bc}) = 0 \tag{B.41}$$

$$\Rightarrow \quad p(\delta_{bc})(1 - p(\delta_{bc})) - p'(\delta_{bc})(1 + \delta_{bc}) = 0 \tag{B.42}$$

Note that $\frac{\partial^2 x(\delta_{bc})}{\partial \delta_{bc}^2} \leq 0$ as it follows from differentiating the left hand side of equation (B.41). Hence $x(\delta_{bc})$ is concave in δ_{bc}. Let $\dot{\delta}_{bc}$ be a solution to the equation $p(\delta_{bc})\big(1 - p(\delta_{bc})\big) - p'(\delta_{bc})(1 + \delta_{bc}) = 0$. Given the concavity of $x(\delta_{bc})$ in δ_{bc}, we note that if there is a unique solution $\dot{\delta}_{bc} \in [0, \bar{\delta}_c]$ or if $\dot{\delta}_{bc} > \bar{\delta}_c$, then for all $\delta_{bc} \in [0, \dot{\delta}_{bc}]$, the PVI threshold increases as a function of the overbid rate. For all, $\delta_{bc} \in [\dot{\delta}_{bc}, \bar{\delta}_c]$ or if $\dot{\delta}_{bc} < 0$, the PVI threshold decreases as a function of the overbid rate. □

Proof of Theorem 3 Item 5

Assume that the PVI threshold $x(\delta_{bc})$ is nondecreasing in δ_{bc}. Without loss of generality, let $x(\delta_{bc}) = \underline{R}$, which implies by definition that when the overbid rate δ_{bc} is used, the critical fund level $\dot{B}(\delta_{bc}) = b$. Now consider an overbid rate δ'_{bc} such that $\delta'_{bc} > \delta_{bc}$. Given that $x(\delta_{bc})$ is nondecreasing in δ_{bc}, this implies $x(\delta'_{bc}) \geq x(\delta_{bc}) = \underline{R}$, which in turn indicates that the critical fund level $\dot{B}(\delta'_{bc}) \geq \dot{B}(\delta_{bc})$. We note through a similar argument that if the latter condition holds, then it would imply that $x(\delta_{bc})$ has to be nondecreasing in δ_{bc}. □

Proof of Theorem 3 Item 6

Since $\frac{\partial V(b)}{\partial t} = 0$ and $\frac{\partial x(\delta^*_{bc})}{\partial t} = 0$, the critical fund level value where $x(\delta^*_{bc}) = \underline{R}$ is the same for different time values. Hence, critical fund level is constant over time. Moreover, given that $\frac{\partial x(\delta^*_{bc})}{\partial t} = 0$, the PVI threshold is constant over time. Hence, it follows from conditions (B.32)-(B.34) that this implies marginal value of accessible funds is constant over time. □

Proof of Theorem 4

We express the value function at time t as follows by conditioning on whether a new property becomes available in the next Δt time units or not:

$$
\begin{aligned}
V^*\big(b_t\big) &= (1-\alpha\Delta)\Big\{\lambda\Delta\Big[\Big[\int_{\underline{C}}^{b}\max_{\delta_{bct}}\Big\{\int_{x(\delta_{bct})}^{\bar{R}}(r+V^*((b-c-c\delta_{bct})_{t+\Delta})p(\delta_{bct}) \\
&\quad+(V^*(b_{t+\Delta})-g(c,\delta_{bct}))(1-p(\delta_{bct}))f(r,c)\mathrm{d}r\Big\}\mathrm{d}c\Big] \\
&\quad+\int_{\underline{C}}^{b}\int_{\underline{R}}^{x(\delta_{bct})}V^*(b_{t+\Delta})f(r,c)\mathrm{d}r\mathrm{d}c\Big]+(1-\lambda\Delta)V^*(b_{t+\Delta})\Big\} \qquad \text{(B.43)} \\
&= (1-\alpha\Delta)\lambda\Delta\Big[\Big[\int_{\underline{C}}^{b}\max_{\delta_{bct}}\Big\{\int_{x(\delta_{bct})}^{\bar{R}}(r+V^*((b-c-c\delta_{bct})_{t+\Delta})p(\delta_{bct}) \\
&\quad+(V^*(b_{t+\Delta})-g(c,\delta_{bct}))(1-p(\delta_{bct}))f(r,c)\mathrm{d}r\Big\}\mathrm{d}c\Big] \\
&\quad+\int_{\underline{C}}^{b}\int_{\underline{R}}^{x(\delta_{bct})}V^*(b_{t+\Delta})f(r,c)\mathrm{d}r\mathrm{d}c\Big] \\
&\quad+V^*(b_{t+\Delta})-\Delta(\alpha+\lambda-\lambda\alpha\Delta)V^*(b_{t+\Delta}) \qquad \text{(B.44)} \\
\Rightarrow\quad \frac{V^*(b_t)-V^*(b_{t+\Delta})}{\Delta} &= (1-\alpha\Delta)\lambda\Big[\Big[\int_{\underline{C}}^{b}\max_{\delta_{bct}}\Big\{\int_{x(\delta_{bct})}^{\bar{R}}(r+V^*((b-c-c\delta_{bct})_{t+\Delta}) \\
&\quad p(\delta_{bct})+(V^*(b_{t+\Delta})-g(c,\delta_{bct}))(1-p(\delta_{bct}))f(r,c)\mathrm{d}r\Big\}\mathrm{d}c\Big] \\
&\quad+\int_{\underline{C}}^{b}\int_{\underline{R}}^{x(\delta bct)}V^*(b_{t+\Delta})f(r,c)\mathrm{d}r\mathrm{d}c\Big]-(\alpha+\lambda-\lambda\alpha\Delta)V^*(b_{t+\Delta}) \qquad \text{(B.45)}
\end{aligned}
$$

Letting $\Delta \to 0$;

$$
\begin{aligned}
\frac{\partial V\big(b_t\big)}{\partial t} &= \lambda\Big[\int_{\underline{C}}^{b}\max_{\delta_{bct}}\Big\{\int_{x(\delta_{bct})}^{\bar{R}}(r+V^*((b-c-c\delta_{bct})_t)p(\delta_{bct})+(V^*(b_t) \\
&\quad-g(c,\delta_{bct}))(1-p(\delta_{bct}))f(r,c)\mathrm{d}r\mathrm{d}c+\int_{\underline{C}}^{b}\int_{\underline{R}}^{x(\delta_{bct})}V^*\big(b_t\big)p(\delta_{bct})f(r,c)\mathrm{d}r\mathrm{d}c\Big] \\
&\quad-(\alpha+\lambda)V^*\big(b_t\big) \qquad \text{(B.46)} \\
&= \lambda\Big[\int_{\underline{C}}^{b}\max_{\delta_{bct}}\Big\{\int_{x(\delta_{bct})}^{\bar{R}}(r+V^*((b-c-c\delta_{bct})_t)p(\delta_{bct})+(V^*(b_t) \\
&\quad-g(c,\delta_{bct}))(1-p(\delta_{bct}))f(r,c)\mathrm{d}r\Big\}\mathrm{d}c+\Big[\int_{\underline{C}}^{\bar{C}}\int_{\underline{R}}^{\bar{R}}V^*\big(b_t\big)f(r,c)\mathrm{d}r\mathrm{d}c
\end{aligned}
$$

$$- \int_{\underline{C}}^{\bar{b}} \int_{x(\delta_{bct})}^{\bar{R}} V^*\big(b_t\big) f(r,c) \mathrm{d}r \mathrm{d}c \Big]\Big] - (\alpha + \lambda) V^*\big(b_t\big) \tag{B.47}$$

$$= \lambda \Big[\int_{\underline{C}}^{b} \max_{\delta_{bct}} \Big\{ \int_{x(\delta_{bct})}^{\bar{R}} \Big[(r + V^*((b - c - c\delta_{bct})_t) p(\delta_{bct})$$

$$+ (V^*(b_t) - g(c, \delta_{bct}))(1 - p(\delta_{bct})) - V^*(b_t) \Big] f(r,c) \mathrm{d}r \Big\} \Big] \mathrm{d}c$$

$$- (\alpha + \lambda) V^*(b_t) + \lambda V^*(b_t) \tag{B.48}$$

Hence, the optimal value function $V^*(b_t)$ is the solution of the differential equation:

$$\frac{\partial V\big(b_t\big)}{\partial t} = \lambda \int_{\underline{C}}^{b} \max_{\delta_{bct}} \Big\{ \int_{x(\delta_{bct})}^{\bar{R}} p(\delta_{bct})(r - [V^*\big(b_t\big) - V^*((b - c - c\delta_{bct})_t)$$

$$+ \frac{1 - p(\delta_{bct})}{p(\delta_{bct})} g(c, \delta_{bct})]) f(r,c) \mathrm{d}r \Big\} \mathrm{d}c - \alpha V\big(b_t\big) \tag{B.49}$$

□

Proof of Theorem 5

Note that equation (B.7) is equivalent to the following for the case with fund expiration:

$$\delta^*_{bct} = \operatorname*{argmax}_{\delta_{bct}} \Big\{ \int_{x(\delta_{bct})}^{\bar{R}} p(\delta_{bct}) \big(r - x(\delta_{bct})\big) f(r,c) \mathrm{d}r \Big\} \tag{B.50}$$

Following the same procedure as in the no fund expiration case, the derivative of the function to be maximized is:

$$p'(\delta_{bc}) \mathbb{E}[r | r \geq x(\delta_{bct})] P(r \geq x(\delta_{bct})) - p'(\delta_{bct}) x(\delta_{bct}) P(r \geq x(\delta_{bct}))$$

$$- p(\delta_{bct}) x'(\delta_{bct}) P(r \geq x(\delta_{bct})) \tag{B.51}$$

Note that $x'(\delta_{bct}) \approx \frac{\partial}{\partial \delta_{bct}} \Big(\frac{(1 - p(\delta_{bct})) g(c, \delta_{bct})}{p(\delta_{bct})} \Big)$ under the assumption that $\frac{\partial (V(b_t) - V((b - c - c\delta_{bc})_t)}{\partial \delta_{bct}}$ is small enough to be ignored. This implies that $x'(\delta_{bct})$ is independent of time and thus the same results for the infinite horizon case apply. □

Proof of Theorem 6 Item 1

The same procedures applied for the proofs of the corresponding results in the no fund expiration case can be used to show that these results hold independent of time. More specifically, for result 1 we note that the upper limit on the integral in the value function definition is b, and a larger value here would imply a larger expected total PVI without any implication of the time. The other results follow from the fact that optimal overbid rates are approximately independent of time. $\square$

Proof of Theorem 6 Item 2

The statement implies that the expected total PVI value is nonincreasing in time. We show through the discrete time approximation of the optimal value function that this holds for all fund levels. Recall that this approximation is expressed as follows:

$$\begin{aligned} V^*(b_{t-T/\tau}) =&(1-\alpha)V^*\big(b_t\big) + \frac{T}{\tau}\lambda \int_{\underline{C}}^{b_t} \max_{\delta_{bct}} \Bigg\{ \int_{x(\delta_{bct})}^{\bar{R}} p(\delta_{bct})\Big(r - \big[V^*\big(b_t\big) \\ &- V^*\big((b-c-c\delta_{bct})_t\big) + \frac{1-p(\delta_{bct})}{p(\delta_{bct})} g(c,\delta_{bct})\big]\Big) f(r,c)\mathrm{d}r \Bigg\}\mathrm{d}c \end{aligned} \tag{B.52}$$

Note that the second component on the right hand side is nonnegative by definition. Given that $\alpha \geq 0$, we get $V^*(b_{t-T/\tau}) \geq V^*(b_t)$ for any T/τ at all fund levels. $\square$

Proof of Theorem 6 Item 3

Let $\frac{\partial V(b_t)}{\partial b}$ be the marginal value of accessible funds. Per Theorem 6 item 2, we have that PVI value $V(b_t)$ is nonincreasing over time. Given that $\frac{\partial}{\partial t}\frac{\partial V(b_t)}{\partial b} = \frac{\partial}{\partial b}\frac{\partial V(b_t)}{\partial t}$ per Young's theorem, we have that $\frac{\partial V(b_t)}{\partial b}$ is also nonincreasing in time. $\square$

Proof of Theorem 6 Item 4

The change in the optimal PVI threshold over time is expressed as:

$$\frac{\partial x(\delta^*_{bct})}{\partial t} = \frac{\partial\Big(V\big(b_t\big) - V\big((b-c-c\delta^*_{bct})_t\big) + \frac{1-p(\delta^*_{bct})}{p(\delta^*_{bct})} g(c,\delta^*_{bct})\Big)}{\partial t} \tag{B.53}$$

We have through the result in Theorem 2 Item 3 that:

$$\frac{\partial\Big(V\big(b_t\big) - V\big((b - c - c\delta^*_{bct})_t\big)\Big)}{\partial t} \leq 0 \tag{B.54}$$

In addition, Theorem 5 establishes the independence of δ^*_{bct} over time, implying that the derivative of the last component in the numerator of (B.53) with respect to t is zero. It follows that $\frac{\partial x(\delta^*_{bct})}{\partial t} \leq 0$. □

Proof of Theorem 6 Item 5

Without loss of generality, let $x(\delta_{bct}) = \underline{R}$, which implies by definition that when the overbid rate δ_{bct} is used, the critical fund level at time t is $\dot{B}(\delta_{bct}) = b$. Now consider the same overbid rate used at time t' such that $\delta_{bct} = \delta_{bct'}$ where $t' > t$. Given that $x(\delta_{bct})$ is nondecreasing in t due to Theorem 6 Item 4, this implies $x(\delta_{bct'}) \geq x(\delta_{bct}) = \underline{R}$, which in turn indicates that the critical fund level $\dot{B}(\delta_{bct'}) \geq \dot{B}(\delta_{bct})$. □

Proof of Theorem 6 Item 6

We show the correctness of this statement through a similar argument as in the proof of Theorem 3 Item 5 above. Assume that the PVI threshold $x(\delta_{bct})$ is nondecreasing in δ_{bct}. Without loss of generality, let $x(\delta_{bct}) = \underline{R}$, which implies by definition that when the overbid rate δ_{bct} is used, the critical time $\dot{T}(\delta_{bct}) = t$. Now consider an overbid rate δ'_{bct} such that $\delta'_{bct} > \delta_{bct}$. Given that $x(\delta_{bct})$ is nondecreasing in δ_{bct}, this implies $x(\delta'_{bct}) \geq x(\delta_{bct}) = \underline{R}$, which in turn indicates that the critical time $\dot{T}(\delta'_{bct}) \geq \dot{T}(\delta_{bct})$. We note through a similar argument that if the latter condition holds, then it would imply that $x(\delta_{bct})$ has to be nondecreasing in δ_{bct}. □

Proof of Theorem 6 Item 7

Assume that the PVI threshold $x(\delta_{bct})$ is nonincreasing in b. Without loss of generality, let $x(\delta_{bct}) = \underline{R}$, which implies by definition that when the overbid rate δ_{bct}

is used, the critical time $\dot{T}(\delta_{bct}) = t$. Now consider the same overbid rate used at fund level b' such that $\delta_{bct} = \delta_{b'ct}$ where $b' > b$. Given that $x(\delta_{bct})$ is nonincreasing in b, this implies $x(\delta_{b'ct}) \leq x(\delta_{bct}) = \underline{R}$, which in turn indicates that the critical time $\dot{T}(\delta_{b'ct}) \leq \dot{T}(\delta_{bct})$. We note through a similar argument that if the latter condition holds, then it would imply that $x(\delta_{bct})$ has to be nonincreasing in b. □

BIBLIOGRAPHY

Aaby, K., Herrmann, J. W., Jordan, C., Treadwell, M., and Wood, K. Montgomery countys public health service uses operations research to plan emergency mass dispensing and vaccination clinics. *Interfaces*, 36(6):569–579, 2006.

Ahmed, F., Kalyanmoy, D., and Abhilash, J. Multi-objective optimization and decision making approaches to cricket team selection. *Applied Soft Computing*, 13(1): 402–414, 2012.

Aobdia, D. and Caskey, J. Investor cost basis and takeover bids, Working Paper, 2012. URL `http://papers.ssrn.com/sol3/papers.cfm?abstract_id=2037551`.

Axel-Lute, M. and Hersh, M. B. The hard part. Technical report, Shelterforce, National Housing Institute, 2011.

Bardach, E. *A Practical Guide for Policy Analysis: The Eightfold Path to More Effective Problem Solving*. Washington, D.C.: CQ Press, 2005.

Bayram, A., Solak, S., Johnson, M. P., and Turcotte, D. Stochastic dynamic models for foreclosed housing acquisition and redevelopment. In *Proceedings of the Industrial Engineering Research Conference*, Reno, NV, 2011a.

Bayram, A., Solak, S., Johnson, M. P., and Turcotte, D. Managing foreclosed housing portfolios for improved social outcomes. In *Proceedings of the Production and Operations Management Society 22nd Annual Conference*, Reno, NV, 2011b.

Berenguer, G. Challenges in nonprofit operations: an operations management perspective, Working Paper, 2013. URL `http://web.ics.purdue.edu/~gberengu/Styles/files/Resume.pdf`.

Bernanke, B. S. Housing, mortgage markets, and foreclosures. In *System Conference on Housing and Mortgage Markets*, Washington, D.C., 2008.

Bertsimas, D. and Popescu, I. Revenue management in a dynamic network environment. *Transportation Science*, 37(3):257–277, 2003.

Bhide, A. Reversing corporate diversification. In *The New Corporate Finance- Where Theory Meets Practice*. New York: McGraw Hill, 1993.

Bodily, S. Police sector design incorporating preferences of interest groups for equality and efficiency. *Management Science*, 24(12):1301–1313, 1978.

Bordoloi, S. and Weatherby, E. Managerial implications of calculating optimal nurse staffing in medical units. *Health Care Management Review*, 24(4):35–44, 1999.

Bratt, R. Challenges for nonprofit housing organizations created by the private housing market. *Journal of Urban Affairs*, 31(1):67–96, 2009.

Burtscher, M., Manser, T., Kolbe, M., Grote, G., Grande, B., Spahn, D., and Wacker, J. Adaptation in anaesthesia team coordination in response to a simulated critical event and its relationship to clinical performance. *British Journal of Anesthesia*, 106(6):801–806, 2011.

Business Insider. U.S. home values lost $798 billion last quarter, 2012. URL `http://articles.businessinsider.com/2011-02-09/markets/29954161_1_peak-zillow-total-loss`.

Calafiore, G. C. Multi-period portfolio optimization with linear control policies. *Automatica*, 44:2463–2473, 2008.

Campbell, A. M., Vandenbussche, D., and Hermann, W. Routing for relief efforts. *Transportation Science*, 42(2):127–145, 2008.

Campbell, J. Y., Giglio, S., and Pathak, P. Forced sales and house prices, Working Paper, 2009. URL `http://www.nber.org/papers/w14866.pdf?new_window=1`.

Cardoen, B., Demeulemeester, E., and Beliën, J. Operating room planning and scheduling: A literature review. *European Journal of Operational Research*, 201(3): 921–932, 2010.

Carøe, C. and Schultz, R. Dual decomposition in stochastic integer programming. *Operations Research Letters*, 24(1):37–45, 1999.

Cassera, M., Zheng, B., Martinec, D., Dunst, C. M., and Swanström, L. Surgical time independently affected by surgical team size. *The American Journal of Surgery*, 198(2):216–222, 2009.

Chalabi, Z., Epsten, D., McKenna, C., and Claxton, K. Uncertainty and value of information when allocating resources within and between healthcare programmes. *European Journal of Operational Research*, 191(2):530–539, 2008.

Chen, C. Foreclosures drag on U.S. recovery. Technical report, Moodys Analytics, 2009. URL `https://www.economy.com/dismal/article_free.asp?cid=116439`.

Chen, S. and Lin, L. Modeling team member characteristics for the formation of a multifunctional team in concurrent engineering. *IEEE Transactions on Engineering Management*, 51(2):111–124, 2004.

Cheng, L., Subrahmanian, E., and Westerberg, A. Design and planning under uncertainty: issues on problem formulation and solution. *Computers and Chemical Engineering*, 27(6):781–803, 2003.

Choi, S. and Wilhelm, W. E. An approach to optimize block surgical schedules. *European Journal of Operational Research*, 2013. URL http://www.sciencedirect.com/science/article/pii/S0377221713008631. Accepted Article.

CNN. Home values plummet $500 billion., 2009. URL http://money.cnn.com/2009/12/09/real_estate/home_value_loss/index.htm.

Collette, Y. and Siarry, P. *Multiobjective Optimization: Principles and Case Studies*. Berlin: Springer, 2003.

Community Wealth. Overview: Community development corporations, 2012. URL http://www.community-wealth.org/strategies/panel/cdcs/index.html.

Creators.com. Robotic surgery is all the rage, but price is high, 2010. URL https://www.creators.com/health/david-lipschitz.html.

Damodaran, A. The value of synergy, Working Paper, 2005. URL http://people.stern.nyu.edu/adamodar/pdfiles/papers/synergy.pdf.

Dantzig, G. B. Optimal solution of a dynamic Leontief model with substitution. *Econometrica*, 23(3):295–302, 1955.

Dizdar, D., Gershkov, A., and Moldovanu, B. Revenue maximization in the dynamic knapsack problem. *Theoretical Economics*, 6(3):157–184, 2011.

Dowsland, K. A. Nurse scheduling with tabu search and strategic oscillation. *European Journal of Operational Research*, 106(2):393–407, 1998.

Drew, D., Skitmore, M., and Lo, H. P. The effect of client and type and size of construction work on a construction's bidding strategy. *Building and Environment*, 36(3):393–406, 2001.

Ebme Articles. Robotic-assisted surgery, 2013. URL http://www.ebme.co.uk/articles/clinical-engineering/83-robotic-assisted-surgery.

Eckenrode, R. T. Weighting multiple criteria. *Management Science*, 12(1):180–192, 1965.

Francis, P., Smilowitz, K., and Tzur, M. The period vehicle routing problem with service choice. *Transportation Science*, 40(4):439–454, 2006.

Fransen, A., Van, J., Merién, A., Wit-Zuurendonk, L., Houterman, S., Mol, B., and Oei, S. Effect of obstetric team training on team performance and medical technical skills: a randomised controlled trial. *BJOG: An International Journal of Obstetrics & Gynaecology*, 119(11):1387–1393, 2012.

Frisch, M. and Servon, L. J. CDCs and the changing context for urban community development: A review of the field and the environment. *Community Development*, 37(4):88–108, 2006.

Galster, G., Levy, D., Sawyer, N., Temkin, K., and Walker, C. The impact of community development corporations on urban neighborhoods. Technical report, Washington, D.C.: The Urban Institute, 2005.

Galster, G., Tatian, P., and Accordino, J. Targeting investments for neighborhood revitalization. *Journal of the American Planning Association*, 72(4):457–474, 2006.

Gass, A. Implementing the neighborhood stabilization program. Technical report, NeighborWorks America, Neighborhood Reinvestment Corporation, 2010.

GLG. Surgical robot claims, 2013. URL `http://www.thegilbertlawgroup.com/practice-areas/product-liability/surgical-robots/`.

Harding, J. P., Rosenblatt, E., and Yao, V. W. The contagion effect of foreclosed properties. *Journal of Urban Economics*, 66(3):164–178, 2009.

Harper, P., Powell, N., and Williams, J. Modeling the size and skill-mix of hospital nursing teams. *Journal of the Operational Research Society*, 61(5):768–779, 2009.

Hiriart-Urruty, J. B. and Lemaréchal, C. *Convex Analysis and Minimization Algorithms: Part 1: Fundamentals*. Berlin: Springer, 1996.

Hobbs, B. F. A comparison of weighting methods in power plant siting. *Decision Science*, 11(1):725–737, 1980.

Holt, C. A. and Sherman, R. Risk aversion and the winner's curse, Working Paper, 2000. URL `http://people.virginia.edu/~cah2k/wincurse.pdf`.

HUD. Preston allocates nearly $4 billion to stabilize neighborhoods in states and local communities hard-hit by foreclosure, 2008. URL `http://www.hud.gov/news/release.cfm?content=pr08-148.cfm`.

Immergluck, D. and Smith, G. The external costs of foreclosure: The impact of single-family mortgage foreclosures on property values. *Housing Policy Debate*, 17 (1):57–79, 2006.

Jeffcott, S. Optimizing team performance in the emergency department. Technical report, Melbourne: Monash University Dept of Epidemiology and Preventative Medicine, NHMRC CRE in Patient safety, 2009.

Johnson, M. P. *Community-Based Operations Research: Decision Modeling for Local Impact and Diverse Populations*. New York: Springer, 2011.

Johnson, M. P. and Smilowitz, K. Community-based operations research. *Tutorials in Operations Research*, 13(1):102–123, 2007.

Johnson, M. P., Turcotte, D., and Sullivan, F. What foreclosed homes should a municipality purchase to stabilize vulnerable neighborhoods? *Networks and Spatial Economics*, 10(3):363–388, 2010.

Johnson, M. P., Solak, S., Drew, R., and Keisler, J. Property value impacts of foreclosed housing acquisitions under uncertainty. *Socio-Economic Planning Sciences*, 47(4):292–308, 2013.

Joint Center for Housing Studies. The state of the nation's housing, 2009. URL `http://www.jchs.harvard.edu/publications/markets/son2009/son2009.pdf`.

Kilic, O. A., Donk, D. P., Wijngaard, J., and Tarim, S. A. Order acceptance in food processing systems with random raw material requirements. *OR Spectrum*, 32(3): 905–925, 2010.

Kingsley, G., Smith, R., and Price, D. The Impacts of Foreclosures on Families and Communities. a report to the open society institute, Washington, D.C.: The Urban Institute. Technical report, 2009. URL `http://www.urban.org/UploadedPDF/411909_impact_of_forclosures.pdf`.

Kleywegt, A. J. and Papastavrou, J. D. The dynamic and stochastic knapsack problem. *Operations Research*, 46:17–35, 1998.

Kleywegt, A. J. and Papastavrou, J. D. The dynamic and stochastic knapsack problem with random sized items. *Operations Research*, 4(1):26–41, 2001.

Lanfranco, A. R., Castellanos, A. E., Desai, J. P., and Meyers, W. C. Robotic surgery: a current perspective. *Annals of Surgery*, 239(1):14, 2004.

Leclerc, P. D. and McLay, L. A. Community-based operations research: Modeling equity for allocating public resources. *Community-Based Operations Research*, 167 (1):97–118, 2012.

Lin, G. Y., Lu, Y., and Yao, D. D. The stochastic knapsack revisited: Switch-over policies and dynamic pricing. *Operations Research*, 56(4):945–957, 2008.

Loch, C. H. and Kavadias, S. Dynamic portfolio selection of NPD programs using marginal returns. *Management Science*, 48(10):1227–1241, 2002.

Louveaux, F. and Schultz, R. Stochastic integer programming. *Handbooks in Operations Research and Management Science*, 10(4):213–266, 2003.

Lu, Y. Solving a dynamic resource allocation problem through continuous optimization. *IEEE Transactions on Automatic Control*, 50(6):890–894, 2005.

McDonald, J. F. and Stokes, H. H. Dynamics of housing price–foreclosure rate interactions. *ISRN Economics*, 2013(4):1–16, 2013.

McLain, T. M. *The use of factor analysis in the development of hand sizes for glove design*. PhD thesis, University of Nebraska at Lincoln, 2010.

Medaglia, A. L., Graves, S. B., and Ringuest, J. L. A multiobjective evolutionary approach for linearly constrained project selection under uncertainty. *European Journal of Operational Research*, 179(3):869–894, 2007.

Mild, P. and Salo, A. Combining a multiattribute value function with an optimization model: An application to dynamic resource allocation for infrastructure maintenance. *Decision Analysis*, 6(3):139–152, 2009.

Morenoff, J. D. and Smapson, R. J. Neighborhood inequality, collective efficacy, and the spatial dynamics of urban violance. Technical report, 2001. URL `http://www.psc.isr.umich.edu/pubs/`.

NeighborWorks. Responsible approaches to neighborhood stabilization: Case studies in action. Technical report, NeighborWorks America, Neighborhood Reinvestment Corporation, 2009.

Nikolaev, A. G. and Jacobson, S. H. Stochastic sequential decision-making with a random number of jobs. *Operations Research*, 58(4):1023–1027, 2010.

Ortega, A., Sánchez, M., Gil, F., and Rico, R. Enhancing team learning in nursing teams through beliefs about interpersonal context. *Journal of Advanced Nursing*, 69(1):102–111, 2013.

Puterman, L. M. *Markov Decision Processes: Discrete Stochastic Dynamic Programming*. New York: Wiley Interscience, 1994.

Russell, C. and Johnson, S. FHFA House Price Index up 0.7 percent in February. Technical report, Federal Housing Finance Agency, 2013.

Sampson, R. J., Raudenbush, S., and Earls, F. Neighborhoods and violent crime: A multilevel study of collective efficacy. *Science*, 277:918–924, 1997.

Schuetz, J., Been, V., and Ellen, I. G. Neighborhood effects of concentrated mortgage foreclosures. *Journal of Housing Economics*, 17(4):306–319, 2008.

Simon, H. The community asset preservation corporation: A new approach to community revitalization, Working Paper. 2009. URL `http://www.bostonfed.org/commdev/REO-and-vacant-properties/123-Simon.pdf`.

Slomp, J. and Suresh, N. C. The shift team formation problem in multi-shift manufacturing operations. *European Journal of Operational Research*, 165(3):708–728, 2005.

Solak, S., Clarke, J., Johnson, E., and Barnes, E. Optimization of R&D project portfolios under endogenous uncertainty. *European Journal of Operational Research*, 207(1):420–433, 2010.

Stable Communities. Neighborhood stabilization program (NSP) strategies, 2012. URL `http://www.stablecommunities.org/nsp-strategies`.

Stolletz, R. and Brunner, J. O. Fair optimization of fortnightly physician schedules with flexible shifts. *European Journal of Operational Research*, 219(3):622–629, 2011.

Swanstrom, T., Chapple, K., and Immergluck, D. Regional resilience in the face of foreclosures: Evidence from six metropolitan areas, Working Paper, 2009. URL http://metrostudies.berkeley.edu/pubs/reports/2009-05.pdf.

Voogd, H. *Multicriteria Evaluation for Urban and Regional Planing*. London: Pion, 1983.

Wall, J., Chandra, V., and Krummel, T. Robotics in general surgery, Working Paper, 2008. URL http://cdn.intechopen.com/pdfs/668/InTech-Robotics_in_general_surgery.pdf.

Wright, P. D. and Mahar, S. Centralized nurse scheduling to simultaneously improve schedule cost and nurse satisfaction. *Omega*, 41(6):1042–1052, 2012.

Yao, R. and Zhang, H. Optimal consumption and portfolio choices with risky housing and borrowing constraints. *Review of Financial Studies*, 18(1):197–239, 2005.

Yushkevich, A. A. and Feinberg, E. A. On homogeneous controlled Markov models with continuous time and finite or countable state space. *Theory of Probability and Its Applications*, 24:156–161, 1979.

Zakarian, A. and Kusiak, A. Forming teams: an analytical approach. *IIE Transactions*, 31(1):85–97, 1999.

Zhang, L. and Zhang, X. Multi-objective team formation optimization for new product development. *Computers & Industrial Engineering*, 64(3):804–811, 2013.